Sergio Santoro

Master in Materials Science

Molecular probes: an innovative technology for monitoring membrane processes

Dissertation for obtaining the Doctoral degree in
Membrane Engineering

Supervisors: Isabel Maria Rôla Coelhoso, Assistant Professor, Faculdade de Ciências e Tecnologia, Universidade Nova de Lisboa

João Paulo Serejo Goulão Crespo, Professor, Faculdade de Ciências e Tecnologia, Universidade Nova de Lisboa

Co-supervisors: Reyes Mallada, Associate Professor, Department of Chemical and Environmental Engineering and Aragon Nanoscience Institute, Universidad de Zaragoza

Enrico Drioli, Emeritus Professor, Department of Environmental and Chemical Engineering, Università degli Studi della Calabria
Alberto Figoli, Researcher, Institute for Membrane Technology (ITM-CNR)

Jury:

President: Prof. José Paulo Barbosa Mota, FCT, Universidade Nova de Lisboa

Examiner(s): Prof. Frederico Castelo Alves Ferreira, IST, Universidade de Lisboa
Prof. Thomas Schafer, University of the Basque Country

Members: Prof. João Carlos Lima, FCT, Universidade Nova de Lisboa
Prof. Reyes Mallada, Universidad de Zaragoza
Dr. Alberto Figoli, Institute for Membrane Technology (ITM-CNR)
Prof. Isabel Maria Rôla Coelhoso, FCT, Universidade Nova de Lisboa
Prof. João Paulo Serejo Goulão Crespo FCT, Universidade Nova de Lisboa

FACULDADE DE
CIÊNCIAS E TECNOLOGIA
UNIVERSIDADE NOVA DE LISBOA

May 2016

Sergio Santoro

Master in Materials Science

Molecular probes: an innovative technology for monitoring membrane processes

Dissertation presented to Faculdade de Ciências e Tecnologia, Universidade Nova de Lisboa for obtaining the Doctoral degree in Membrane Engineering

May 2016

Molecular probes: an innovative technology for monitoring membrane processes

"To all the dreamers,
to those who speak to the wind.
To the ones in love, to the day-
dreamers, to all who will still give their
life away to make a dream come true.
To the rejects, the not wanted, to all
whom are left out. To the crazy ones,
them being real or just assumed to be.
To the good hearted men, to those who
still want to believe that real feelings
exist. To those who can still be touched.
A tribute to the great soakers, to big
ideas, to dreams. To those who will
never give up, to who is mocked or
judged. To the everyday poets. To the
possible winners and so to all the losers
who are still urged to rise again and to
keep fighting. To the forgotten heroes
and to those who wander around. To
those, that after having fought and lost
for their ideals, still feel they are
invincible. To those who are not scared
to express their ideas. To those who
went around the world and to who one
day will do the same. To those who do
not want to distinguish between reality
and fiction. To all the errant knights. And
somehow, it is fair and well said…..to all
the performers."

Don Quixote
Miguel de Cervantes

Acknowledgements

"Inside us there is something that has no name, that something is what we are." Though only my name appears on the cover of this dissertation, a great many people from Portugal, Spain and Italy have contributed to its production. I owe my gratitude to all those people who have made this dissertation possible.

My deepest gratitude is to Prof. João Paulo Crespo. I have been amazingly fortunate to have an advisor who gave me the freedom to explore on my own, and at the same time the guidance to recover when my steps faltered.

I would like to express my sincere gratitude to Prof. Isabel Coelhoso for the continuous support of my Ph.D study: her guidance helped me in all the time of research and writing of this thesis.

I will always be grateful to Prof. João Carlos Lima, who introduced me to the wonders of the Photochemistry. I am indebted to him for his continuous encouragement and guidance.

This dissertation would not have been possible without Dr. Artur Moro. He has been always there to teach me, listen, give advice, read my reports, comment on my views and help me understand and enrich my ideas.

I am grateful to Dr. Carla Portugal for holding me to a high research standard and enforcing strict validations for each research result by insightful comments and constructive criticisms.

Thanks also go to my colleagues and friends of the Universidade Nova de Lisboa, who expressed an interest in the project and provided useful feedback.

I will always be grateful to Prof. Reyes Mallada because she provided me the opportunity to join her team at the Institute of Nanoscience of Aragon. I benefited from her advice, particularly so when exploring new ideas. Her positive outlook and confidence in my research inspired me.

I owe my gratitude to Dr. Victor Sebastian for the continuous support of research during my stay in Spain, for his patience, motivation, and immense knowledge.

Dr. Manuel Arruebo's insightful comments were thought-provoking and they helped me focus my ideas.

The members of the Institute of Nanoscience of Aragon have contributed immensely to my personal and professional time at Zaragoza. The group has been a source of friendships as well as good advice and collaboration.

I would also like to express my thanks to Dr. Alberto Figoli who has been always played a key role in my studies and research. It was though his persistence, understanding and kindness that I completed my graduate training and my PhD. The joy and enthusiasm he has for her research was contagious and motivational for me.

I would like to thank Dr Alessandra Criscuoli for the patient guidance, encouragement and advice. I have been extremely lucky to have a supervisor who cared so much about my work, and who responded to my questions and queries so promptly.

A very special thanks goes out to Giovanni Desiderio and Dr. Giuseppe Lombardo. They truly made a difference in the last part of my studies.

I am grateful to all my friends from the Institute on Membrane Technology for being my surrogate family.

My sincere thanks also goes to Prof. Enrico Drioli, Dr. Curcio Efrem and all the members of the The Erasmus Mundus Doctorate in Membrane Engineering (EUDIME) for the assistance throughout my PhD program and the exchange of ideas in the annual meetings.

"Quando ti viene nostalgia non è mancanza. E' presenza di persone, luoghi, emozioni che tornano a trovarti." Grazie ai luoghi e agli amici di sempre, che mi sono mancati e che hanno fatto sentire sempre la loro presenza. Soprattutto quando ne avevo bisogno.

Grazie al mio fianco, Marika, gioia che ha contagiato la mia esistenza. Con la promessa che il più bello dei mari è quello che non navigammo e i più belli dei nostri giorni non li abbiamo ancora vissuti.

Grazie ad Adriana, riparo nella tempesta e arcobaleno nel sereno, e a Francesco, il fratello che non ho mai avuto.

Grazie a Letizia, che mi ha insegnato a restare bambino. E' difficile chiederti scusa per un mondo che è quel che è, io nel mio piccolo tento qualcosa per farlo assomigliare a te.

Grazie a mia mamma e mio papà, invincibili eroi del quotidiano. A voi devo quello che sono ed il senso che ho acquisito della vita.

Grazie a tutta la mia famiglia, ai miei nonni e alla gente del mio paese, perché *"sono solo un punto lungo una retta lucida e infinita"*.

Abstract (300 words)

The ultimate objective of this study is to use molecular probes as an innovative and alternative technology contributing to the advance of membrane science by monitoring membrane processes in-situ, on-line and at sub-micron scale.

An optical sensor for oxygen sensing was developed by the immobilization of tris (1, 10-phenanthroline) ruthenium (II) ($Ru(phen)_3$) in a dense polymeric membrane made of polystyrene (PS) or Poly(3-hydroxybutyrate-co-3-hydroxyvalerate) (PHBV). The emission of the probe was quenched by both the temperature and by the oxygen. Moreover, the oxygen sensitivity was affected by the oxygen permeability of the membrane. The evaluation of the oxygen concentration is prone to errors since the emission of a single probe depends on several parameters (i.e. optical path, source intensity). The correction of these artefacts was obtained by the immobilization of a second luminescent molecule non-sensitive to the oxygen, Coumarin. The potential of the luminescent ratiometric sensor for the non-invasive monitoring of oxygen in food packaging using polymeric films with different oxygen permeability was evaluated. Emphasis was given to the efficiency of the optical sensor for the on-line, in-situ and non invasive monitoring of the oxygen by comparing the experimental data with a model which takes into account the oxygen permeability of the packaging materials evaluated independently.

A nano-thermometer based on silica nano-particles doped with $Ru(phen)_3$ was developed. A systematic study shows how it is possible to control the properties of the nano-particles as well as their temperature sensitivity. The nano-thermometer was immobilized on a membrane surface by dip-coating providing information about the temperature on the membrane surface.

Hydrophobic porous membrane made of Poly(vinylidene fluoride) was prepared via electrospinning and employed in a direct contact membrane distillation process. Using a designed membrane module and a membrane doped with $Ru(phen)_3$ the on-line mapping of the temperature on the membrane's surface was evaluated.

Resumo

O objectivo final deste trabalho é a utilização de sondas moleculares como uma tecnologia inovadora e alternativa contribuindo para o avanço da ciência em processos de membranas, monitorizando esses processos *in-situ*, on-line e numa escala submicrométrica.

Foi desenvolvido um sensor óptico para a detecção de oxigénio imobilizando tris (1, 10-fenantrolina) de ruténio (II) (Ru(phen)$_3$) numa membrana polimérica densa de poliestireno (PS) ou de poli (3-hidroxibutirato-co -3-hidroxivalerato) (PHBV). A sensibilidade da sonda para o oxigénio é afectada pela permeabilidade da membrana a este gás. Verificou-se que a avaliação da concentração de oxigénio é propensa a erros uma vez que a emissão de uma única sonda depende de vários parâmetros, tais como, o percurso óptico, a intensidade de fonte, entre outos. A correcção destes erros foi obtida pela imobilização de uma segunda molécula luminescente não-sensível ao oxigénio, a cumarina. O potencial deste sensor raciométrico luminescente para a monitorização não invasiva de oxigénio em embalagens de alimentos usando filmes poliméricos com diferentes permeabilidades ao oxigénio foi avaliada. Os resultados obtidos através da monitorização não invasiva do oxigénio com o sensor foram comparados com os obtidos usando um modelo que tem em conta a permeabilidade ao oxigénio dos materiais de embalagem avaliada independentemente.

Desenvolveu-se ainda, um nano-termómetro baseado em nano-partículas de sílica dopadas com Ru(phen)$_3$. Um estudo sistemático mostra como é possível controlar as propriedades das nano-partículas, bem como a sua sensibilidade à temperatura. O nano-termómetro foi imobilizado sobre a superfície de uma membrana por *dip-coating* sendo possível obter deste modo, a temperatura na superfície da membrana.

Foi ainda preparada uma membrana porosa hidrofóbica de poli (fluoreto de vinilideno) usando a técnica de *electrospinning* que foi utilizada num processo de destilação directa num contactor de membrana. Usando um módulo de membranas desenhado e a membrana dopada com Ru(phen)$_3$, foi possível obter o mapeamento da temperatura na superfície da membrana.

Resumen

El objetivo final de este estudio es el uso de una tecnología innovadora basada en el uso de sondas moleculares que actúan como sensores. La tecnología desarrollada contribuye al avance de la ingeniería de membranas, específicamente al control in situ de los procesos fisico-químicos que tienen lugar en su estructura porosa. El desarrollo de esta tecnología ha hecho posible obtener un buen control en la cuantificación de la temperatura y concentración de oxígeno presente en las membranas, alcanzándose una resolución sub-micrométrica.

Se ha desarrollado un sensor óptico (sonda) para detectar y cuantificar la presencia de oxígeno mediante la inmovilización de tris (1, 10-fenantrolina) rutenio (II) (Ru(phen)$_3$) en una membrana polimérica densa de poliestireno (PS) o poli (3-hidroxibutirato-co -3-hidroxivalerato) (PHBV). La emisión espectral de la sonda era sensible tanto a la temperatura de la membrana como a la presencia de oxígeno. Por otra parte, la sensibilidad de la sonda al oxígeno se vio afectada por la permeabilidad de las moléculas de oxígeno a través de la membrana. La cuantificación de la concentración de oxígeno no es trivial y suele estar sujeta a errores de emisividad generados por artefactos espectrales, ya que la emisión de una única sonda depende de varios parámetros, como por ejemplo el camino óptico o la intensidad de la fuente de excitación. La corrección de estos artefactos se obtuvo mediante la inmovilización de una segunda molécula luminiscente no sensible al oxígeno, cumarina.

En este proyecto se ha evaluado el potencial del sensor luminiscente radiométrico para la monitorización no invasiva de oxígeno en el envase de alimentos, utilizando para ello películas poliméricas con diferente permeabilidad al oxígeno. Se ha estudiado en mayor profundidad la eficiencia del sensor óptico para el análisis on-line, utilizando para ello la medida in situ y no invasiva de la luminiscencia de las sondas. La monitorización de la presencia de oxígeno se realizó mediante la comparación de los datos experimentales de la emisión de las sondas con los datos de permeación de oxígeno a través del embalaje.

Además, se ha elaborado una sonda térmica, nanotermómetro, basada en el dopado de nanopartículas de silice con Ru(phen)$_3$. Un estudio sistemático muestra cómo es posible controlar las propiedades luminiscentes de las nanopartículas, así como su sensibilidad a la medida de la temperatura. El nano-termómetro se inmovilizó sobre la superficie de la membrana, proporcionando información muy precisa sobre la temperatura en la superficie de la misma.

Finalmente, se ha desarrollado una membrana porosa hidrófoba de poli(fluoruro de vinilideno) mediante la técnica de electrohilado. Dicha membrana se ha empleado en un proceso de destilación por contacto directo. Mediante el uso de las anteriores sondas descritas basadas en Ru(phen)$_3$ y el desarrollo de un   módulo de membrana con acceso óptico, se ha podido estudiar la distribución térmica de la membrana en las diferentes condiciones de destilación estudiadas.

Riassunto

L'obiettivo finale di questo studio è l'impiego di sonde molecolari come tecnologia innovativa ed alternativa che contribuisca al progresso della scienza delle membrane favorendo il monitoraggio del processo a membrana *in-situ*, on-line e su scala inferiore al micron.

E' stato sviluppato un sensore ottico per il monitoraggio dell'ossigeno tramite l' immobilizzazione di tris (1,10-fenantrolina) rutenio (II) ($Ru(phen)_3$) in una membrana polimerica densa fatta di polistirolo (PS) e poli(3-idrossibutirrato-co-3-idrossivalerato) (PHBV). L'emissione della molecola è influenzata sia dalla temperatura che dall'ossigeno. Inoltre, la sensibilità all'ossigeno è condizionata dalla permeabilità all'ossigeno della membrana. Tuttavia, la determinazione della concentrazione di ossigeno è soggetta ad errori, poiché l'emissione di una singola molecola dipende da diversi parametri (per esempio cammino ottico, intensità sorgente). La correzione di questi artefatti è stata ottenuta tramite l'immobilizzazione di una seconda molecola luminescente non sensibile all'ossigeno, ovvero la Cumarina. Abbiamo valutato le potenzialità del sensore basato sul rapporto delle intensità delle emissioni delle due molecole luminescenti nel monitorare la concentrazione di ossigeno nell'imballaggio alimentare fatto da film polimerici con diversa permeabilità all'ossigeno. E' stata data enfasi all'efficienza del sensore ottico per il monitoraggio non invasivo, *in-situ* e on-line dell'ossigeno, confrontando i dati sperimentali con un modello che tiene conto delle permeabilità all'ossigeno dei materiali di imballaggio valutate indipendentemente.

È stato sviluppato un termometro costituito da nano-particelle di silice drogate con $Ru(phen)_3$. Uno studio sistematico mostra come sia possibile controllare le proprietà delle nano-particelle, nonché la loro sensibilità alla temperatura. Il nano-termometro è stato immobilizzato su una superficie di una membrana mediante *dip-coating* fornendo informazioni riguardo la temperatura sulla superficie della membrana.

Abbiamo preparato tramite *electrospinning* una membrana idrofoba porosa fatta di poli(fluoruro di vinilidene) che è stata impiegata in un processo di distillazione a membrana per contatto diretto.

La mappatura on-line della temperatura sulla superficie della membrana è stata consentita dall'impiego di un modulo a membrana appositamente progettato e dal drogaggio della membrana con $Ru(phen)_3$.

x

Nomenclature

A: Packaging area, m^2

a.u.: Arbitrary unit

b: Optical path, cm

BOPP: Biaxially oriented polypropylene

(byp): (2,2'-bipyridine)

c: Concentration probe, mol

CA: Contact angle, °

$C_{O_2}^{in}$: Oxygen concentration in the enclosed package

$C_{O_2}^{out}$: Oxygen concentration in the atmosphere (21%)

Coumarin: 7-Methoxy-4-methylcoumarin

C(T): Temperature compensation

d_p: Pore size, μm

(dpp): (4,7-diphenyl-1,10-phenanthroline)

dR/dT: Temperature sensitivity of the ratiometric response, $°C^{-1}$

ENM: Electrospun Nanofibrous Membrane

EDS: X-ray microanalysis

f_1: Fractional intensity

I: Intensity of emission, a

FPP: Tetrakis pentrafluoropheny porphine

I: Intensity of emission in the presence of oxygen

I_0: Intensity of emission in absence of oxygen, a.u.

I_{21}: Intensity of emission at atmospheric pressure, a.u.

I_{exc}: Intensity of exciting light, a.u.

$I(N_2)$: Fluorescence intensities in the absence of oxygen

$I(O_2)$: Fluorescence intensities in the 100% oxygen

k: Constant of excitation/detection geometry

k_q: Rate of bimolecular quenching

K_{SV}: Stern-Volmer constant, $\%^{-1}$

$K_{SV}(T_{ref})$: Stern-Volmer constant at 25°C, $\%^{-1}$

l: Thickness of packaging, m

N_A: Avogadro's number, mol^{-1}

N_2: Nitrogen

O_2: Oxygen

OEP: Octaethylporphyrin

OEPK: Octaethylporphyrinketone

P: Porosity, %

$p(O_2)$: Oxygen partial pressure, bar

$P(O_2)$: Oxygen permeability, $m^2 s^{-1}$

PAN: Poly(acrylonitrile)

PBA: 1-pyrene butyric acid, OEP: octaethylporphyrin

PHVB: Poly(β-hydroxybutyrate-β-hydroxyvalerate)

PDMS: Poly(dimethylsiloxane)

Pe: Oxygen permeability, barrer

(phen): Phenanthroline (ppy):[2-phenylpyridinato-C2,N]

PS: Polystyrene

PSS: Poly(sodium 4-styrene sulfonate)

PtTFPP: Ttetrakis(pentafluorophenyl)porphyrin

PDMS: Polydimethylsiloxane,

PVA: Polyvinyl alcohol

R: Ratiometric response

R_m: Non-temperature dependent ratiometric response

R_0: Ratiometric response in absence of oxygen

R_0: Ratiometric response in an atmosphere of oxygen

R_m: Non-temperature dependent ratiometric response in absence of oxygen

$R_0(T)$: Ratiometric response at a certain oxygen level and temperature

$R_0(Tref)$: Ratiometric response in absence of oxygen at 25°C

R_{21}: Ratiometric response at atmospheric pressure, a.u.

$Ru(phen)_3$: Tris(1,10-phenanthroline)ruthenium(II)

s: Electrical conductivity, $\mu S\ cm^{-1}$

T: Temperature, °C

TGA: Thermogravimetric analysis

TTA: Thenoyltrifluoroacetonate,

V: Volume enclosed by the packaging, m^3

yO_2: Volumetric oxygen concentration, %

Greek symbols

β: Geometric parameter of the permeation cell, m^{-1}

δ: Collision radius, m

ε: Molar extinction coefficient, $m^2 mol^{-1}$

λ: Wavelenght, nm

Φ: Quantum yeld, %

v: Viscosity, cP

ρ: Density, $cm^3 g^{-1}$

Contents

List of Figures

List of Tables

Chapter 1

Introduction: state of art and thesis motivations

The following chapter includes the state-of-the-art related with the technology of interest in the present thesis (molecular probes for oxygen and temperature monitoring in membrane processes), the motivations for the explored approach and the main objectives of this thesis.

1.1 Membrane technology: advances and limitations

Membranes have been considered an interesting technology providing a crucial contribute in solving critical issues of the 21th century, such as pollution, energy and water demands. Membrane processes have been gained considerable interest for environmental friendly, non energetic intensive and economical separation of species in a wide range of application (i.e. water purification and desalination, recovery or release of target molecules of interest in medical and pharmaceutical field, production of biomass, bio-fuel and biogas).

The key activity of the membrane is the preferential transport of chemical species useful for separation processes or controlled release molecules [1].
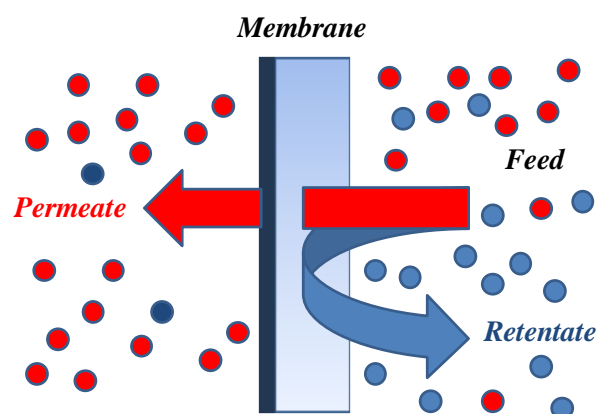
Figure 1.1: Membrane separation.

In the evaluation of the membrane performance, three parameters must be considered [1]:

      i)   Selectivity: favouring the selective transport of the target molecules;

      ii) Permeability: ensuring high mass transport of permeant species;

      iii) Stability: guarantying long term and stable performance of the transport.

Efforts have been devoted for the improvement of membrane processes on the basis of production of high-performance membrane materials and the optimization of operating conditions of the processes. The high-performance of the membrane is usually guaranteed by the employment of novel materials and designed membrane morphologies adequate for the separation of interest, whereas the optimization of the membrane processes is guaranteed by dedicated membrane modules and optimized operating conditions aimed to improve the interactions between the permeant species and the membrane modules which govern the mass transport trough the membrane [2].

In fact, the breakthrough in membrane science was achieved as a consequence of development of extremely selective and ultra-thin membranes and of high surface-area membrane modules which made membrane processes competitive and economical viable [3-4]. Furthermore, progresses in material science and nanotechnology favoured the development of new material with tailored properties and high performance [5-7].

Besides these advances, there are major issues limiting the membrane processes performance in terms of selectivity, permeability and stability, in particular fouling, concentration and thermal polarization [8-10]. In fact, in the recent years, the development of membrane modules and the design of membrane process are becoming increasingly important to minimize those major persistent factors and to maximize the membrane performance [11].

For this reason, the evaluation of membrane properties and membrane performance at sub-micron scale, *in-situ* and on-line are crucial for better understanding the chemical and physical interactions between the permeant species and the membrane surface in order to improve membrane technology overcoming its limitations.

1.2 Monitoring of membrane processes

Membrane technology applications focus considerable interest on the evaluation of the performance of membranes and efforts are directed towards the improvement of the techniques enable to detect on-line the membrane processes performance. It is well know that there are dramatically changes during the processes because of variations in membrane properties, such as deterioration of the material, swelling or fouling, and of operating conditions, such as temperature polarization or feed composition.

The efficiency of the membrane is usually expressed in terms of permeability obtained by quantifying the permeate. On the other hand, the quantitative analyses of the permeate concentration and the evaluation of its different chemical composition with respect to the feed and the retentate allows the evaluation of the selective mass transport. Then, the long-term observation of those properties consents to estimate the stability of the membrane and of the membrane process.

The qualitative and the quantitative analyses of the streams in/out-coming to/from the membrane module provide a global information about the performance of the process that is a consequence of permeant/membrane interactions at molecular scale and the chemical and physical parameters (i.e. temperature, concentration of the permeants in the boundary layer) which affect the process. Furthermore, it is well known that those interactions and parameters dramatically change along the module and time as a consequence of the membrane nature and of the operating conditions.

In fact, for a complete picture the "wish list" for monitoring membrane processes is: in real time, non-invasive, *in situ*, at a molecular scale and using pattern recognition approaches [12].

Unfortunately, conventional techniques fail in providing information at microscopic level, *in situ* and in real time for studying those phenomena of interest.
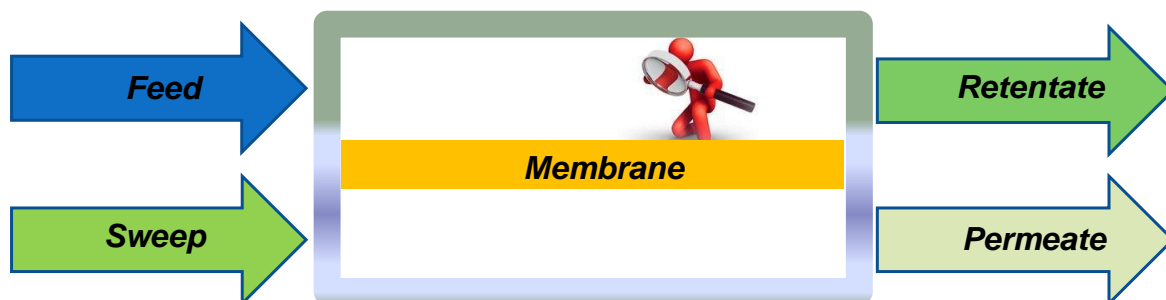
Figure 1.2: Membrane process.

1.3 Importance of temperature and oxygen in membrane processes

Oxygen is fundamental in a wide range of applications involving membrane technologies such as gas separation for oxygen enriched air, fuel cell for energy production, aerobic membrane reactor treating wastewater, membrane contactors employed in liquid oxygenation (i.e. water, blood) [13-16].

Furthermore, oxygen is essential for life and its monitoring provides information about biological activity crucial for the monitoring of the aerobic bio-fouling on membrane surface, the evaluation of food quality stored in packaging and efficiency of membrane bioreactor [17-19].

Temperature is an omnipresent factor influencing nearly every chemical process, including membrane processes. In fact, it is well know that temperature dramatically affects the performance of the membrane, usually increasing the productivity of the processes by increasing the membrane permeability [1]. Moreover the temperature improves the yield of reactions in membrane reactors [20]. On the other hand, temperature significantly affects microbial growth and the physicochemical properties of organic molecules dissolved in the treated solutions [21].

Nowadays, electrochemical sensors such as thermocouple for the monitoring of the temperature and Clark electrode for the detection of the oxygen levels are employed as accurate and inexpensive technologies with a rapid response time employed in monitoring membrane processes [22-23]. However, the miniaturization of the sensors is the most critical issue of these technologies that are unable to monitor the parameters of interest with a high spatial resolution at micron and submicron scale, typically demanded in innovative research fields such as nano-medicine, biotechnology and micro-fluidics as well as in membrane technology [24-25].

1.4 Molecular probes: an innovative technology for monitoring membrane process

Luminophores are chemical compounds that can re-emit light upon light excitation usually employed as markers in bio-medical applications. Their employment as molecular probes could be considered a promising and suitable alternative technology in monitoring membrane processes *in-situ*, on-line, non-invasive and at sub-micron scale [26].
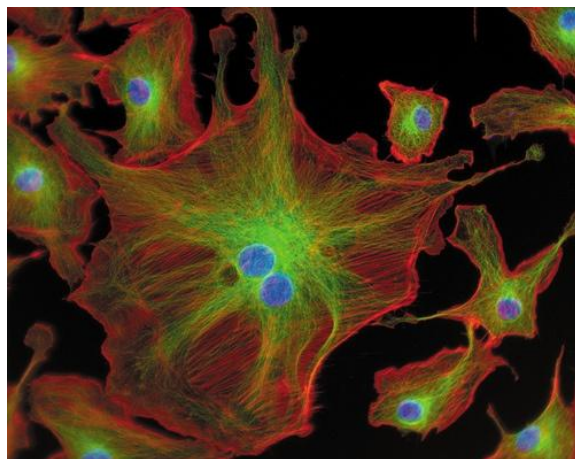
Figure 1.3: Bovine pulmonary artery endothelial cells marked with different luminophores. Source: www.flickr.com.

In fact, the emission of the luminophores (fluorescence or phosphorescence) strongly depends on their chemical compositions and molecular structures, but it is also affected by environmental conditions (i.e. pH and temperature) and vicinity (i.e. solvents and presence of quenchers) [27].

Optical sensors are successfully applied in different fields, such as: marine, environmental, medical, chemical and molecular biotechnology analysis, industrial production monitoring, bioprocess control and automotive industry [28] and they are based on the immobilization of luminophores in a matrix. The properties of the emission of optical sensor (intensity, lifetime or quantum yield) enable to monitor changes in its vicinity or in the environmental, providing physical or chemical information [29].

The role of the matrix load with the luminophore is to support and protect the probe by the encapsulation guaranteeing at the same time high degree of interactions with the target in case of chemical sensing.

The desired properties of the molecular probes are: high emission, long photochemical stability and elevated and exclusive sensitivity towards the chemical or physical parameter of interest. In this contest, a wide variety of molecular probes and optical sensors for oxygen and temperature sensing were developed since are two key factors affecting chemical processes [30-31].

The immobilization of molecular probes into/onto membranes could be considered an interesting technology for monitoring and mapping oxygen and temperature in membrane modules and processes.

1.5 Oxygen molecular probe

Optical sensors are based on quenching of phosphorescence of luminophores immobilized generally in a polymeric matrix. In fact, the luminescence of oxygen molecular probes is quenched by the analyte: higher oxygen concentration leads lower intensity of emission.

Table 1.1: List of optical sensor prepared employing common molecular probes for oxygen sensing.

Molecular Probe	Support	$I(N_2)/I(O_2)$	Reference
PBA	PDMS	1.5	[32]
Perylene	PS	1.5	[33]
PtOEP	PS	4.5	[34]
PdOEP	PS	11.5	[35]
PtOEPK	PS	20	[36]
PdOEPK	PS	28	[36]
PtTFPP	Silica	117	[37]
Ir(ppy)$_3$	PS	1.2	[38]
Os(ddp)$_3$	PDMS	4.5	[37]
Ru(ddp)$_3$	PDMS	4.4	[39]
Ru(phen)$_3$	PSS	2.3	[41]
Ru(byp)$_3$	PSS	1.7	[41]

$I(N_2)$: the fluorescence intensities in the absence of oxygen, $I(O_2)$: the fluorescence intensities in the 100% oxygen, PBA: 1-pyrene butyric acid, OEP: octaethylporphyrin, OEPK: octaethylporphyrinketone, FPP: tetrakis pentrafluoropheny porphine, (ppy): [2-phenylpyridinato-C2,N], (dpp): (4,7-diphenyl-1,10-phenanthroline), (phen): phenanthroline, (byp): (2,2'-bipyridine), PDMS: Polydimethylsiloxane, PS: Polystyrene, PSS: poly(sodium 4-styrene sulfonate).

The development of oxygen sensor is based on the selection of the molecular probes. Since the 60's, polycyclic aromatic hydrocarbons (PAHs) dissolved in polymers, soaked into porous glasses, or covalently immobilized on glass supports have been studied as organic luminescent probes for oxygen monitoring [41-42]. However, PAHs suffer from a lack of stability due to aggregation, related to their low solubility in some polymers, and adequate sensitivity to oxygen is achievable only in polymers highly permeable to oxygen.

In recent years more advanced probes, typically organo-metallic compounds, are employed for the development of optical sensors because of their long excited state lifetimes, which increase the sensitivity to lower concentrations of oxygen. In general, organo-metallic compounds sensitive to oxygen are classified into two categories: transition metal polypyridyl complex (in general complexes of Ru^{2+}, Re^+, Os^{3+} and Ir^{3+}) and metallo-porphines, (in particular Pt^{2+} and Pd^{2+}porphyrins).

Numerous sensors are based on the employment of Pt^{2+} and Pd^{2+}porphyrins because of the high phosphorescence quantum yields at room temperature and, in particular, high sensitivity to oxygen [34,43]. However, porphyrins are very reactive towards singlet oxygen, which leads to photobleaching and limits the long term stability of these sensors.

Nowadays, efforts are devoted to chemical modification of the probes to ensure long term stability or to the development of sensors based on the lifetime monitoring [44]. Unfortunately, the monitoring of the decay time is more sophisticated with respect to the monitoring of the emission intensity, limiting the application of these sensors in real situations.
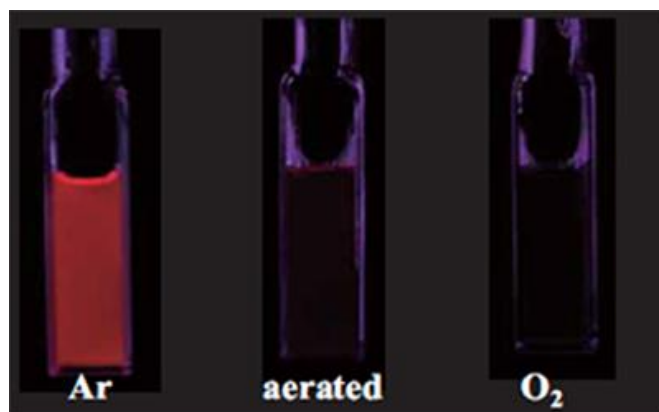
Figure 1.4: Luminescence of an oxygen molecular probe in argon (Ar), aerated and oxygen atmosphere. Source: http://www.scivaxls.com.

On the other hand, transition Ru polypyridyl complexes, such as tris(bipyridine)ruthenium(II) (Ru(bpy)$_3$) and tris(phenantroline)ruthenium(II) (Ru(phen)$_3$) show photostability combined with significant luminescence sensitive to oxygen, but lower with respect to metallorphines due to shorter excited state lifetime [45-46].

1.6 Temperature molecular probes

The thermal sensitivity of the luminophores is related to the fact that vibrational modes are activated by increasing the temperature favouring the non-radiative deactivation upon the excitation of the luminophore.
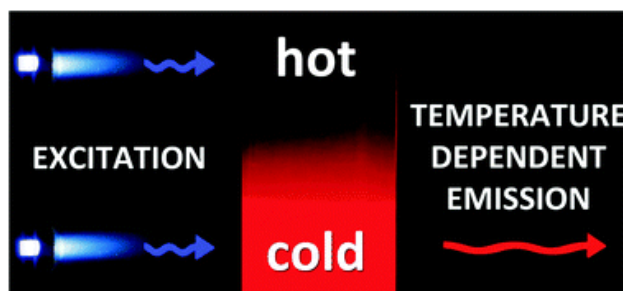
Figure 1.5: Representative scheme of working of an optical sensor for temperature detection [46].

Popular organic dyes were studied as valid candidates for *in-situ* luminescent nano-thermometry in biological media. The interest is related to the fact that luminescent molecular probes enable high spatial resolution with fast response, often in a time scale comparable to that of cellular processes, combined with a non-invasive monitoring.

Table 1.2: List of optical sensor prepared employing common molecular probes for temperature sensing

Molecular Probe	Support	Temperature range (K)	Reference
Rhodamine B	Silica	283-368	[48]
Fluorescein	Starch	273-333	[49]
Ru(phen)$_3$	PAN	273-393	[50]
Ru(byp)$_3$	PVA	50–290	[51]
PtOEP	PS	300-450	[52]
Eu(TTA)	PS	278-333	[53]

(phen): phenanthroline, (byp): (2,2'-bipyridine), OEP: octaethylporphyrin, TTA: thenoyltrifluoroacetonate, PAN: Poly(acrylonitrile), PVA: Polyvinyl alcohol , PS: Polystyrene.

Among the organic dyes, Rhodamine B and Fluorescein have been extensively studied because of their good brightness, emission in the visible and linear temperature dependence of the intensity of the emission in ambient conditions (273-333 K) [47-48]. Furthermore, Fluorescein has been employed as pH sensitive molecular probes. However, limitations in the employment of organic dyes are related to their weak thermal stability.

Once again, luminescent metal–ligand complexes have been considered as promising molecular probes for temperature sensing. In fact, organo-metallic complexes showed a pronounced temperature sensitivity combined with thermal stability. However, a ubiquitous problem consists to the

fact that the emission of phosphorescent luminescent metal–ligand complexes is generally affected by the oxygen that often are immobilized in matrix with low oxygen permeability to minimize interferences related to oxygen concentration drifts.

In fact, in the last decade, metallo-porphines of platinum (i.e. Platinum octaethylporphyrin) and Ru polypyridyl complexes have been selected in several studies as fluorescent nano-thermometers immobilized in different matrixes.

1.7 Objectives and thesis outline

Membrane is an emerging technology allowing non-intensive separation processes without the employment of chemicals. The development of high performance membranes based on innovative and devoted materials and the design of the membrane processes allowed the achievement of the success of membrane technologies in different fields, from gas separation to water treatment, in particular desalination.

Besides the easy scale-up of membrane processes which favour the employment of membrane technologies at industrial scale, the performance of the process is related to the chemical-physical interactions at molecular level between the permeant species and the membrane. For this reason, it is evident the capital importance of studying of membrane processes at molecular level in order to better understand the selective permeation of chemicals, providing an important feedback for the preparation of innovative materials and to overcome the limitations of membrane science. In fact, major factors limiting membrane technology (i.e. concentration polarization, thermal polarization, fouling) are related to phenomena taking part on membrane surface. The study of these critical issues is really challenging because of the lack in term of experimental data related to the problems of studying them with high spatial resolution without disturbing the membrane processes.

Luminophores, molecules emitting light upon light exposure, are successfully employed as molecular probes for the in-situ, at submicron scale, non-invasive and on-line monitoring of several parameters (i.e. temperature, oxygen, and pH) typically demanded in innovative fields of nano-science. The aim of this work is to propose molecular probe as an innovative technology for monitoring membrane processes.

In this study, tris (1,10-phenanthroline) ruthenium (II) chloride hydrate, (Ru(phen)$_3$, was selected as molecular probe on the basis of its high brightness, photostability and pronounced oxygen and temperature sensitivity.

The selected probe was immobilized in dense polymeric membrane made of polystyrene (PS) and Poly(3-hydroxybutyrate-co-3-hydroxyvalerate) (PHBV) prepared via solvent evaporation. Experiments showed that the intensity of the emission of the films due to the immobilized emissive molecule is quenched by the oxygen concentration. A systematic study demonstrated that the oxygen sensitivity of the membrane is affected by oxygen permeability of the polymeric matrix as well as the concentration of the molecular probes. The intensity of the emission was found to be sensitive to the

operating conditions, in particular fluctuations of the optical path, drifts in the intensity of the excitation light and temperature variations, limiting the effectiveness of the oxygen sensing. Therefore, a second probe, 7-Methoxy-4-methylcoumarin (Coumarin), non-sensitive to the oxygen concentration was immobilized in the polymeric membrane, allowing the corrections of artefacts induced by changes in the geometry and intensity of the light source. On the other hand, the implementation of simple model compensated the thermal effect, obtaining a signal that depends exclusively on the oxygen concentration. This work performed at the Universidade Nova de Lisboa was submitted to Journal of Membrane Science.

The developed oxygen sensitive membranes were employed as optical sensor for the on-line and non invasive monitoring of oxygen in food packaging. The sensor was placed in a degassed atmosphere sealed by polymeric films reproducing a typical configuration in modified atmosphere packaging (MAP): the polymeric packaging in an interface between the enclosed degassed atmosphere (without oxygen) and the aerated atmosphere (oxygen concentration of 21v%). Packaging films made of polymer with different oxygen permeability such as of biaxially oriented polypropylene (BOPP) and polydimethyl siloxane (PDMS) were tested. The oxygen content in the enclosed atmosphere was evaluated by measuring the fluorescence emission of the optical sensor using a bifurcated optical fiber connected to the excitation source and the detector. The experiments showed the efficiency of the optical sensor in the on-line and non-invasive monitoring of the oxygen permeated trough the packaging materials. As expected, the increase of the oxygen concentration is more pronounced in the MAP sealed with PDMS than BOPP due to its oxygen permeability one order of magnitude higher. Moreover, the results were confirmed by the solution-diffusion model which predicted the rate of permeation of oxygen trough the packaging material considering its oxygen permeability evaluated with an independent method. This work was carried out at the Universidade Nova de Lisboa and submitted to Journal of Food Engineering.

The second part of this work was devoted to the development of a system based on Ru(phen)$_3$ useful for the monitoring of temperature. The molecular probe was immobilized in silica nano-particles prepared following the Stöber method. The encapsulation in silica allows the protection of the luminophore from other environmental variables. However the injection of the luminophore in the precursor of the colloidal solution dramatically affects the mono-dispersivity of the nano-particles due to steric affects. On the other hand, the growth of a shell made of silica doped with the luminophore on mono-dispersed silica nano-particle allowed the preparation of mono-disperse nano-particles. The produced nano-particles showed high temperature sensitivity phosphorescence ascribable to Ru(phen)$_3$. Furthermore the chemical and physical properties of the nano-particles are tuneable in terms of diameter by the concentration of the silica precursor, phosphorescence activity and temperature sensitivity by the concentration of the probe and easy to be functionalized turning from hydrophilic to hydrophobic their character. The immobilization of the developed nano-thermometer on the surface of porous hydrophobic membrane by dip-coating was proposed as an innovative technology which enables the monitoring of temperature on membrane surface. The work was

developed at the Universidad de Zaragoza and submitted to Journal of Colloids and Interface Science.

Once again, Ru(phen)$_3$ was selected as molecular probe and immobilized into/onto hydrophobic porous membrane made of Poly(vinylidene fluoride). The membranes prepared using electrospinning present excellent performance in direct contact membrane distillation process because of their open pore morphology made of a 3D network of nano-fibers. The membranes presented luminescent activity due to the immobilized molecular probe which enables the mapping of temperature on membrane surface and the evaluation of the thermal polarization. A paper is in preparation to be submitted to Journal of Membrane Science.

The studies presented in this thesis provide an important advance in studying membrane processes and may be further applied to deep understanding mass-transport, evaluate the membrane performance and design operating conditions and membrane modules.

1.8 References

[1] Baker, R W. Overview of Membrane Science and Technology, in: *Membrane Technology and Applications.* Wiley, second edition, 2004.

[2] Figoli A, Santoro S, Galiano, F, and Basile, A. Pervaporation membranes: preparation and characterization, in: Vapour Permeation and Membrane Distillation Principles and Applications. Elsevier Woodhead Publishing, 2015.

[3] Uemura, T, and Henmi, M. Thin-Film Composite Membranes for Reverse Osmosis, in : *Advanced Membrane Technology and Applications*. Wiley, 2008.

[4] Koutsou, C P, Karabelas, AJ, and Kostoglou, M. Membrane desalination under constant water recovery – The effect of module design parameters on system performance. *Separation and Purification Technology*, 147: 90-113, 2015.

[5] Lau, M L, Ismail, A F, Misdan, N, and Kassim, M A. A recent progress in thin film composite membrane: A review. *Desalination,* 287: 190-199, 2012.

[6] Bastan, D, Esmaeili, N, and Asadollahi, M. Polymeric mixed matrix membranes containing zeolites as a filler for gas separation applications: A review. *Journal of Industrial and Engineering Chemistry,* 19(2): 375-393, 2013.

[7] Briscoe, W H. Polymers and Nanoscience, In: *Colloidal Foundations of Nanoscience*. Elsevier, 2014.

[8] Mohammad, A W, Teow, T Y, Ang, W F, Chung, Y T, Oatley-Radcliffe, D L, and Hilal, N. Nanofiltration membranes review: Recent advances and future prospects. *Desalination*, 356: 226-254, 2015.

[9] Ali A, Macedonio F, Drioli, E, Aljlil S, and Alharbi, A O. Experimental and theoretical evaluation of temperature polarization phenomenon in direct contact membrane distillation. *Chemical Engineering Research and Design,* 91(10): 1966-1977, 2013.

[10] Jogdand, A, and Chaudhuri, A. Modeling of concentration polarization and permeate flux variation in a roto-dynamic reverse osmosis filtration system. *Desalination,* 375: 54-70, 2015.

[11] She, Q, Wang, R, Fane, A G, and Tang, C Y. Membrane fouling in osmotically driven membrane processes: A review. *Journal of Membrane Science*, 499: 201-233, 2015.

[12] Abetz, V, Brinkmann, T, Dijkstra, M, Ebert, K, Fritsch, D, Ohlrogge, K, Paul, D, Peinemann, K-V, Nunes, SP, Scharnagl, N, and Schossig, M. Developments in Membrane Research: from Material via Process Design to Industrial Application. *Advanced Engineering Materials,* 5: 328-358, 2006.

[13] Nyström, M, and Mänttäri, M. Introduction: Opportunities and Challenges of Real Time Monitoring on Membrane Processes, in: *Monitoring and Visualizing Membrane-Based Processes*. Wiley, 2009.

[14] Belaissaoui, B, Le Moullec, Y, Hagi, H, and Favre, E. Energy efficiency of oxygen enriched air production technologies: Cryogeny vs membranes. *Separation and Purification Technology*, 125: 142-150, 2014.

[15] Banham, D, Ye, S, Pei, K, Ozaki, J-I, Kishimoto, T , and Imashiro, I. A review of the stability and durability of non-precious metal catalysts for the oxygen reduction reaction in proton exchange membrane fuel cells. *Journal of Power Sources*, 285: 334-348, 2015.

[16] Razavi, S M , and Miri, T. A real petroleum refinery wastewater treatment using hollow fiber membrane bioreactor (HF-MBR). *Journal of Water Process Engineering*, 8: 136-141, 2015.

[17] Tabesh, H, Amoabediny, Rasouli, A, Ramedani, A, Poorkhalil, A, Kashefi, A, and Mottaghy, K. Simulation of blood oxygenation in capillary membrane oxygenators using modified sulfite solution. *Biophysical Chemistry* 195: 8-15, 2014.

[18] Wisniewski, N, and Reichert, M. Methods for reducing biosensor membrane biofouling. *Colloids and Surfaces B: Biointerfaces*,18(3-4):197-219, 2000.

[19] Mills, A. Oxygen indicators and intelligent inks for packaging food. Chem. *Soc. Rev. 34*, 1003–1011, 2005.

[20] Murat S, Insel H C, Cokgor, E U, and Orhon, D. Effect of low dissolved oxygen on simultaneous nitrification and denitrification in a membrane bioreactor treating black water. *Bioresource Technology,* 102 : 4333-4340, 2011.

[21] Iulianelli A, Ribeirinha P, Mendes A, and Basile, A. Methanol steam reforming for hydrogen generation via conventional and membrane reactors: A review. *Renewable and Sustainable Energy Reviews,* 29: 355-368, 2014.

[22] Arévalo, J, Ruiz, L M, Pérez, J, and Gómez, M A. Effect of temperature on membrane bioreactor performance working with high hydraulic and sludge retention time. *Biochemical Engineering Journal*, 88: 42-49, 2014.

[23] Childs, P R N. Advances in temperature measurement. *Advances in Heat Transfer 36*: 111-181, 2003.

[24] Ramamoorthy, R, Dutta, P K, and Akbar, S A. Oxygen sensors: Materials, methods, designs and applications. *Journal of Materials Science* 38(21): 4271 – 4282, 2003.

[25] Gosse, C, Bergaud, C, and Löw, O. Molecular Probes for Thermometry in Microfluidic Devices, in: *Thermal Nanosystems and Nanomaterials, Topics in Advanced Physics* 118. Springer-Verlag, 2009.

[26] Grist M, Chrostowski L, and Cheung, KC. Optical oxygen sensors for applications in microfluidic cell. *Culture,* 10(10): 9286-9316, 2010.

[27] Chu C S, Lo, Y-L, and Sung, T-W. Review on Recent Developments of Fluorescent Oxygen and Carbon Dioxide Optical Fiber Sensors. *Photonic Sensors* 1(3): 234-250, 2011.

[28] Stich, M I J, Fischer, L H, and Wolfbeis, O S. Multiple fluorescent chemical sensing and imaging, *Chem. Soc. Rev.*, 39: 3102-3114, 2010.

[29] Quaranta, M, Borisov, SM, and Klimant, I. Indicators for optical oxygen sensors. *Bioanal Rev*, 4:115-157, 2012

[30] Amao, Y. Probes and Polymers for Optical Sensing of Oxygen. *Microchim. Acta,* 143(1): 1-12, 2003.

[31] Brites, C D S, Lima, P P, Silva, N J O, Angel, M, Amaral, V S, Palacio, F, and Carlos, L D. Thermometry at the nanoscale. *Nanoscale,* 4: 4799-4829, 2012.

[32] Sharma, A, and Wolfbeis, O S. Fiber optic Oxygen Sensor Based on Fluorescence Quenching and Energy Transfer. *Applied Spectroscopy,* 42(6): 1009-1011, 1988.

[33] Fujiwara, Y, Ishikawa, Y, and Amao, Y. *Nippon Kagaku Kaishi*, 2002.

[34] Lee, S-K, and Okura, I. Photoluminescent determination of oxygen using metalloporphyrin-polymer sensing systems. *Spectrochimica Acta Part A,* 54(12): 91-100, 1998.

[35] Amao, Y, Miyashita, T, and Okura. Optical oxygen sensing based on the luminescence change of metalloporphyrins immobilized in styrene-pentafuorostyrene copolymer film. *Analyst,*125(5): 871-875, 2000.

[36] Hartmann, P, and Trettnak, W. Effects of polymer matrices on calibration functions of luminescent oxygen sensors based on porphyrin ketone complexes. *Anal Chem.*, 68: 2615-2620, 1996.

[37] Chu, C-S. and Lo, Y-L. Optical fiber dissolved oxygen sensor based on Pt(II) complex and core-shell silica nanoparticles incorporated with sol–gel matrix. *Sensors and Actuators B,* 151(1): 83-89, 2010.

[38] Amao, Y, Ishikawa, Y, and Okura, I. Optical Oxygen Sensing Material: Terbium(III) Complex Adsorbed Thin Film. *Bull Chem Soc Jpn*, 74: 2445-2449, 2001.

[39] Xu, W, Kneas, K A, Demas, J N, and DeGraff, B A. Oxygen sensors based on luminescence quenching of metal complexes: Osmium complexes suitable for laser diode excitation. *Anal. Chem*, 68(15): 2605-2609, 1996.

[40] Carraway, E R, Demas, J N, and DeGraff, B A. Luminescence quenching mechanism for microheterogeneous systems. *Anal. Chem.*, 63(4): 332-336, 1991.

[41] Amao, Y, and Okura, I. Optical oxygen sensing materials: chemisorption film of ruthenium(II) polypyridyl complexes attached to anionic polymer. *Sensors and Actuators B*, 88(2): 162-167, 2003.

[42] Bergman, I. Rapid-response Atmospheric Oxygen Monitor based on Fluorescence Quenching. *Nature,* 218: 396, 1968.

[43] Basu, B J, Thirumurugan, A, Dinesh, A R, Anandan, C, and Rajam, K. Optical oxygen sensor coating based on the fluorescence quenching of a new pyrene derivative. *Sensors and Actuators B*, 104(1): 15-22, 2005.

[44] Papkovsky, P B, Olah, J, Troyanovsky, I V, Sadovsky, N A, Rumyantseva, V D, Mironov, F A, Yaropolov, A I, and Savitsky, A P. Phosphorescent polymer films for optical oxygen sensors. *Biosens. Bioelectron.* 7: 199-206, 1992..

[45] Puklin, E, Carlson, B, Gouin, S, Costin, C, Green, E, Ponomarev, S, Tanji, H, Gouterman, M, 2000, Ideality of pressure-sensitive paint. I. Platinum tetra(pentafluorophenyl)porphine in fluoroacrylic polymer. *J. ApplPolym. Sci.,* 77(3): 2795-2804

[46] Gillanders, R N, Tedford, M C, ,Crilly P J, and Bailey, R T. A composite thin film optical sensor for dissolved oxygen in contaminated aqueous environments. *Anal. Chem. Acta,* 545(2): 189-194, 2005.

[47] Wang, Z, McWilliams, A R, Evans, C E B, Lu, X, Chung, S, Winnik, M A, and Manners, I. Covalent attachment of RuIIphenanthroline complexes to polythionylphosphazenes: the development and evaluation of single-component polymeric oxygen sensors. *Adv. Funct. Mater.,* 12(6-7): 415-419, 2002.

[48] Wang, X-D, Wolfbeis, O S, and Meier, R J. Luminescent probes and sensors for temperature. *Chem. Soc. Rev.,*42(19): 7834-7869, 2012.

[49] Ross, D, Gaitan, M, and Locascio, L E. Temperature measurement in microfluidic systems using a temperature-dependent fluorescent dye. *Anal. Chem.,* 73(17): 4117-4123, 2001.

[50] Guan X, and Su, Z. Synthesis and characterization of fluorescent starch using fluorescein as fluorophore: potential polymeric temperature/pH indicators. *Polym. Adv. Technol.,* 19(5): 385-392, 2008.

[51] Baleizao, C, Nagl, S, Schäferling, M, Berberan-Santos, M N, and Wolfbeis, O S. Dual Fluorescence Sensor for Trace Oxygen and Temperature with Unmatched Range and Sensitivity. *Anal. Chem.,* 80(16): 6449-6457, 2008.

[52] Mills, A, Tommons, C, Bailey, R T, Tedford, M C, Crilly, P J. Luminescence temperature sensing using poly(vinyl alcohol)-encapsulated $Ru(bpy)_3^{2+}$ films. *Analyst*, 131(4): 495-500, 2006.

[53] Stehr, J, Lupton, J M, Reufer, M, Raschke, G, Klar, T A, and Feldmann, J. Sub-Microsecond Molecular Thermometry Using Thermal Spin Flips. *Adv. Mater.,* 16(23-24): 2170-2174, 2004.

[54] Basu, B J, and Venkatraman, S. Fabrication of a Bi-luminophore Temperature Sensitive Coating by Embedding Europium Thenoyltrifluoroacetonate (EuTTA) and Perylene in Polystyrene. *J. Fluorescence,* 19(3): 479-485, 2009.

Chapter 2

Development of Oxygen and Temperature Sensitive Membranes Using Molecular Probes as Ratiometric Sensor

2.1 Introduction

Membrane processes are governed by the physical-chemical interactions between the boundary layer of the solutions in contact with the membranes and the membrane surfaces [1]. Efforts in membrane science have been devoted on the development of innovative materials and optimization of the operating conditions in order to maximize the selective permeant-membrane interactions increasing the performance of the process in terms of productivity, selectivity and stability [1]. Moreover, it is notorious that these interactions dynamically change on membrane surface due to variations of the operating conditions and membrane properties related to phenomena such as the as concentration and/or thermal polarization, fouling, swelling and membrane deterioration [1-6].

Nowadays, employing common analytic technologies it is possible monitoring the global performance of the process estimating the permeability and the selectivity of the membrane and to evaluate the long-term stability of the separation processes. However, they lack in providing on-line information for studying parameters of interest at low scale and understanding the phenomena which affect the global processes at large scale. In fact, the optimal monitoring processes would be in real time, non-invasive, in situ, at a molecular scale and using pattern recognition approaches [7].

Optical sensors, based on the immobilization of luminescent molecular probes in/onto polymeric matrices, are an attractive technology for non-invasive monitoring, allowing to obtain highly sensitive devices for continuous detection of temperature changes and/or oxygen content in a given medium [8]. The molecular size of probes consents the on-line detection with a high resolution, also at micrometric and sub-micrometric scale using adequate technology (i.e. fluorescent microscopy) [9-10]. Further advantages are related to the fact that the activation stimuli and the responses of the optical sensors consist of light, allowing for the development of non-invasive sensors with a short response time [11]. For these reasons, molecular probes could be considered a promising technology for on-line, non-invasive and high resolution monitoring of membrane process.

Oxygen (O_2) and temperature (T) are two fundamental parameters affecting every chemical and biological process, included membrane processes. Nowadays, electrochemical sensors such as thermocouple for the monitoring of the temperature and Clark electrode for the detection of the oxygen levels (yO_2) are used as accurate and inexpensive technologies with a rapid response time [11-13]. However, the miniaturization of the sensors is the most critical issue of these technologies that are unable to monitor the parameters of interest with a high spatial resolution at micron and submicron scale, typically demanded in innovative research fields [13-17]. On the other hand, these parameters have been successful detected employing molecular probes which provided crucial information for the studying and understanding of many phenomena of scientific interest in different areas (i.e. chemistry, medicine, biology, environment, aerospace) and the monitoring of industrial processes in several fields (i.e. bioprocess, food packaging, automotive, clinical diagnostic) [17-22]. The aim of this work is the development of oxygen and temperature sensitive membranes based on the dispersion of molecular probes in polymeric matrices useful for a non invasive, on line and at submicron scale monitoring of oxygen and temperature in membrane processes.

The identification of the most adequate materials and the optimization of the procedure for the preparation of the optical sensors are crucial for the development of the optical sensor.

The sensitivity of the device strongly depends on the properties of polymer, in particular its oxygen permeability [23]. In general, polymers with high oxygen permeability, such as poly(dimethylsiloxane) (PDMS), are employed for the development of the optical sensor in order to guarantee interactions between the permeating target molecules (O_2) and the immobilized molecular probes. However, they lack in mechanical properties and thus a rigid support is often required [24].On the contrary, glassy polymers such as polystyrene (PS) present lower, but reasonable, oxygen permeability and good mechanical properties which allow the preparation of self-consistent films, improving their versatility [25].

Nevertheless, the core of the optical sensor is the molecular probe. In the last decades, efforts have been made towards the development of luminescent probes with high sensitivity to oxygen and long stability [26-29].

Luminescent transition metal polypyridyl complexes present unmatched photostability, and have been largely used in the preparation of optical sensors. In particular, Ru(II) polypyridyl complexes have been employed more frequently since they are rather easy to synthesize. Disadvantages are related to the relatively short excited state lifetime, with respect to metallorphines, that limits their sensitivity. Also, they suffer from pronounced cross talk to temperature since their triplet states are subjected to severe thermal quenching [30]. In fact, it is well known for optical sensors based on fluorescence (or phosphorescence) quenching that both the emission intensity and the excited state life time are affected by the temperature [30-32].

The higher limitations for practical applications, common to all optical sensors based on the fluorescence/phosphorescence emission intensity detection, are related to the strong impact that operating conditions (geometry of the detection, optical path, fluctuations of the excitation source, probe concentration, etc.) produce in the intensity of the signals measured.

A strategy to overcome these drawbacks is the simultaneous use of two luminescent probes (dispersed in the same polymeric matrix) and the combination of their emission intensities in a ratiometric signal which allows for the correction of errors produced by unknown fluctuations of the operative conditions [33-35].

Tris(1,10-phenanthroline)ruthenium(II) (Ru(phen)$_3$), a luminescent transition metal polypyridyl complex, was used as oxygen sensitive probe in order to ensure long life-time to the sensor. The performance of polystyrene (PS) and poly(β-hydroxybutyrate-β-hydroxyvalerate) (PHBV) as sensor matrix was evaluated. The design of Ru(phen)$_3$ based ratiometric sensors involved the use of a second fluorescent probe non-sensitive to oxygen as a reference for correcting artifacts induced by optical path drifts and fluctuations of the intensity of the exciting light. At this respect, the monitoring efficiency of 7-Methoxy-4-methylcoumarin (Coumarin), Dansyl Chloride and Quinine Sulfate were evaluated.

Finally, in order to overcome the vulnerability of the ratiometric signal to the temperature, a correction model was implemented to compensate temperature drifts along the monitoring of O_2 concentration.

2.2 Materials and Methods

2.2.1 Materials

Polystyrene (PS, Mw: 192,000) was purchased from Sigma Aldrich Chemistry (Spain), whereas Poly(3-hydroxybutyrate-co-3-hydroxyvalerate)(PHBV, Mw: 300,000) containing 3 mol% of 3-hydroxyvalerate units was obtained from Tianan Biologic Material Co. Ltd. (China). Tris(1,10-phenanthroline)ruthenium(II) (Ru(phen)$_3$) was synthesized according to the procedure reported in literature [36]. The other molecular probes 7-methoxy-4-methylcoumarin (Coumarin), Dansyl Chloride and Quininehemisulfate salt monohydrate (Quinine Sulfate) and the solvent (Chloroform) were purchased from Sigma Aldrich Chemistry (Spain).

The chemical structures of the polymers and of the probes employed are represented in Figure 2.1.
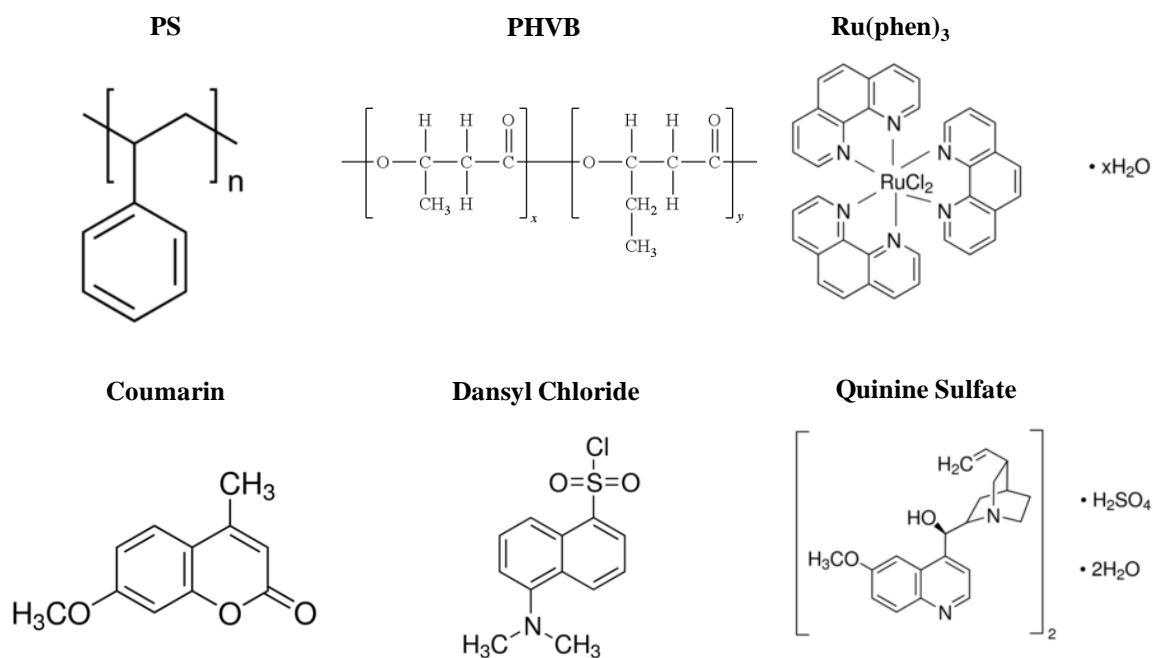
Figure 2.1: Membrane separation: Chemical structures of polymers and molecular probes employed in the development of oxygen and temperature sensitive membranes.

2.2.2 Methods

2.2.2.1 Fluorescence measurements

Fluorescence measurements were performed on a Horiba-Jobin-Yvon SPEX Fluorolog 3.22 spectrofluorimeter equipped with a 450 W Xe lamp. All spectra were collected with 5 nm slit bandwidth for excitation and emission and corrected.

Preliminary tests for the selection of the materials and evaluation of the response of the membranes to oxygen level were performed using a cuvette (10 mm optical path) with a cup presenting an inlet and an outlet for degassing the atmosphere by feeding Argon. The optical sensor was placed on the surface of a triangular prism made of porous glass in order to establish an angle of 45º between excitation and emission light while allowing for non-hindered gas transport to the polymeric membrane (Figure 2.2).
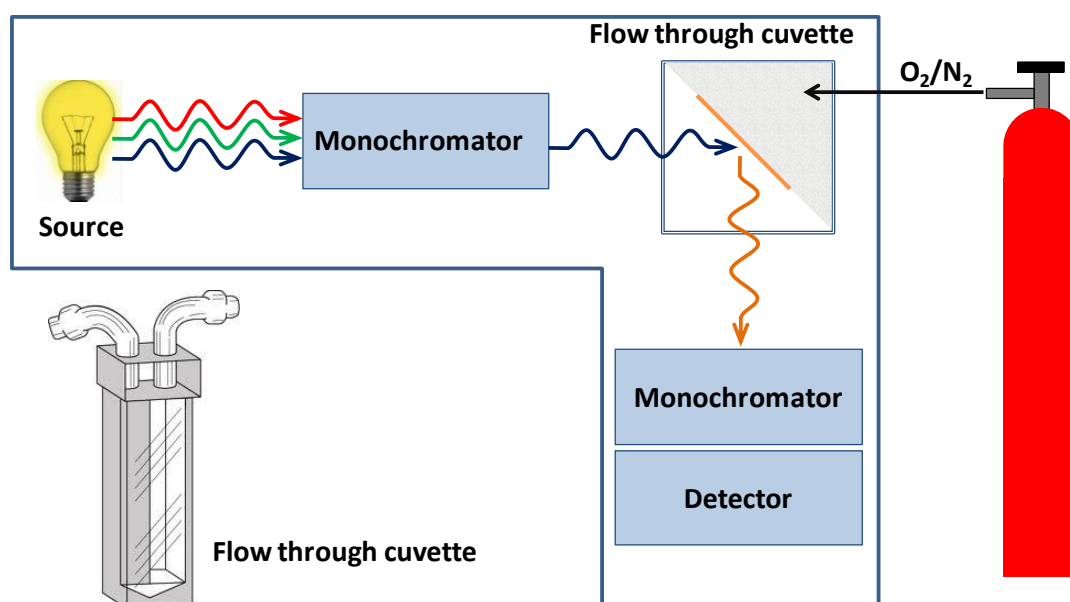
Figure 2.2: Scheme of the spectrofluorimeter and cuvette used for preliminary experiments.

The sensitivity of the membranes based on the two-probe system to the oxygen concentration and temperature was evaluated using the scheme represented in Figure 2.3. The sample was placed on a porous support in a steel cell employed for membrane processes with a quartz window which allows to excite the sensor and to collect its emission using the bifurcated optical fiber bundle connected to the spectrofluorometer. Mixtures of oxygen/nitrogen with different oxygen concentrations (0%, 10%, 21%, 50% and 100% v/v) purchased from Praxair (Spain) were fed to the cell and, subsequently, it was sealed using the two valves shown in Figure 2.3. The pressure of the cell during the experiments was kept at 1 atm. The area of the sample was 1 cm^2. The distance between the optical fiber and the

sample was 1.5 cm. The chamber was kept at a constant temperature which was varied from 25°C to 50°C to study the effect of temperature.

The absorption spectra of the molecular probes dissolved in chloroform were also recorded in a Shimadzu UV2501PC spectrophotometer, using a quartz cuvette with a 10 mm path length at 21°C.
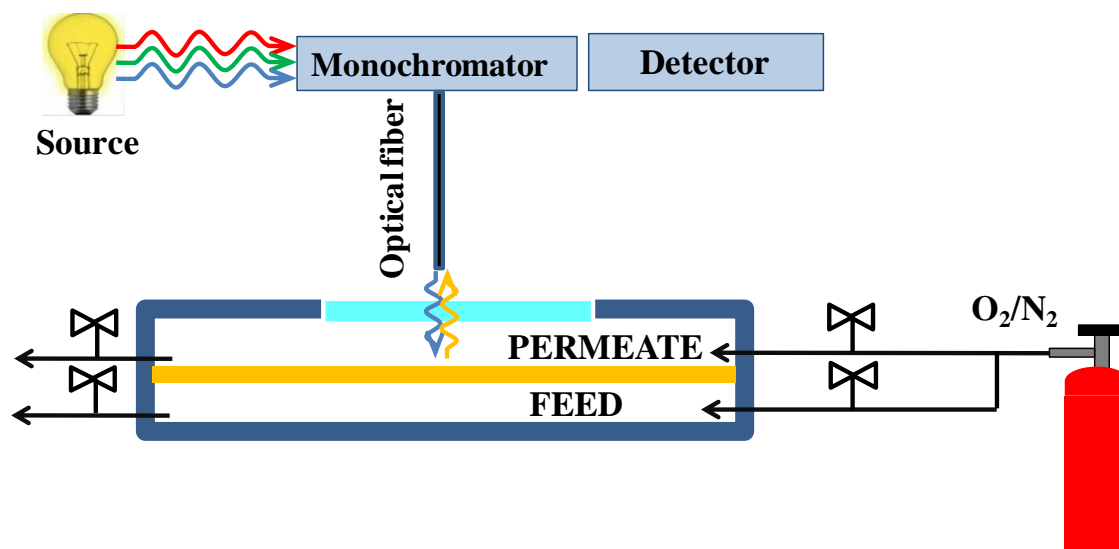
Figure 2.3: Scheme of experiments for the evaluation of the oxygen and temperature sensitivity.

2.2.2.2 Oxygen and temperature sensitive membrane preparation

In this work, the membranes were prepared by dry-casting a dope solution of polystyrene (PS) solubilized in 10 ml of chloroform (25 w/v %). After the solubilization of the polymer in the solvent by stirring the solution at 30°C overnight, 1ml of chloroform containing the probe (ranging from 10^{-3} M to 10^{-5} M) was injected in the polymeric solution. The amount of the oxygen sensitive probes with respect to the polymer was varied from 8×10^{-7} mol g^{-1} to 8×10^{-9} mol g^{-1}. In the case of the two dye systems, a second injection of 1 ml of chloroform containing the reference (Coumarin, Quinine Sulfate or Dansyl Chloride) was also performed. The concentration of the reference was equal to the concentration of the oxygen sensitive luminescent probe; except for Dansyl Chloride that was one order of magnitude higher.

In order to assure a homogeneous dispersion of the probes through the polymer matrix, the dope solution was stirred for 2 hours and sonicated for 1 hour. Then, the polymeric solution was cast using a casting knife with thickness of 0.75 mm. After evaporation of the solvent at room temperature (ca. 48 hours), the prepared membranes were placed in an oven at 65°C over night in order to favor the removal of solvent traces, generating membranes with thicknesses of 144±3 μm.

The procedure for the preparation of the PHVB membranes was similar to the one employed previously, except the solubilization of the pellets of polymer in chloroform was facilitated by heating the polymeric solution at 60ºC for 90 min.

2.2.2.3 Characterization of the membranes with the ratiometric sensor

The membrane's morphology was observed by using a scanning electron microscope (Quanta FEG 250). Membranes cross sections were prepared by freeze fracturing the samples in liquid nitrogen, to produce a clean brittle fracture. Thermogravimetric analyses were performed using a Mettler Toledo TGA/SDTA 851e equipment.

Gas permeation experiments were performed on a fixed volume/pressure increase instrument [37], constructed by GKSS (Geesthacht, Germany) for the evaluation of the diffusion coefficient, solubility and permeability of gases through the PS membrane and with the ratiometric sensor. The gases tested were: N_2, O_2, and CO_2 at constant temperature of 25 ± 1 °C.

2.3 Results and Discussion

2.3.1 Oxygen sensitive membrane

$Ru(phen)_3$, known as a phosphorescent molecule with long lived luminescence and good oxygen sensitivity [24] was tested as potential oxygen sensitive probe in the preparation of the oxygen sensitive membranes at a concentration of $8x10^{-7}$ mol g^{-1} in PS. The emission spectra of the probe immobilized in PS in degassed (0% oxygen) and aerated (21% oxygen) conditions, together with the background emission spectrum of bare PS, are reported in Figure 2.4. The emission was collected exciting the membrane at the maximum of absorption of the Ruthenium complex in PS (459 nm). $Ru(phen)_3$ showed its maximum emission at 589 nm and it is clearly distinguishable from the background luminescence of PS.

As reported in Figure 2.4, the intensity of the emission of $Ru(phen)_3$ increased 20% as a consequence of the decrease of the oxygen concentration from 21% to 0% (v/v).

On the basis of this result, upon incorporation on PS, $Ru(phen)_3$ can be considered a robust probe for oxygen detection under ambient conditions, exhibiting reproducible response and high emission intensity.
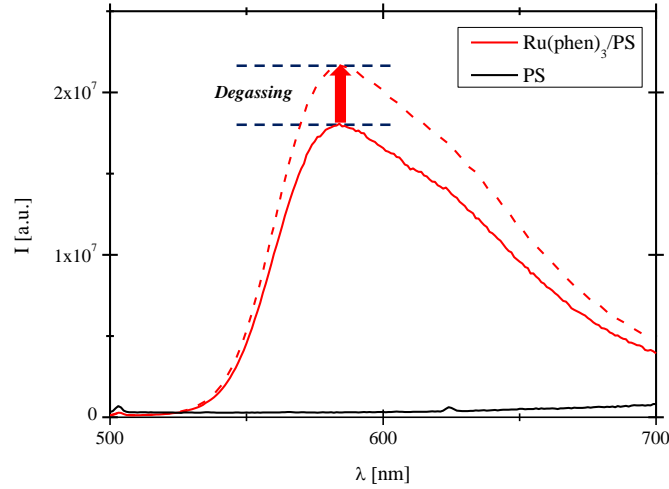
Figure 2.4: Effect of the oxygen concentration on the emission spectra of Ru(phen)₃(b) immobilized in PS films (T=21°C, probe concentration 8x10⁻⁷mol g⁻¹). Experiments were performed using the set-up reported in Figure 2.2.

2.3.2 Development of an oxygen sensor based on ruthenium

Ruthenium based optical sensors were developed using different probe concentrations and different polymeric matrices. Figure 2.5.a reports the effect of the concentration of $Ru(phen)_3$ on the polymeric membrane emission intensities.

The intensity of the peak at 589 nm increased by increasing the amount of $Ru(phen)_3$, as predicted by the equation:

$$I = kI_{exc}\Phi[\varepsilon bc] \qquad (2.1)$$

where k is a parameter related to excitation/detection geometry, I_{exc} is the intensity of the exciting light, Φ is the quantum yield, ε and c are respectively the molar extinction coefficient and the concentration of the luminophore and b is the optical path.

By looking at Figure 2.5.b it is possible to observe that the ratio of the emission intensity of $Ru(phen)_3$ in the absence of oxygen (I_0) and the emission intensity at different oxygen concentrations (I) increases linearly according to the well-known Stern-Volmer linear equation:

$$\frac{I_0}{I} = 1 + K_{SV}[O_2] \qquad (2.2)$$

A slight increase in sensitivity was observed upon increasing $Ru(phen)_3$ concentration in the membrane, which is probably due to the increase of the signal-to-noise ratio at higher concentrations. Nevertheless, this improvement in sensitivity can be considered within the error of the system, since

an 100-fold increase in probe concentration sensitivity resulted in approximately 1.5-fold increase in sensitivity.

a)   b)
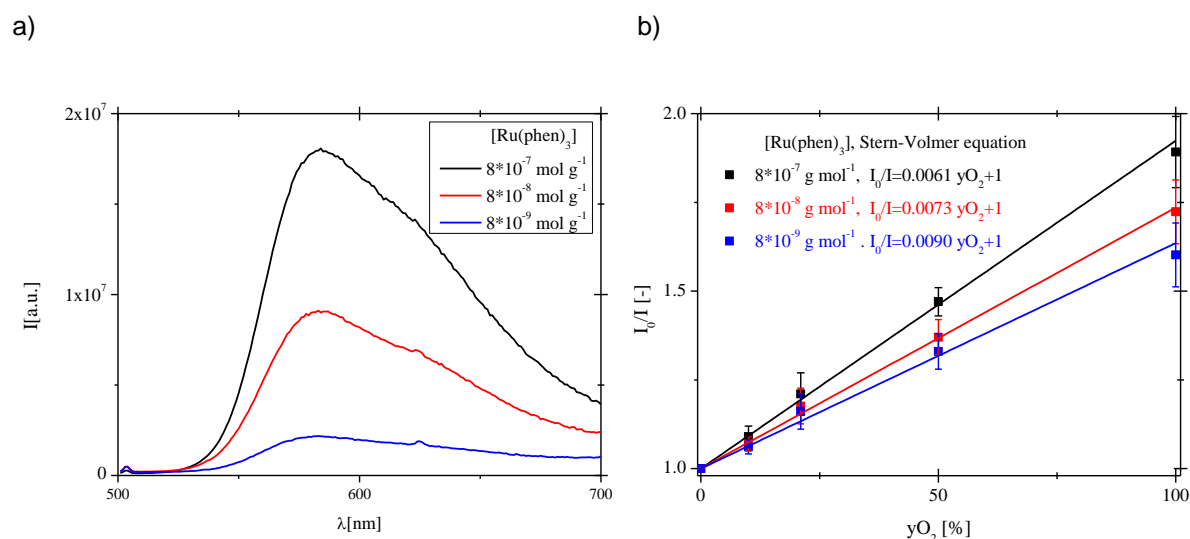
Figure 2.5: Effect of the concentration of Ru(phen)₃ on the absolute intensity of the emission (a) and on the Stern-Volmer plot (b) (T=21°C). Experiments were performed using the set-up reported in Figure 2.2.

The sensitivity of optical sensors can be tuned by adjustment of the polymer matrix oxygen permeability. Thus, the sensitivity to oxygen of the probe dispersed in two different polymeric matrixes with different oxygen permeability coefficients was evaluated: PS, which combines a reasonable oxygen permeability with good mechanical properties consenting to prepare a self-consistent device, whereas PHBV, a biopolymer of low environmental impact and lower oxygen permeability [37-38].The amount of the probe dispersed in both polymeric matrixes was 8×10^{-7} mol g^{-1}.

By looking at Figure 2.6, it is possible to notice that the sensitivity of the sensor prepared using PS is higher than that observed for the probe dispersed in PHVB, due to the higher oxygen permeability of PS. In fact, the sensitivity of optical sensor increases by increasing the oxygen permeability of the matrix containing the molecular probe, as predicted by the equation:

$$\frac{I_0}{I} = 1 + \frac{4\alpha\pi N_A \sigma}{1000}\tau_0 P(O_2)p(O_2) \qquad (2.3)$$

where N_A is Avogadro's number, σ is the collision radius of the oxygen-dye complex, τ_0 is lifetime of the excited state in absence of oxygen, $p(O_2)$ is the oxygen partial pressure and $P(O_2)$ is the oxygen permeability in the polymer which is 0.34 barrer for PHVB and 3.6 barrer in the case of PS [37-38].
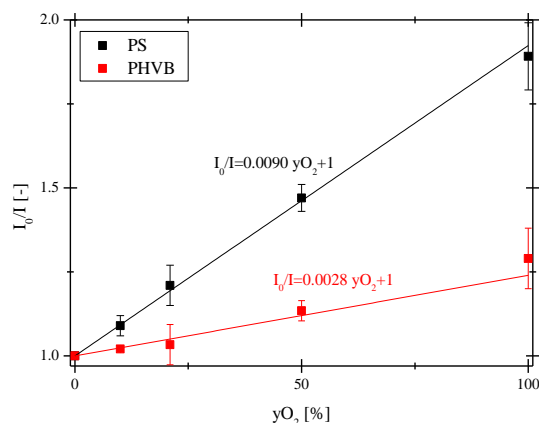
Figure 2.6: Stern-Volmer plots obtained for membranes prepared with PS and PHVB (T=21°C, probe concentration 8x10⁻⁷mol g⁻¹). Experiments were performed using the set-up reported in Figure 2.3.

2.3.3 Development of a ratiometric sensor based on ruthenium

The disadvantage on the use of Ru(phen)$_3$ as molecular probe for oxygen monitoring is its single emission band because of the emission multi-parameter dependence (i.e. oxygen level, optical path, chromophore concentration, intensity of excitation light, temperature) limiting the robustness of the oxygen detection is strongly reduced with single emissive sensors.

To overcome this limitation a second fluorescent molecule (reference) non-sensitive to oxygen was added to the membranes in order to develop a ratiometric sensor. Using this additional probe it is expected to improve the robustness of the measurements by discrimination of the emission changes exclusively attributable to O$_2$ concentration differences. The ideal reference probe is required to have a well discernible emission from Ru(phen)$_3$ and low sensitivity to oxygen. Three different fluorophores complying with the mentioned requisites were evaluated: Quinine Sulfate, Dansyl Chloride and Coumarin.

The absorbance, excitation and emission spectra obtained for the different probes at a concentration of 10 µM in chloroform solutions are reported in Figure 2.7. The analysis of these spectra revealed that:

(i) the emission of Ru(phen)$_3$ results red-shifted with respect to the emission of all the tested references. Ruthenium complex presents an absorption band centered at 453 nm, but also absorption in the UV range that can be used to simultaneously excite the sensor and the reference;

(ii) Coumarin and Quinine both show absorptions in the 300-400 nm region, and emissions well distinguishable from Ruthenium. Coumarin showed the highest emission intensity;

(iii) the emission of Dansyl Chloride is very low compared with the other probes at the same conditions.
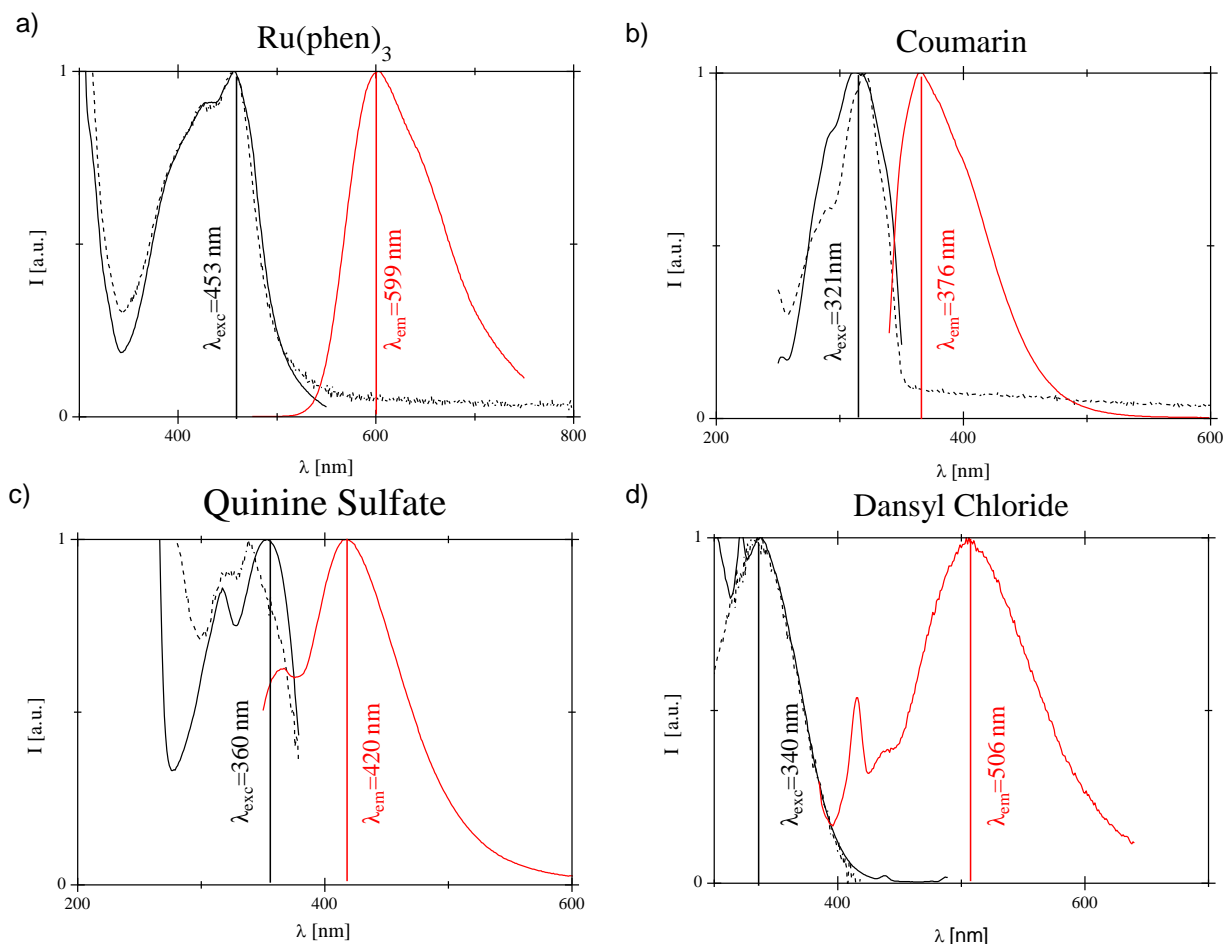
Figure 2.7: Normalized spectra of Absorbance (black dashed), excitation (black solid) and emission (red solid) of solution of Chloroform containing 10 µM at 21°C of Ru(phen)₃ (a), Coumarin (b), Quinine Sulfate (c) and Dansyl Chloride (d).

In order to develop the two probe system, membranes containing equimolar amounts of the oxygen sensitive probe (Ru(phen)$_3$) and the reference equal to 8×10^{-7} mol g^{-1} were prepared. In the case of Dansyl Chloride, the concentration has been increased to 8×10^{-6} mol g^{-1} because of its lower quantum yield. Because of the high absorption of Ru(phen)$_3$ in the UV-region, the films have been excited at the maximum of absorption of the reference probes in PS, i.e. 326 nm for Coumarin, 308 nm for Quinine Sulfate and 330 nm for Dansyl Chloride. The effect of removing oxygen in the dual emissions of PS films is reported in Figure 2.8.
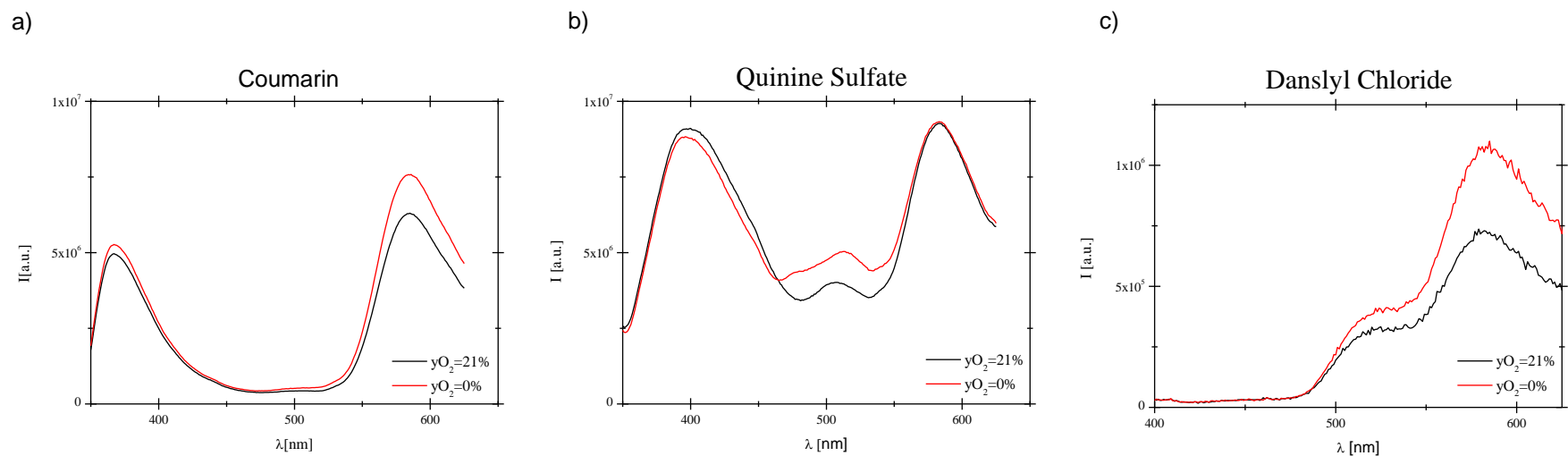
Figure 2.8: Emissions of membranes containing the oxygen sensitive probe (8×10^{-7} mol g^{-1}, λ_{max}=589nm) and different reference compounds: (a) Coumarin (8×10^{-7} mol g^{-1}, λ_{max}=363nm), (b) Quinine Sulfate (8×10^{-7} mol g^{-1}, λ_{max}=403nm), (c) Dansyl Chloride (8×10^{-6} mol g^{-1}, λ_{max}=506nm). Experiments were performed at T=21°C using the set-up reported in Figure 2.2.

The membrane prepared with Coumarin as reference presented two perfectly discernible bands: the emission of Coumarin at 363 nm and the emission of Ru(phen)$_3$ at 589 nm. The emission of Coumarin was not significantly dependent on oxygen concentration; whereas those ascribed to Ru(phen)$_3$ increased by decreasing the oxygen level (Figure 2.8.a).

Membrane prepared using Quinine Sulfate as reference was non-sensitive to the oxygen concentration (Figure 2.8.b). In fact the emissions of Ru(phen)$_3$ at 589 nm did not varied by removing the oxygen from the cuvette. This effect could be due to the formation of dimmers between the complex of Ruthenium (positively charged) and Quinine Sulfate (negatively charged).

The emission of Dansyl Chloride overlapped the emission of the oxygen sensitive probe. (Figure 2.8.c). This overlap, combined with the low emission intensity of Dansyl Chloride, makes the Dansyl Chloride region of emission quite sensitive to changes in ruthenium emission. In fact, the intensity of Dansyl Chloride increased upon oxygen removal, limiting its employment as a reference.

Table 2.1 : Comparison of the emissive properties of the ratiometric sensors made of Ps doped with the reference probe and Ru(phen)$_3$: wavelength of emission (λ); intensities of emission in aerated condition (I_{21}); ratio of emission intensities of reference over Ruthenium complex (R_{21}) at atmospheric pressure; sensitivity of the intensity of the reference (I_0/I_{21}); sensitiviy of the ratiometric response (R_0/R_{21}) to oxygen removal.

Reference Probe	λ[nm]	I_{21} [10^6 a.u.]	I_0/I_{21}	R_{21}	R_0/R_{21}
Coumarin	363	8.4	1.02	1.38	1.24
Quinine Sulfate	403	9.1	0.97	1.01	1.03
Dansyl Chloride	506	2.7	1.28	0.35	1.17

On the basis of its high emission, non-sensitivity to oxygen concentration and non-overlap of emission bands, Coumarin was selected as reference for the development of the dual probe system sensor for the monitoring of oxygen concentration.

2.3.4 Oxygen sensitivity of the two probe system fluorescent membrane

The sensitivities of PS membrane containing an equimolar amount of Coumarin and Ru(phen)$_3$ were tested using the scheme reported in Figure 2.3. The oxygen concentration in the cell was varied from 0% to 100%. Experiments were performed using 2 different samples in order to evaluate the reproducibility of the response. The results obtained are summarized in Figure 2.9.

The emission of Coumarin, considering the experimental error, is non-dependent on the oxygen concentration, whereas the behaviour of Ru(phen)$_3$ is predicted by the Stern-Volmer equation.

The high experimental errors and the low value of the correlation factor (0.922) are a clear evidence of the expectable ineffective employment of a sensor using the emission of a single probe. This limitation is due to low reproducibility in the operative conditions and, in particular, to the slight changes of geometry of the experiments using the optical fibre. However, the ratio of the emissions of the two probes:

$$R = I_{Coumarin}/I_{Ru(phen)_3}; \quad (2.4)$$

not only shows the same linear increase with oxygen concentration, but also the correlation factor becomes higher than 0.99.The error becomes of around 1%, due to the cancelation of errors resulting from the ratio of signals.

a)   b)
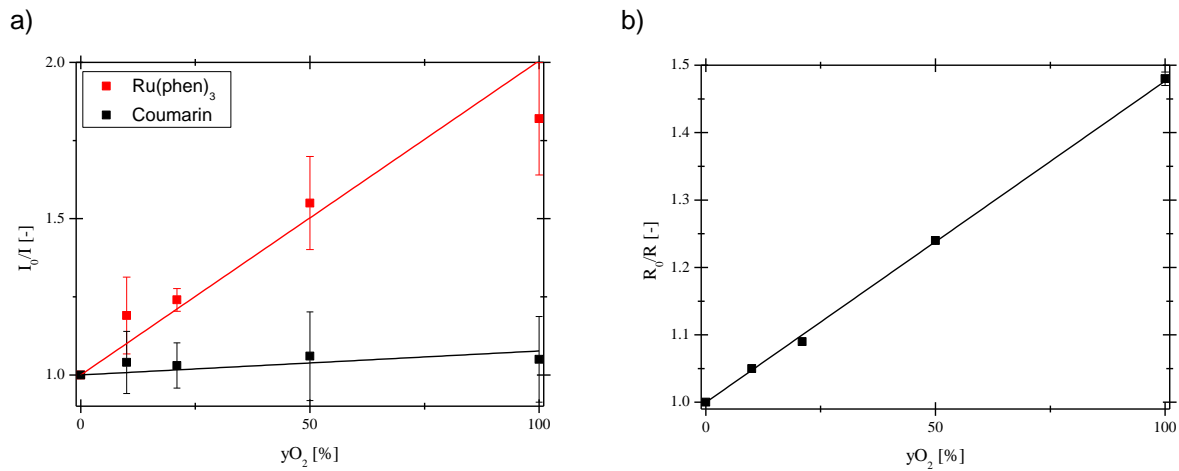
Figure 2.9: Oxygen sensitivity at T=21°C of (a) the intensities of emission of Ru(phen)$_3$ and Coumarin in PS and (b) the ratiometric signal. Experiments were performed using the set-up reported in Figure 2.3.

That is, the ratiometric signal is much more robust than the single emission of the Ruthenium complex, being independent from the optical path and the excitation light intensity. In fact, combining Eqs 2.1 and 2.4, and considering that the PS membranes contain an equimolar amount of the two probes, the ratio of the probes' intensities

$$R = (\Phi\varepsilon)_{Coumarin}/(\Phi\varepsilon)_{Ru(phen)_3}, \quad (2.5)$$

depends only on their photophysical properties, i.e. extinction coefficients (ε) and the quantum yield (Φ), that is affected by the oxygen content following the Stern-Volmer equation.

Since the Coumarin is non-sensitive to the oxygen, we can assume that the linear response of the ratiometric response to the oxygen level is the Stern-Volmer constant which expresses the dynamic quenching of ruthenium complex. Furthermore, transition-metal complexes, in particular immobilized in silicone rubber, often do not exhibit perfectly linear Stern-Volmer calibration plots due to the presence of micro heterogeneities within the polymer, leading to downward curvature of the trend [40]. In this case, the linearity of the trend in the whole range of oxygen concentration

(from 0% to 100%) is an evidence of the sensor structural and chemical homogeneity. This was confirmed by characterizing the doped PS membrane with molecular probes in comparison with the bare PS membrane. SEM analyses showed that the morphology and the thickness of the optical sensor are not affected by the addition of the molecular probes. In fact, PS membrane containing $Ru(phen)_3$ and Coumarin presents a symmetric dense morphology comparable with that one observed in the membrane of bare PS (see Annex I). Furthermore, the amount of the probes is so low that it was not possible to detect the presence of atomic Ruthenium by analysis of energy-dispersive X-ray microanalysis (EDS).

Table 2.2: Permeability, diffusion coefficient and solubility of different gases in the membranes of PS and PS doped with $Ru(phen)_3$ and Coumarin. $[Probe]=8x10^{-7}$ mol g^{-1}.

	PS			Doped PS		
Gases	O_2	N_2	CO_2	O_2	N_2	CO_2
P [barrer]	2.34±0.12	0.35±0.02	13.09±0.65	2.47±0.12	0.42±0.02	12.24±0.61
D [10^{-12} m^2 s^{-1}]	12.05±0.63	4.08±0.21	5.26±0.26	10.02±0.51	3.57±0.18	4.14±0.21
S [cm^3(STP) cm^{-3} bar^{-1}]	0.15±0.01	0.06±0.01	1.87±0.09	0.19±0.01	0.09±0.01	2.22±0.11

The thermogravimetric analysis (TGA) shows that doped PS presents and the pure polymer are identically stable (Annex II). In fact, in both cases, the degradation occurs in the range of 350°C-420C° and the melt point was evaluated at 398°C.

Regarding the permeability measurements, PS is a glassy polymer with moderate gas permeability. The most permeable specie is carbon dioxide, whereas O_2 showed a moderate permeability due to the combination of a high diffusion and low solubility. The immobilization of the molecular probes in the polymeric matrix did not affect significantly the barrier properties of the PS membrane.

2.3.5 Temperature sensitivity of the two probe system fluorescent membrane

Ideally, an oxygen optical sensor should be independent from all other environmental conditions, including temperature. However, it is well known that the temperature affects the emission of the luminophores and the diffusion coefficient of gases (i.e. oxygen) in the polymer, thus affecting the measurements.

The effect of the temperature on the sensor emission when exposed at constant atmospheric pressure (yO_2=21%) was evaluated. Results are summarized in Figure 2.10.

a)   b)
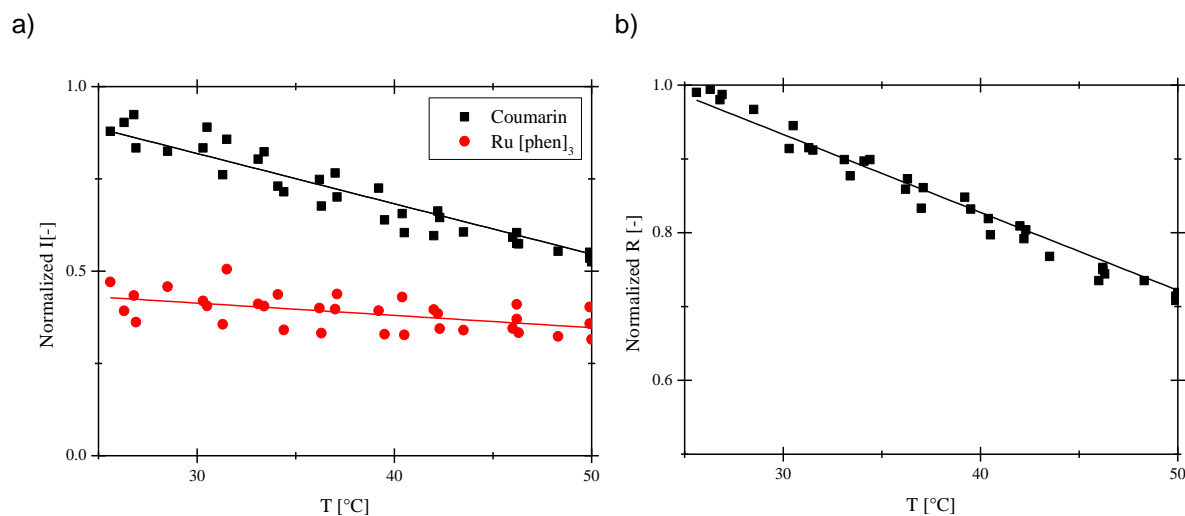
Figure 2.10: Effect of the temperature on (a) the intensities of the emission of Ru(phen)$_3$ and Coumarin in PS and (b) the ratio of their intensities , recorded at yO_2=21%.

As expected, the emission intensities of both probes decrease linearly with the increase of the temperature (Figure 2.10.a). However, the Coumarin emission decreases 45% by increasing temperature from 25ºC to 50ºC, whereas Ruthenium complex registered an emission decrease of only 20%, upon the same temperature change, evidencing that Coumarin is more sensitive to the temperature than Ru(phen)$_3$. As a consequence of the different sensitivity of the two probes towards the temperature, the ratio of the intensities of their emissions decreases by increasing the temperature. Again, the single probe emissions depend dramatically on changes of environmental conditions. As a consequence, the precise evaluation of the temperature using the single probe emission is prone to errors as can be seen through the data scattering shown in Figure 2.10.a. Once more, the employment of the ratio of the emission intensities of the two probes allows for an accentuated error reduction (<3%) without affecting significantly the sensitivity. In fact, a decrease of 30% of the normalized ratio ($R/R_{25°C}$) was obtained after increasing the temperature from 25°C to 50°C.

2.3.6 Simultaneous effect of oxygen and temperature

The use of the two probes and the combination of their emission in a ratiometric signal allows for the correction of artifacts due to the geometry of the experiment and the source intensity fluctuations, favoring consequently the development of a robust sensor for the detection of temperature or oxygen. However, a ubiquitous problem arises from the fact that probes for oxygen also respond to temperature, forbidding the simultaneous detection of the two parameters. In fact,

since the response of the ratiometric sensor depends on both, temperature and O_2 concentration, the simultaneous estimation of these parameters is only possible using systems with fixed geometry.

In Figure 2.11, it is possible to observe the simultaneous effect of both oxygen and temperature on the ratiometric response.

a)   b)
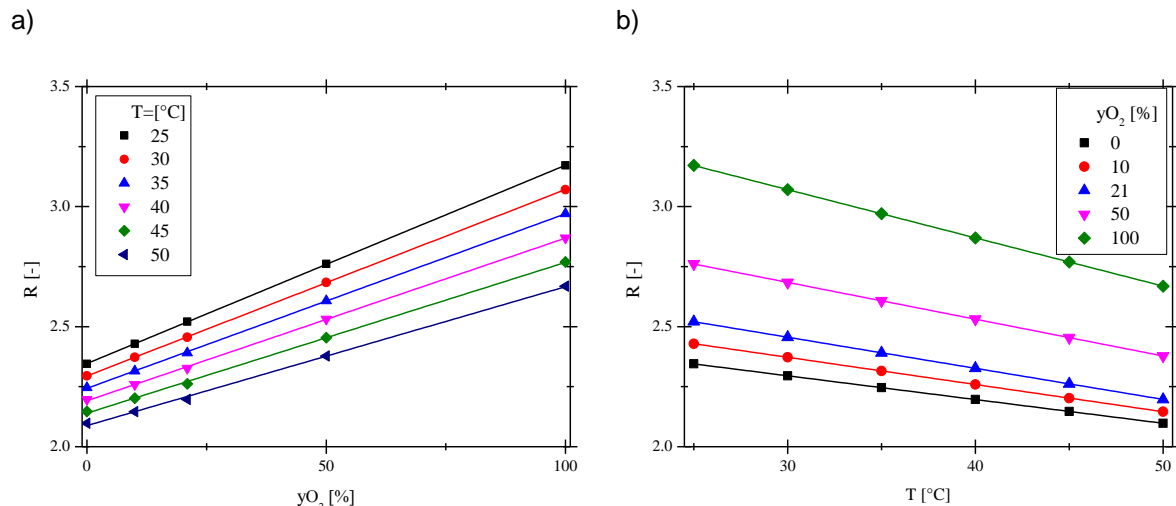
Figure 2.11: Effect of the temperature on the oxygen sensitivity (a) and of oxygen on the temperature sensitivity (b). Experiments were performed using the set-up reported in Figure 2.3.

a)   b)
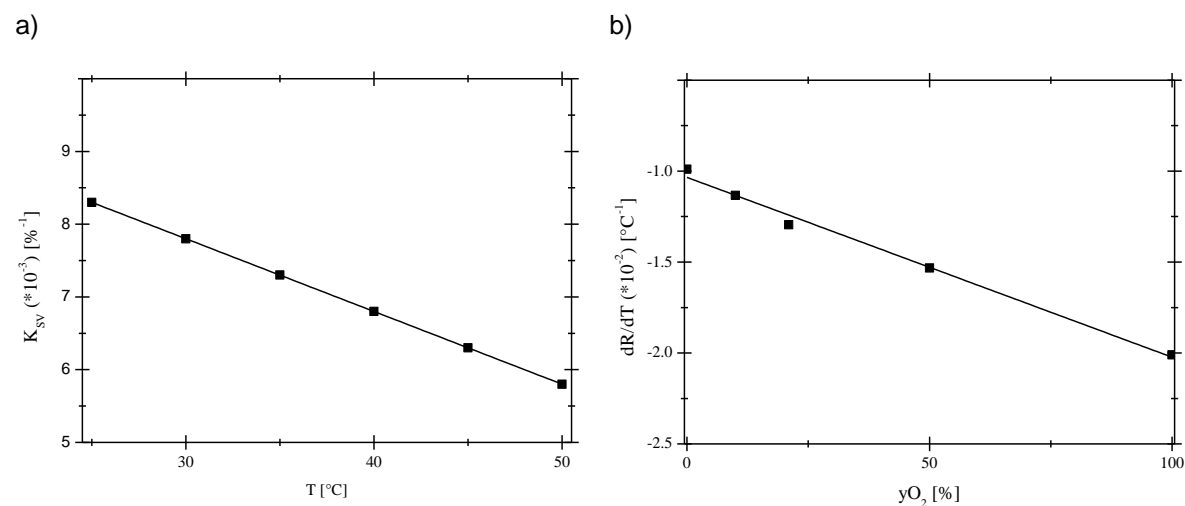
Figure 2.12: Effect of the temperature on Stern-Volmer constant (a) and of oxygen on the temperature sensitivity (b).

The ratiometric response linearly increases by increasing the oxygen at different temperature as a consequence of the quenching of Ru(phen)$_3$. Moreover, the effect of the temperature is to favor the non-radioactive deactivation of both Coumarin and Ru(phen)$_3$ decreasing the value of the ratio of their intensities. Furthermore, by looking at figure 2.12.a it is possible to notice that the increase of temperature decreases the oxygen sensitivity of the membrane (K_{SV}).

On the other hand, the temperature linearly decreases the ratiometric response of the membrane since the intensity of Coumarin is more affected by the temperature than the emission of the complex of Ru (Figure 2.11.b). In addition the variation of the oxygen concentration increases the value of the ratiometric response due to the quenching of $Ru(phen)_3$ and decrease the thermal sensitivity of the dual emission of the membrane (Figure 2.12.b).

2.3.7 Temperature compensation of the oxygen sensor

Lo et al. (2008) [41] developed a simple model for evaluation of the oxygen concentration non-dependent on the temperature, using as probe the emissive complex platinum(II) meso-tetrakis(pentafluorophenyl)porphyrin (PtTFPP). The model allowed them to evaluate the temperature compensation C(T) for the sensor response using the emission intensity of the complex.

The same model was applied to the emission ratios obtained in this work, (R), according to Equation 2.6:

$$C(T) = \frac{R_0(T_{ref})}{R(T)} - \frac{R_0(T_{ref})f_1 K_{SV}(T_{ref})yO_2}{R(T)\{1+K_{SV}(T_{ref})yO_2\}}, \qquad (2.6)$$

where $R_0(T_{ref})$ is the ratio of the intensities in the absence of oxygen at the reference temperature (T=25°C), and R(T) is the ratiometric response at a certain oxygen level and temperature of the measurement, $K_{SV}(T_{ref})$ is the Stern–Volmer constant at the reference temperature (T=25°C) for the ratiometric sensor, $f_1(T)$ is the fractional intensity of the component contributing to the total luminescence at the given temperature of the measurement is assumed to be 1 since no deviation from linear Stern-Volmer equation was observed, as already pointed out in section 1.3.4.

The non-temperature dependent ratio, R_m, was determined by Equation 2.7:

$$R_m = C(T)R. \qquad (2.7)$$

Experiments were performed at different temperatures ranging from 25°C to 50°C and distinct oxygen concentrations (yO_2=0%, 21%, 50% and 100%) for evaluation of the temperature compensation effect. It was observed that the ratiometric response obtained in the whole range of temperatures follows a Stern-Volmer behavior (R^2>0.99). As shown in Figure 2.13.a the sensitivity of R_0/R signal to $y(O_2)$ decreases with the increase of temperature. This effect is clearly visible by the decrease of the R_0/R vs. $y(O_2)$ profile slope as well as by the linear decrease of the ratiometric sensor Stern-Volmer coefficient at increasing temperatures.

According to Equation 2.6, the value of the temperature compensation factor C(T) depends on the temperature and oxygen concentration. The non-temperature ratiometric signal, R_{m0}/R_m, where R_{m0} is the non-temperature dependent ratio in absence of oxygen, was obtained after correction of R_0/R values using Eq. 1.7. The sensitivity of R_{m0}/R_m vs. yO_2 (%) is plotted in Figure 2.13.b. As shown, R_{m0}/R_m exhibits good sensitivity to yO_2 without influence of temperature, confirming the

robustness of the developed ratiometric sensor. In fact, the different Stern-Volmer plots at

a)

b)
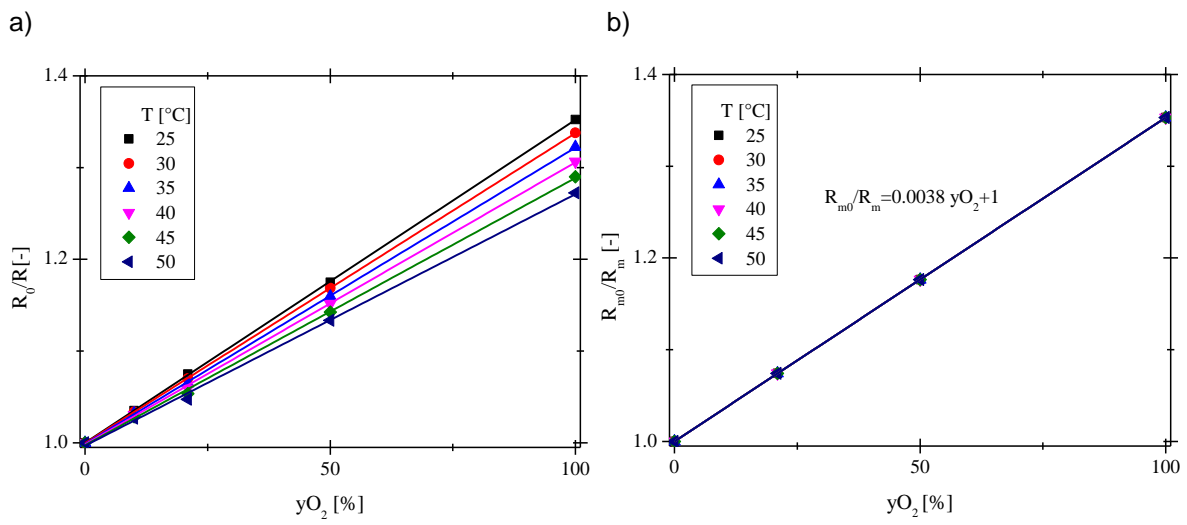
different temperatures are perfectly overlapped.

Figure 2.13: (a) Effect of the temperature on the Stern-Volmer ratiometric response and (b) Stern-Volmer trend of the compensated ratiometric response at different temperatures.

2.4 Conclusions

In this work oxygen and temperature sensitive membranes were developed. The fluorescent membrane was based on the use of the Ru(phen)$_3$ as molecular probe for oxygen monitoring. Studies confirmed that the sensitivity of the sensor increased by employing polymer matrices with high oxygen permeability. However, the detection based on the use of the Ruthenium complex suffers of inaccuracy related to optical path and excitation geometry drifts. In order to correct this artifact, Coumarin was selected as a reference among different fluorescent luminophores for development of the ratiometric response because of its non-sensitivity to oxygen and well discernible emission band from those observed for the Ruthenium complex. The employment of the reference allowed to correct artifacts induced by fluctuations in the excitation light intensity, excitation geometry and optical path. The ratiometric sensor showed a linear response in the whole range with a sensitivity of $R_{100}/R_0 \sim 1.5$ at room temperature (21°C).

As expected, the ratiometric optical sensor was found to be sensitive to the temperature. In fact, the ratiometric response decreased 30% by increasing the temperature from 25°C to 50°C. However, temperature compensation of the signal consents to calibrate the ratiometric optical sensor, thus obtaining a response independent from the temperature, the optical path, excitation geometry and fluctuations in the excitation light intensity of the source and transmission properties of the optical fiber. The reproducibility of the measurements in the range 25-50ºC is highlighted by the low error value of 0.1%, throughout the whole O$_2$ concentration range.

Given the combination of (i) high mechanical stability (provided by the PS matrix), (ii) high sensitivity and selectivity (provided by the two-probe system) and (iii) high reproducibility in the output signal/response, this membrane presents a significant step for monitoring O$_2$ and temperature in membrane processes at laboratory and industrial scales. On-going work envisages the application of the developed membrane on the monitoring of oxygen permeation in food packaging and for the monitoring of the temperature on PVDF membrane surfaces, for the evaluation of the thermal polarization in membrane distillation processes.

2.5 References

[1] Baker, R W. Concentration Polarization, in: *Membrane Technology and Applications*. Wiley, second edition, 2004.

[2] Figoli A, Santoro S, Galiano, F, and Basile, A. Pervaporation membranes: preparation and characterization, in: *Vapour Permeation and Membrane Distillation Principles and Applications*. Elsevier Woodhead Publishing, 2015.

[3] Martinez-Diez, L, and Vázquez-González, M I. A method to evaluate coefficients affecting flux in membrane distillation. *J. Membr. Sci.,* 173(2): 225-234, 2000.

[4] Paipuri, M, Kim, S H, Hassan, O, Hilal, N, and Morgan, K. Numerical modelling of concentration polarisation and cake formation in membrane filtration processes. *Desalination*, 365: 151-159, 2015.

[5] Tijing, L D, Woo, Y C, Choi, J-S, Lee, S, Kim, S-H, and Shon, H K. Fouling and its control in membrane distillation—A review. J. Membr. Sci, 475: 215-244, 2015.

[6] Tarleton, E S, Robinson, J P, and Salman, M, 2006, Solvent-induced swelling of membranes measurements and influence in nanofiltration. *J. Membr. Sci.,* 280(1-2): 442-451.

[7] Nyström, N, and Mänttäri, M.Opportunities and Challenges of Real Time Monitoring on Membrane Processes, in: *Monitoring and Visualizing Membrane-Based Processes*. Wiley, 2009.

[8] Stich, M I J, Fischer, L H, and Wolfbeis, O S. Multiple fluorescent chemical sensing and imaging. *Chem. Soc. Rev.*, 39(8): 3102-3114, 2010.

[9] Dmitriev, R I, Zhdanov, A V, Nolan, Y M, and Papkovsky, D B. Imaging of neurosphere oxygenation with phosphorescent probes. *Biomaterials*, 34(37): 9307-9317, 2013.

[10] Chauhan, V M, Hopper, R H, Ali, S Z, King, E M, Udrea, F, Oxley, C H, and Aylott, J W. Thermo-optical characterization of fluorescent rhodamine B based temperature-sensitive nanosensors using a CMOS MEMS micro-hotplate. *Sensors and Actuators B,* 192(1): 126-133, 2014.

[11] Baleizão, C, Nagl, S, Schäferling, M, Berberan-Santos, M N, and Wolfbeis, O S. Dual fluorescence sensor for trace oxygen and temperature with unmatched range and sensitivity. *Anal. Chem.,* 80(16): 6449-6457, 2008.

[12] Childs, P R N. Advances in temperature measurement. *Advances in Heat Transfer 36*: 111-181, 2003.

[13] Ramamoorthy, R, Dutta, P K, and Akbar, S A. Oxygen sensors: Materials, methods, designs and applications. *Journal of Materials Science*, 38 (21): 4271-4282, 2003.

[14] Brites, C D S, Lima, P P, Silva, N J O, Angel, M, Amaral, V S, Palacio, F, and Carlos, L D. Thermometry at the nanoscale. *Nanoscale,* 4: 4799-4829, 2012.

[15] Gosse, C, Bergaud, C, and Löw, O. Molecular Probes for Thermometry in Microfluidic Devices, in: *Thermal Nanosystems and Nanomaterials, Topics in Advanced Physics* 118. Springer-Verlag, 2009.

[16] Marek, P, Velasco-Veléz, J J, Haas, T, Doll, T, and Sadowski, G. Time-monitoring sensor based on oxygen diffusion in an indicator/polymer matrix. *Sensors and Actuators B,* 178: 254-262, 2013.

[17] Grist M, Chrostowski L, and Cheung, KC. Optical oxygen sensors for applications in microfluidic cell. *Culture,* 10(10): 9286-9316, 2010.

[18] Balaji Ganesh, A, and Radhakrishnan, T K. Fiber-optic sensors for the estimation of oxygen gradients within biofilms on metal. *J. Opt. Lasers Eng.*, 46(33): 321-327, 2008.

[19] Sakaguchi, R, Kiyonaka, S, and Mori, Y. Fluorescent sensors reveal subcellular thermal changes. *Current Opinion in Biotechnology*, 31(1): 57-64, 2015.

[20] Tsukada, K, Sakai, S, Hase, K, and Minamitani, H.Development of catheter type optical oxygen sensor and applications to bioinstrumentation. *Biosens. Bioelectron.,* 18(12): 1439-1445, 2003.

[21] Gouin, J F, Baros, F, Birot, D, and André, J C. A fibre-optic oxygen sensor for oceanography. *Sensors and Actuators B,* 39(1-3): 401-406, 1997.

[22] Wang, X-D, Chen, H-X, Zhao, Y, Chen, X, Wang, X-R, and Chen, X.Optical oxygen sensors move towards colorimetric determination. *TrACTrends in Anal. Chem.,* 29(4): 319-338, 2010.

[23] Douglas, P, and Eaton, K. Response characteristics of thin film oxygen sensors, Pt and Pdoctaethylporphyrins in polymer films. *Sensors and Actuators B,* 82(2-3): 200-208, 2002.

[24] Wolfbeis, O S. Fiber optic chemical sensors and biosensors. *Anal. Chem.*, 80(12):4269-4823, 2008.

[25] Amao, Y. Probes and Polymers for Optical Sensing of Oxygen. *Microchimica Acta,* 143(1): 1-12, 2003.

[26] Basu, B J, Thirumurugan, A, Dinesh, A R, Anandan, C, and Rajam, K. Optical oxygen sensor coating based on the fluorescence quenching of a new pyrene derivative, *Sensors and Actuators B*,104(1): 15-22, 2005.

[27] Amao, Y, Miyashita, T, and Okura, I. Optical oxygen sensing based on the luminescence change of metalloporphyrins immobilized in styrene-pentafuorostyrene copolymer film. *Analyst*, 125(5): 871-875, 2000.

[28] Gillanders, R N, Tedford, M C, Crilly, P J, and Bailey, R T. A composite thin film optical sensor for dissolved oxygen in contaminated aqueous environments. *Anal. Chem. Acta*, 545(2): 189-194, 2005.

[29] Wang, Z, McWilliams, A R, Evans, C E B, Lu, X, Chung, S, Winnik, M A, and Manners, I. Covalent attachment of RuIIphenanthroline complexes to polythionylphosphazenes: the development and evaluation of single-component polymeric oxygen sensors. *Adv. Funct. Mater.*, 12(6-7): 415-419, 2002.

[30] Liebsch, G, Klimant, I, and Wolfbeis, O S. Luminescence lifetime temperature sensing based on sol–gels and poly(acrylonitrile)s dyed with ruthenium metal–ligand complexes. *Adv. Mater.*, 11(15): 1296–1299, 1999.

[31] Coyle, L M, and Gouterman, M. Correcting lifetime measurements for temperature. *Sensors and Actuators B*, 61(1-3): 92-99, 1999.

[32] Stich, M I J, Nagl, S, Wolfbeis, O S, Henne, U, and Schaeferling, M. A Dual Luminescent Sensor Material for Simultaneous Imaging of Pressure and Temperature on Surfaces. *Adv. Funct. Mater.* 18(9): 1399-1406, 2008.

[33] Chu, C-S, and Lo, Y-L. Ratiometric fiber-optic oxygen sensors based on sol–gel matrix doped with metalloporphyrin and 7-amino-4-trifluoromethyl coumarin. *Sensors and Actuators B*,134(2): 711-717, 2008.

[34] Park, E J, Reid, K R, Tang, W, Kennedy, R T, and Kopelman, R. Ratiometric fiber optic sensors for the detection of inter- and intra- cellular dissolved oxygen. *J.Mater. Chem.*, 15: 2913-2919, 2005.

[35] Poteau, X, and MacCraith, B. Ratiometric sensor for dissolved oxygen in seawater. *Proc. SPIE* 4876: 886-893, 2003.

[36] Cywinski, P J, Moro, A J, Stanca, S E, Biskup, C, and Mohr, G J. Ratiometric porphyrin-based layers and nanoparticles for measuring oxygen in biosamples. *Sensors and Actuators B*,135(2): 472-477, 2009.

[37] Jansen, J C, Friess, K, and Drioli, E. Organic vapour transport in glassy perfluoropolymer membranes: A simple semi-quantitative approach to analyze clustering phenomena by time lag measurements. *J. Membrane Sci.*, 367(1-2): 141-151, 2011.

[38] Corre, Y M, Bruzaud, S, Audic, J L, and Grohens, Y. Morphology and functional properties of commercial polyhydroxyalkanoates: A comprehensive and comparative study. *Polymer Testing*, 31(2): 226-235, 2012.

[39] Murphy, T M, Freeman, B D, and Paul, D R. Physical aging of polystyrene films tracked by gas permeability. *Polymer*, 54(2): 873-880, 2013.

[40] Roche, P, Al-Jowder, R, Narayanaswamy, R, Young, J, and Scully, P. A novel luminescent lifetime-based optrode for the detection of gaseous and dissolved oxygen utilising a mixed ormosil matrix containing ruthenium (4,7-diphenyl-1,10-phenanthroline)$_3$Cl$_2$. *Analytical and Bioanalytical Chemistry*, 386(5): 1245-1257, 2006.

[41] Lo, Y-L, Chu, C-S, Yur, J-P, and Chang, Y-C. Temperature compensation of fluorescence intensity-based fiber-optic oxygen sensors using modified Stern–Volmer model. *Sensors and Actuators B*,131(2): 479-488, 2008.

Chapter 3

Monitoring oxygen permeation through packaging films using ratiometric luminescent sensors

3.1 Introduction

Food packaging provides not only a method for transporting food safely, but extends shelf-life by protecting food from harmful bacteria, contamination, and degradation that would occur otherwise [1]. In this contest, oxygen is a crucial factor in food storage since its presence allows a myriad of aerobic microorganisms to grow and is involved in the degradation of ascorbic acid and in the oxidation of a wide range of flavours and nutrients [2-4]. Modified atmosphere packaging (MAP) can be used to extend food shelf life, in which the atmosphere within the food package is flushed with an inert gas, such as nitrogen or carbon dioxide, reducing the oxygen content to typically 0.5–2% [4].

In recent years, efforts have been devoted to develop different food safety measures to ensure the security and quality of food, enhancing product safety by the employment of new materials and technologies [4-7].

A new generation of packaging materials with barrier properties and that can release active compounds (antimicrobial, antioxidants, enzymes, flavours, nutraceuticals) or absorb undesirable substances (oxygen, ethylene, moisture) at controlled rates suitable for enhancing the quality and safety of a wide range of foods during extended storage is being developed [8-9]. On the other hand, efforts are devoted among the food industry, retailers, consumers, and their stakeholders for developing a simple, low-cost, rapid, reliable, non-invasive and non-destructive device to evaluate real-time freshness of food products [10]. In this sense, the oxygen concentration in the food-package is an useful index of the food quality.

Oxygen indicators employed in this field usually fall into two categories:

(i) lumophoric, the luminescence of molecular probes decrease with increasing partial pressure of oxygen;

(ii) colorimetric, the colour of the indicator changes as a consequence of oxygen-binding reaction, redox reaction or light-activated redox reaction [11].

Some organometallic compounds immobilized in appropriate matrix are used as colorimetric sensor related to the capability to reversibly bind molecular oxygen [12-14]. These sensors present an advantage that is the colour change easily perceived by the human eye, without requiring any specialist analytical equipment, providing an instant insurance about the food quality to the consumer [15]. However, reversible colorimetric indicators suffer of several drawbacks such as, lack of quantitative information about oxygen concentration, instability and low spectral changes upon oxygen binding, thus limiting their employment.

Luminophores, in particular metal polypyridyl complex and metalloporphines, are widely explored for the development of oxygen sensors based on luminescence quenching due to the energy transfer from the luminophore to oxygen [16-17]. Optical sensors prepared by the dispersion of luminophores in polymeric films present the advantage to consent a quantitative evaluation of oxygen.

Optical sensors, consisting in dispersion of molecular probes in polymers, respond directly to oxygen partial pressure in a gas or in a liquid: higher oxygen levels result in lower intensities of

emission and luminescence lifetimes [19-20]. Oxygen is an excellent quencher of photoluminescence due to its energetic levels and ground state paramagnetic properties, and quenching mechanism is summarized in Figure 3.1: the excited state of the molecular probe transfers energy to the quencher (i.e. oxygen) which on the other hand is excited to singlet oxygen via non-radiative energy transfer oxygen from the luminophore to the ground state triplet oxygen, while the molecular probe returns to its ground state without the emission of light (Figure 3.1).

The quenching requires diffusion of oxygen to a collisional distance of the excited probe molecule and can be quantified by the Stern-Volmer equation:

$$\frac{I_0}{I} = \frac{\tau_0}{\tau} = 1 + k_q \tau_0 [O_2]; \qquad (3.1)$$

where I and I_0 are the luminescence intensities in the presence and absence of the quencher, τ and τ_0 are the lifetimes of the luminophore in the presence and absence of the quencher, k_q is the bimolecular quenching constant and is directly proportional to the permeability of the matrix containing the molecular probes.
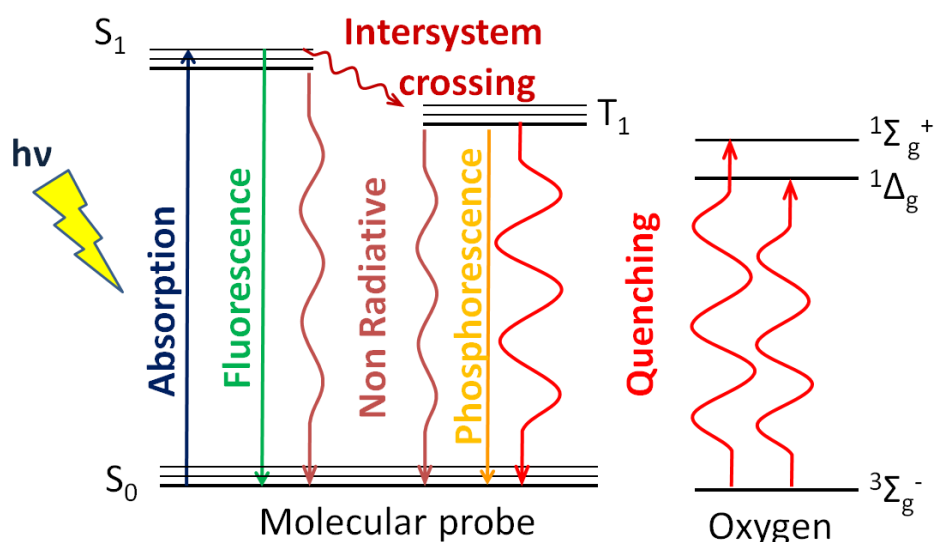
Figure 3.1: Mechanism of dynamic quenching.

Ru(phen)$_3$ is a luminophore widely studied as molecular probe for oxygen detection because of its good sensitivity to oxygen, long lifetime and good chemical stability [21-22].

However the measurements of the intensity of the emission are prone to changes in the optical path, b, fluctuations in the intensity of the excitation light intensity, I_{exc}, and variations in the excitation/detection geometry, k, as reported in the following equation:

$$I = k I_{exc} \Phi [\varepsilon b c]. \qquad (3.2)$$

This limits the use of luminescence probe in robust optical sensing when a specialized analytical equipment with fixed setup is absent.

The use of a second luminophore and the combination of its emission with that of the oxygen sensitive probe translates into a ratiometric signal (R) allowing for the correction of these artifacts and consequently, to the development of a robust oxygen sensor [22-25], non-dependent on operating conditions of the measurements, but solely on the photochemical properties of the two probes (quantum yield Φ and molar extinction coefficient ε):

$$R = (\Phi\varepsilon)_{Coumarin}/(\Phi\varepsilon)_{Ru(phen)_3} . \qquad (3.3)$$

In our previous work a polymeric ratiometric optical sensor was developed based on tris 1,10-phenanthroline ruthenium ($Ru(phen)_3$) as oxygen sensitive probe and 7-Methoxy-4-methylcoumarin (Coumarin) used as reference in order to correct artifacts due to the operating conditions, which allowed us to obtain a signal depending exclusively from the oxygen content [26].

In this study the developed ratiometric optical sensor is used for the online and non-invasive monitoring of oxygen in food packaging experiments. The optical sensor was employed for measuring changes of oxygen concentration inside a package due to its permeation from the atmosphere. Films with different oxygen permeability, namely, biaxially oriented polypropylene (BOPP) and polydimethylsiloxane (PDMS), were employed as packaging material enclosing a modified atmosphere package (MAP). PDMS was selected on the basis of its high oxygen permeability in order to evaluate the response of the optical sensor with a rapid change of the atmosphere composition, whereas BOPP is a barrier polymer employed to estimate the resolution of the sensor in a real situation. The values of oxygen concentration using the sensor were compared with the ones predicted by using the permeability of these polymers, obtained in independent experiments and confirmed by gas chromatography analysis.

3.2 Experimental section

3.2.1. Materials and Methods

The oxygen sensitive probe Tris(1,10-phenanthroline)ruthenium(II) ($Ru(phen)_3$) was synthesized according to the procedure reported in literature [27]. Polystyrene (PS, Mw: 192,000), 7-methoxy-4-methylcoumarin (Coumarin) and Chloroform were purchased from Sigma Aldrich Chemistry (Spain).

Biaxially oriented polypropylene (BOPP) was purchased from Termofilm-Embalagens Técnicas LDA (Portugal), whereas SSP-M823 polydimethyl siloxane membrane (PDMS) from Specialty Silicone Products Inc. (United States).

Fluorescence measurements were performed using a Horiba-Jobin-Yvon SPEX Fluorolog 3.22 spectrofluorimeter equipped with a 450 W Xe lamp equipped with a randomized biforcuted fiber-optical bundle FL-3000. All spectra were collected with 5 nm slit bandwidth for excitation and emission and corrected.

Gas chromatography measurements were performed using a Trace GC Ultra, Thermo Electron Corporation, with a thermal conductivity detector. The oven temperature was fixed at 35ºC; whereas the injector heated at 200ºC. The carrier gas is Helium at 1 mL min^{-1}. The column used was a Supelco Carboxen 1010 with 30 meters and a 50 minutes run.

3.2.2. Preparation of the optical sensor

The optical sensor was prepared by dry-casting of a polymeric solution made of PS (25 wt%) dissolved in chloroform. The solution was stirred at 30°C overnight till an homogenous polymeric solution was obtained. The probes, Ru(phen)$_3$ and Coumarin at a concentration of 10^{-3}M were solubilized in chloroform and subsequently injected in the polymeric solution. The dope solution was stirred for 2 hours and sonicated for 1 hour and, then, cast using a casting knife with thickness of 0.75 mm.

A self-consistent film of PS with 144±3 µm thickness was obtained by solvent evaporation (48 hours). The prepared films were placed in an oven at 65°C over night in order to favor the removal of solvent traces.

The optical sensor showed a good stability in terms of immobilization of the probes. In fact, samples of 1 cm^2 were immersed for 48 hours in 10 mL of water, methanol and ethanol and in all cases, measurements of absorbance confirmed the absence of probes in the solvents.

3.2.3 Response of the sensor

The optical sensor presents the advantage that can be placed in the food package and the stimuli to the sensor and the information consists of light, allowing a non invasive monitoring of the oxygen content in the enclosed package.

In order to perform experiments for evaluating the efficiency of the sensor in monitoring the oxygen concentration in food packaging, the set-up showed in Figure 3.2 was developed.

This rig is composed by a stainless steel cell of a volume of 12.56 cm^3 with a sealed compartment separated from the atmosphere by a film (area of 7.07 cm^2) supported on a porous stainless. The optical sensor (area=1 cm^2) was placed between the film and the stainless support.

One of the surfaces of the film was exposed to the atmosphere ($C(O_2)^{out}$=21%); whereas the other one was exposed to the sealed compartment of the cell, which should represent the enclosed atmosphere of the food package. Four different mixtures of gas with different oxygen concentrations (0, 10, 21, 50 %) were fed to the chamber for the calibration of the sensor. Each concentration was flushed for 20 minutes at a pressure of 1.1 bar. Then the cell was sealed by closing the two valves maintaining a pressure of 1 bar and the spectra were collected after 5 min required to guarantee the gases diffusion in the polymeric matrix and the optical sensor to achieve the steady state.

For evaluating the oxygen permeation trough the film and reproduce real conditions in food package, the cell was filled with an inert atmosphere of argon and sealed by closing the two valves, simulating a modified atmosphere (0% of O_2).

The oxygen content in the enclosed atmosphere was evaluated by measuring the fluorescence emission of the optical sensor using a bifurcated optical fiber (distance between the optical sensor and the optical fiber was ca. 2 mm) connected to a spectrofluorometer. Emission spectra were collected for 24 hours to follow the oxygen permeation trough the film made of oriented BOPP and 3 hours in the case of PDMS film. After collecting the last spectra, a sample from the enclosed atmosphere was collected using a gas tight syringe and injected in the GC to validate the results obtained using the optical sensor.
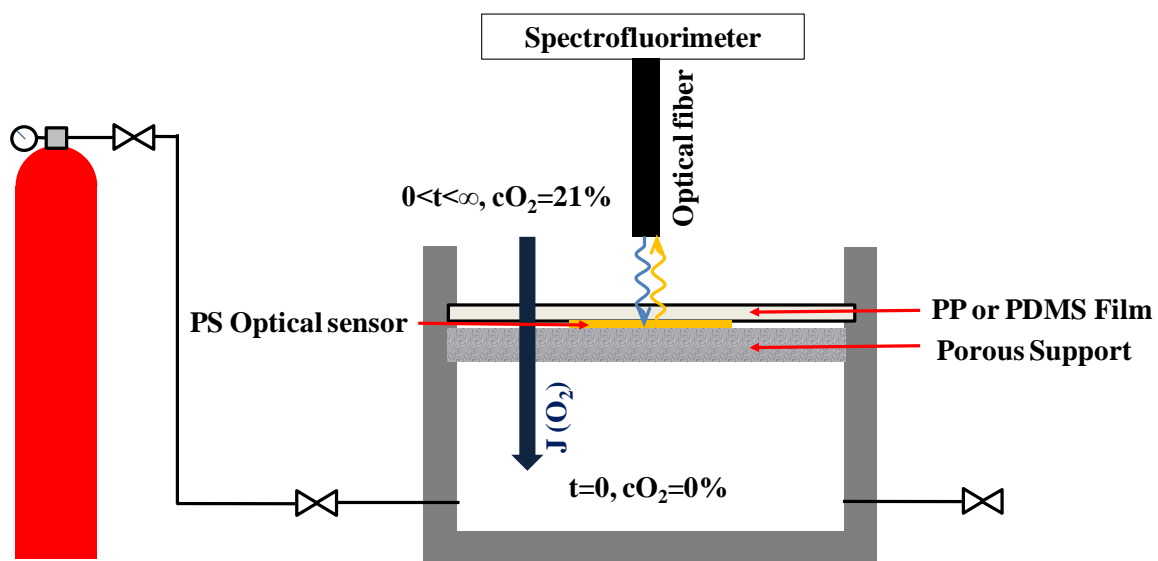
Figure 3.2: Set up used for experiments.

3.2.4 Oxygen permeability trough dense films

Polymeric films provide a barrier protection to gas ensuring and adequate quality to the food for a long period (shelf life). The transport of gas or vapor through the package affects the quality of the food and, in many situations, the role of packaging is in the direction of reducing to as low as possible the oxygen exchange between the internal and the external side of the package. However, the barrier properties of the film can be inhibited by leakages. For this reason, the transport properties of the material used to make the package and the monitoring of the oxygen concentration in the package are crucial in food industry.

The permeation of gas and vapor through a dense polymeric material is described by the solution diffusion model: molecules on the high-pressure side of the film dissolve into the polymer, diffuse

down the concentration gradient and desorb on the low-pressure side of film [28]. This is a typical situation in food packaging, where the food is stored in an atmosphere kept at a lower partial pressure of oxygen with respect to the environment (Figure 3.3).

The permeability coefficient Pe, derived using Fick's first law to model diffusion and Henry's law to model adsorption and desorption [29], is the product of a solubility coefficient, S, and a diffusion coefficient or diffusivity, D:

$$\mathbf{Pe = DS}. \quad (3.4).$$

In the case of multilayer films, the total permeability (Pe_{TOT}) is obtained by the following equation, according to a resistance in series model:

$$\frac{l_{TOT}}{Pe_{TOT}} = \sum_{i=1}^{n} \frac{l_i}{Pe_i}; \quad (3.5),$$

where l_{TOT} is the total thickness of the multilayer film and l_i and Pe_i are the thickness and the permeability of the single layer i, respectively.

The evolution of the concentration of oxygen in the enclosed package ($C_{O_2}^{in}$) along time starting from an enclosed atmosphere without oxygen ($C_{O_2}^{in\,t=0}$=0%) can be predicted by a mass balance of oxygen using the following equation:

$$C(O_2)^{in} \, [\%] = C(O_2)^{out} - C(O_2)^{out} \exp\left[\left(\sum_i \frac{Pe_i\, A_i}{l_i\, V}\right) t\right]; \quad (3.6)$$

where $C_{O_2}^{out}$ is the oxygen concentration in the atmosphere (21%), Pe is the oxygen permeability of a film of thickness l and area A employed for sealing a package of volume V. Considering that the molecular probe is immobilized in PS, the oxygen first diffuses trough the package and, then, in the PS matrix. For this reason, the multilayer composition of the system must be considered.
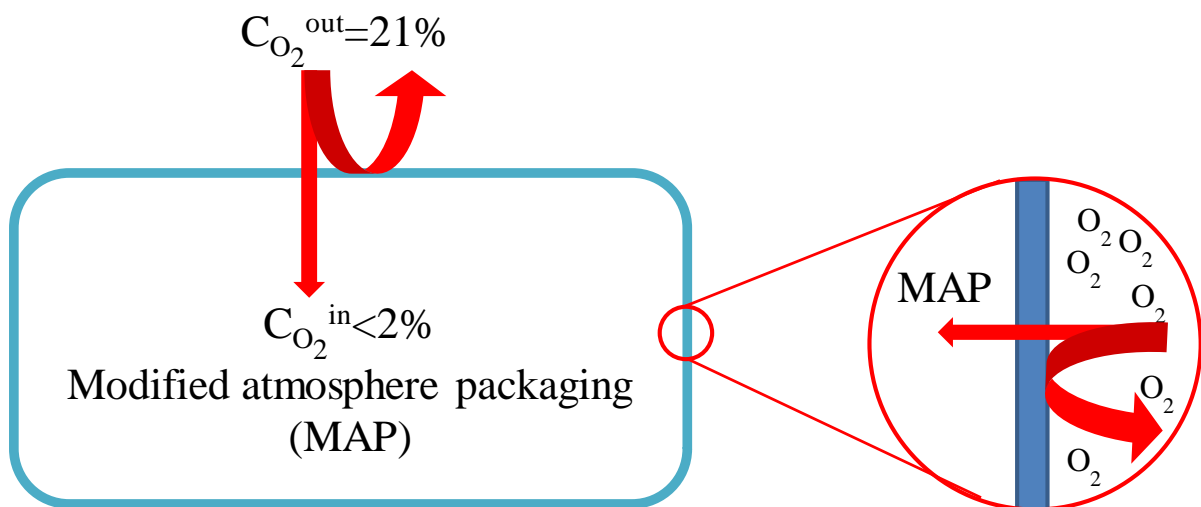
Figure 3.3: Permeation of oxygen in food package

The oxygen permeability of the films employed was measured independently using the set-up described in Figure 3.4.
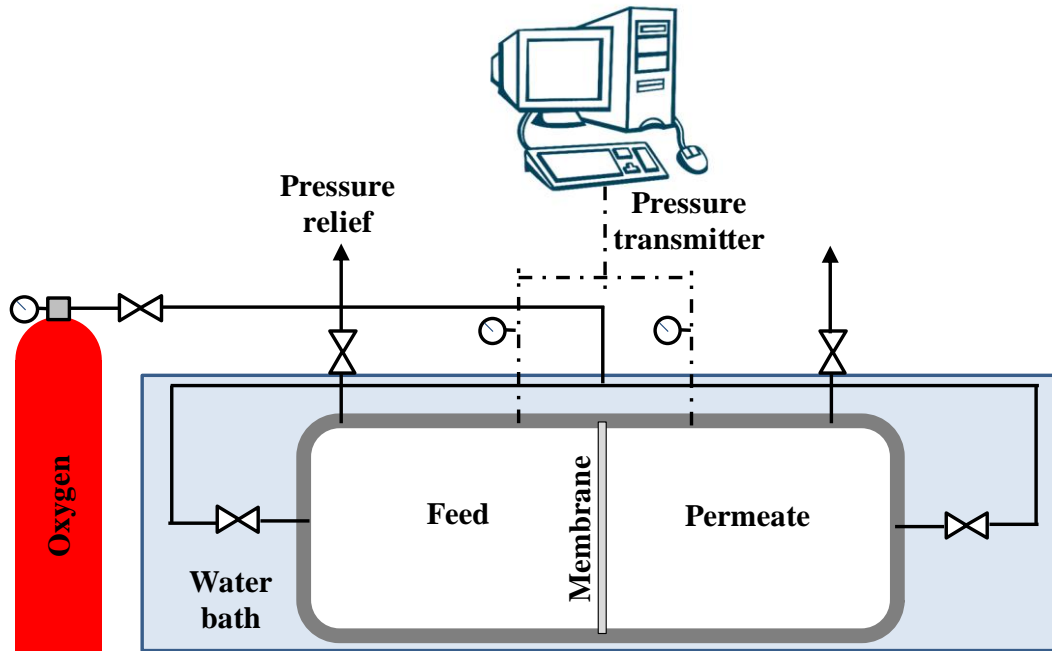
Figure 3.4: Set-up for measuring oxygen permeability.

In this case; the rig is composed by two identical stainless sealed compartments separated by the membrane with an effective area of 12.6 cm^2. The oxygen was fed in both compartments and after evacuation of the permeate compartment a driving force of around 0.5 bar between the feed and permeate was established, favoring the transport of gas.

The permeability of the pure gas through the membrane was calculated from the pressure data of the feed and permeate compartments measured using two transducers; according to the following equation:

$$\frac{1}{\beta} ln\left(\frac{[p_{feed}-p_{perm}]_0}{[p_{feed}-p_{perm}]}\right) = Pe\frac{t}{l}; \quad (3.7)$$

where p_{feed} and p_{perm} are the pressures in the feed and permeate compartments respectively (bar), Pe is the permeability (m^2 s^{-1}), t is the time (s) and l is the membrane thickness (m). The geometric parameter β (m^{-1}) is:

$$\beta = A\left(\frac{1}{V_{feed}} + \frac{1}{V_{perm}}\right); \quad (3.8)$$

where A is the membrane area (m^2) and V_{feed} and V_{perm} are the volume of the feed and permeate compartments (m^3), respectively.

3.3. Results and discussion

3.3.1 Optical sensor sensitivity

The sensitivity of the optical sensor based on the dispersion of Ru(phen)$_3$ was evaluated by measurement of fluorescence performed by fixing in a cuvette the film with an angle of 45° with respect to the source. The emission was collected by exciting the optical sensor at the maximum of the absorption of Ru(phen)$_3$ in PS (460 nm).

In Figure 3.5.a it is reported the emission of the optical sensor in aerated condition (C(O$_2$)=21%) with an emission maximum at 590 nm. Subsequently, argon was fed in the cuvette in order to remove oxygen, obtaining an increase of the emission intensity due to the higher number of emissive probes as a consequence of the lower number of quencher molecules. In fact after 30 min of feeding argon in the cuvette, an increase of ca. 20% of the emission was observed due to the decrease of the oxygen level in the cuvette from 21% to 0%.

In Figure 3.5.b it is reported the rate of increase of the maximum of emission (I/I$_0$, %) due to the removal of the oxygen, which follows an asymptotic trend. In fact, the intensity of emission increases linearly for the first 5 min and then evolves to a plateau achieved in 10 min (Figure 3.5.b). The increase is well fitted by the equation:

$$\frac{I_t}{I_{t=0}} \ [\%] = a - bc^t; \quad (3.10)$$

where "a" is the asymptotic value of 119.86; "b" is the response range, equal to 19.6, and "c" is the rate, equal to 0.71.

a)   b)
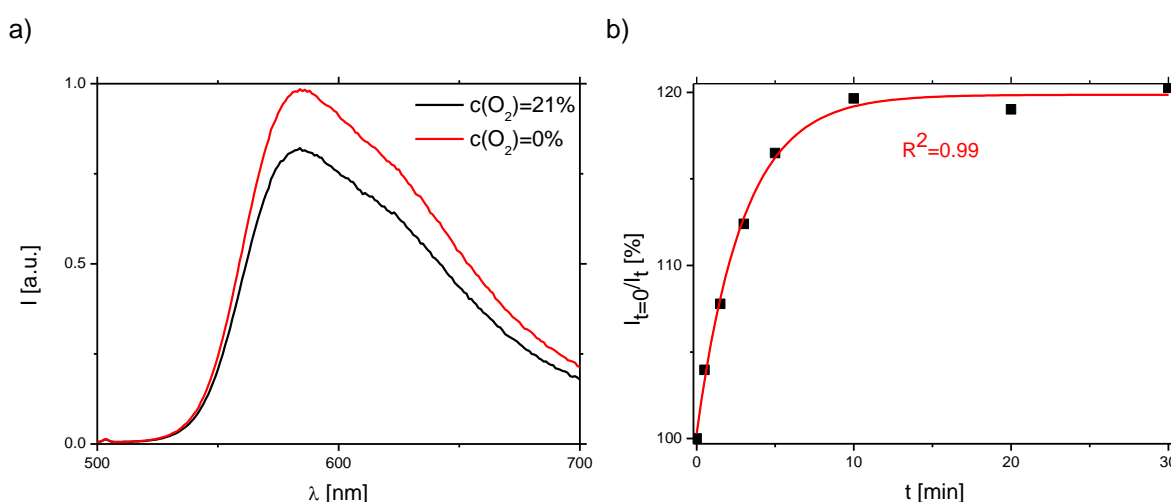
Figure 3.5: Intensity of the emission of Ru(phen)$_3$ in aerated and inert atmosphere (a) and kinetics of the maximum of emission during degassing.

Previous studies [26] showed that the intensity of the single emission of the probes suffers drifts related to the operating conditions. In order to develop a robust optical sensor, a second probe

(Coumarin) was dispersed for correcting related artifacts using the ratio of their intensity as the signal, which depends solely on the oxygen concentration.

The optical ratiometric sensor was placed in the sealed cell shown in Figure 3.2 within PDMS or BOPP films and the signal obtained by exciting and collecting the emission in situ with an optical fiber. The excitation wavelength was fixed at 325 nm in order to simultaneously excite both Coumarin and $Ru(phen)_3$. By looking at the emission spectra in aerated atmosphere ($C(O_2)$=21%) reported in Figure 3.6, it is possible to notice the emissions of the two probes: 382 nm for Coumarin and 590 nm for $Ru(phen)_3$. The emission of the $Ru(phen)_3$ is lower with respect to emission of the Coumarin once the sensor was excited at the wavelength of absorption of the Coumarin, whereas $Ru(phen)_3$ absorbs at 460 nm. However, the advantage of the combination of these two probes and the excitation at 325nm is to have two discernible peaks using a single wavelength of excitation. The difference in the emission spectra of the films is attributed to the different optical properties of PS and BOPP.
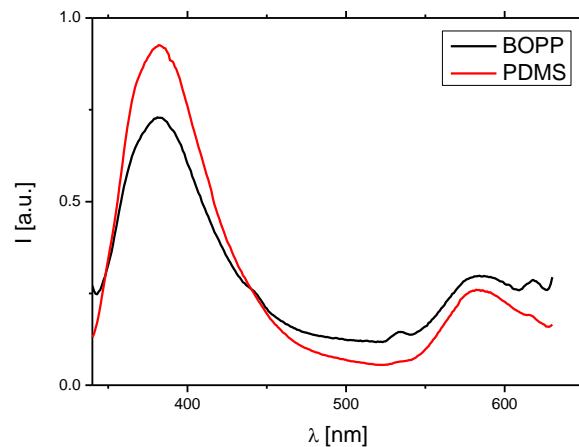
Figure 3.6: Emission of the optical sensor collected beyond PDMS and BOPP films.

The sensitivity of the sensor was evaluated by varying the oxygen concentration from 0% to 50%. By looking at the single emission it is possible to notice that the emission of Coumarin is not evidentially affected by the oxygen concentration. In fact the ratio of the intensity in the absence of oxygen (I_0) divided by the intensity of the emission at a certain oxygen concentration (I) is almost 1. On the other hand, the intensity of the emission of the Ruthenium complex is quenched by the oxygen and the ratio I_0/I increases by increasing the oxygen concentration. Nevertheless, it is possible to notice that, the intensity of the emission of the single probe is affected by errors; in particular, in the case of the PDMS. This is due to the fact that the feed of the gases in the chamber produces subtle variations of the pressure which slight move the optical sample, changing the focus of excitation and the optical path. This effect is more pronounced for experiments performed with the PDMS film, which is an elastomeric polymer, whereas BOPP is more rigid and the optical sensor is more properly fixed between the polymeric film and the porous support.

Nevertheless; the combination of the emission in the ratiometric signal allows for the correction of these artifacts obtaining a signal measurement depending solely on the oxygen concentration. In both cases the ratiometric response "R" linearly increased by increasing the oxygen concentration with a coefficient of determination (R^2) of 0.99, confirming the robustness of the optical sensor in real situation. Furthermore the two linear coefficients are really similar: 0.168 in the case of BOPP and 0.164 for PDMS, which is related to the exclusive sensitivity of Ru(phen)$_3$ to the oxygen concentration.
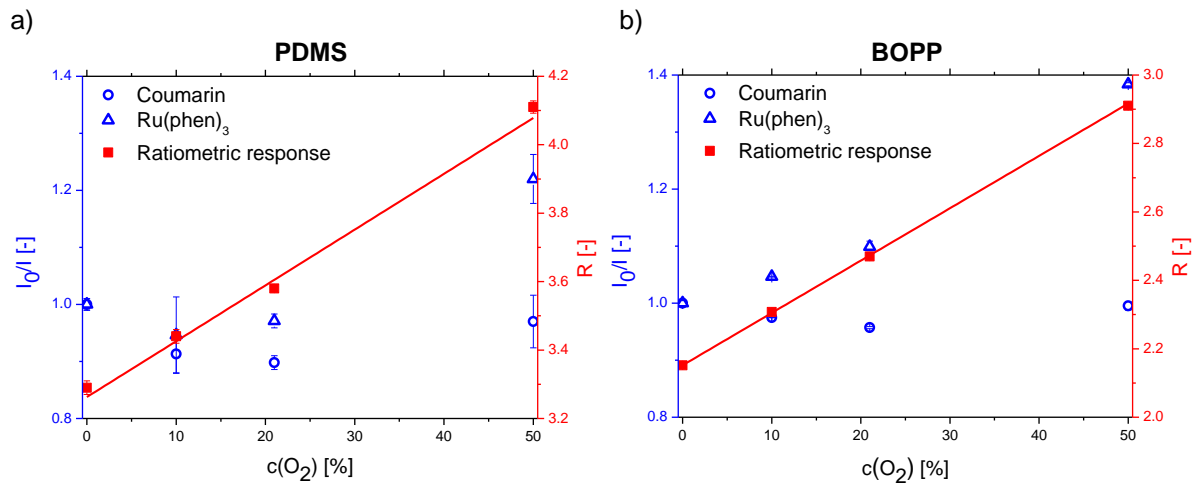
Figure 3.7: Calibration of the optical sensor in food packaging mimicking experiments.

3.3.2 Food packaging mimicking experiments

In Table 1 are reported the measured oxygen permeability values of the different polymeric materials employed in this work, evaluated using the set-up reported in Figure 3.4.

Table 3.1 Oxygen permeability and thickness of the optical sensor (PS) and the films used for food packaging simulations.

Film	Permeability [$cm^2\ s^{-1}$]	Thickness [μm]
PS	$(1.9\pm0.3)\ 10^{-8}$	144 ± 3
PDMS	$(2.7\pm0.3)\ 10^{-6}$	66 ± 4
BOPP	$(9.9\pm0.7)10^{-9}$	40 ± 4

PDMS is not commonly used in food packaging because of its high permeability to gases, in particular to oxygen. In fact, its permeability is two orders of magnitude higher than the observed for the optical sensor made of PS. This polymer is very much used in food packaging because it

combines moderate oxygen permeability with low cost, while limitations are related to its flexibility. Nevertheless, a lower permeability was observed for BOPP which is also widely used because of its high strength and puncture resistance combined with good barrier properties to moisture, gases and odors.

In Figures 3.7 and 3.8 are reported the results of the permeation of oxygen in an enclosed atmosphere sealed using PDMS or BOPP films, monitored by the optical sensor made of PS. The experimental results are compared with the predicted values evaluated using Eq.3.6 and employing the value of permeability obtained with independent experiments (Table 3.1).

In the case of PDMS, inert sealed atmosphere is equilibrated with the external atmosphere in terms of oxygen concentration in 3 hours. In fact, GC measurements confirmed that after 3 hours the oxygen concentration in the enclosed atmosphere was 21%, reaching the equilibrium with the external atmosphere. Furthermore, the evolution of the oxygen content with time in the sealed cell evaluated using the optical sensor is predicted by the model (Equation 3.6), assuming that the global permeability is given by the multilayer film combining the two polymers (PS and PDMS) as reported in Equation 3.5.
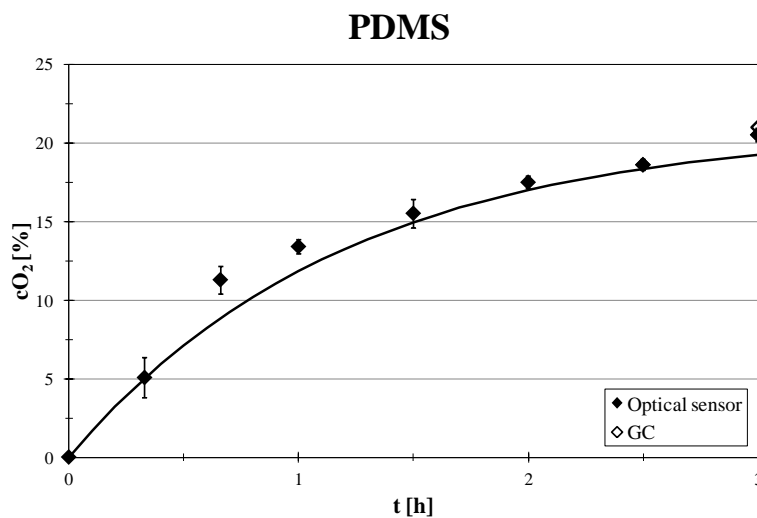
Figure 3.8: Oxygen concentration in the food packaging simulation for PDMS employing the ratiometric optical sensor. Results obtained using the optical sensor were predicted by the model and confirmed by chromatographic analyses (GC).

On the other hand, for the BOPP film, after 24 hours the oxygen concentration of the enclosed atmosphere increased from 0% to 3.6%. The line in Figure 3.8 is a simulation of the oxygen concentration inside the package using the values of the permeability of BOPP and PS presented in Table 3.1. However, as it can be noticed the experimental data is not fitted by the model in the first part of the experiment (solid line in Figure 3.8.b). This is due to the inaccuracy of Henry's law to describe the sorption in glassy polymers In fact, a dual mode sorption behavior is usually observed for the diffusion of small molecules in low concentrations through glassy polymers. It results from the combination their adsorption in the free-volume of the membrane and solution-

diffusion trough the polymeric chains. The model assumes two populations of molecules in the polymer: the ordinary dissolution in the continuous amorphous network and those in the cavity created by the additional free volume in the polymer [30]. At short times, the Langmuir adsorption is dominant since the free volume is filled in a short time, whereas Henry's law contributes at longer times since the dissolution of permeants in the polymeric network is slower. Therefore, in the beginning of the experiment a sigmoid curve can be fitted to the experimental data (dashed line in Figure 3.8.b). Nevertheless, after 24 hours the oxygen concentration measured by the sensor was 3.6%, which is very close to the value measured by GC analysis (3.1%) and predicted by the model using a constant permeability (2.8%). According to the model, the equilibrium of the enclosed atmosphere (21% of O_2) will be achieved after 600 hours (25 days) confirming the good barrier properties of BOPP.

a)

b)
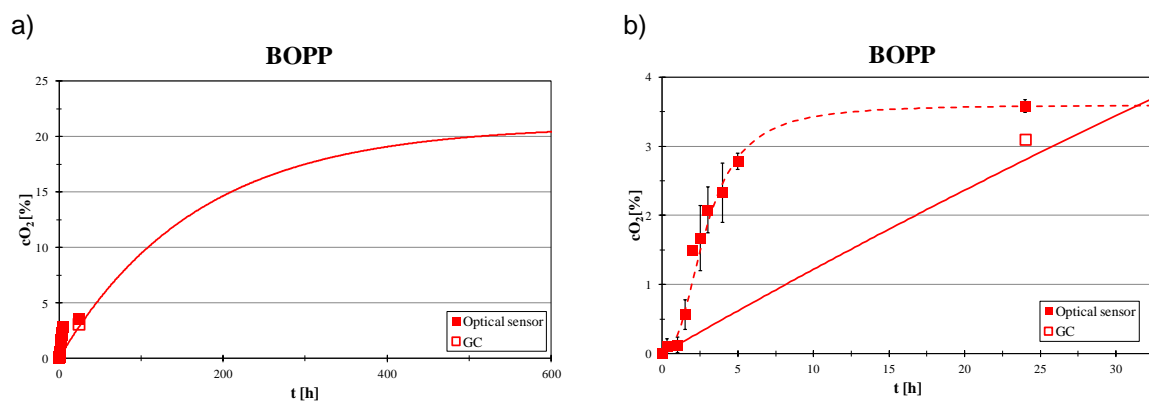
Figure 3.9: Oxygen concentration in the food packaging simulation for BOPP: a) Results obtaining using the optical sensor compared with by the model (constant permeability) and confirmed by chromatographic analyses (GC); b) Model (solid line), Dual mode model (dashed line) and results in the food packaging simulation for 24 hours using BOPP.

3.4 Conclusions

An optical sensor for oxygen monitoring was developed using Ru(phen)$_3$ as an oxygen sensitivity probe. The employment of Coumarin as a reference allowed for corrections of artifacts due to the operating conditions, which affected the emission of the oxygen sensitive probe. This strategy allowed the development of a robust optical sensor useful for on- line and non- invasive monitoring of oxygen concentration in real situations such as food packaging.

Experiments of food packaging simulation were performed by placing the optical sensor in an enclosed atmosphere using films of PDMS or BOPP. The experiments evidenced the sensitivity of the sensor for monitoring oxygen concentration variations due to the permeation of gases from the atmosphere to the package through polymer films with different oxygen permeabilities. Experiments carried out with PDMS evidenced the rapid response of the optical sensor in an atmosphere subjected to quick variations of oxygen concentration. On the other hand, it was possible to evaluate the sensitivity of the developed sensor at low oxygen concentration by measuring the evolution oxygen concentration in BOPP package.

Furthermore the solution diffusion model, with constant permeability successfully predicted the evolution of oxygen concentration inside the package in the case of PDMS, whereas a dual-mode sorption model was observed for BOPP package at low temporal scale where.

3.5 References

[1] Siracusa, V, Rocculi, P, Romani, S, and Della Rosa, M. Biodegradable polymers for food packaging: a review. *Trends in Food Science & Technology*, 19(12): 634-643, 2008.

[2] Marsh, K, and Bugusu, B. Food Packaging—Roles, Materials and Environmental Issues. *J. of Food Science*, 72(3): 39-55, 207.

[3] Miller, K S, and Krochta, J M. Oxygen and aroma barrier properties of edible films: A review. *Trends in Food Science & Technology* 8(7): 228-237, 1997.

[4] Brody, A L, Strupinsky, B R, and Kline, R. Introduction, In: *Active Packaging for Food Applications*. CRC Press Book, 2001.

[5] Duncan, T V. Applications of nanotechnology in food packaging and food safety: barrier materials, antimicrobials and sensors. *J. Colloid Interface Sci.*, 363(1): 1-24, 2001.

[6] Jung, J, Puligundla, P, and Ko, S. Proof-of-concept study of chitosan-based carbon dioxide indicator for food packaging applications. *Food Chem.*, 135(4): 2170-2174, 2012.

[7] Smigic, N, Djekic, I, Tomasevic, I, Miocinovic, J, and Gvozdenovic. Implication of food safety measures on microbiological quality of raw and pasteurized milk. *Food Control* 25(2): 728-731, 2012.

[8] Figoli, A, Mascheroni, E, Limbo, S, Drioli, E. Membranes for Food Packaging, In: *Membrane Technology: Membranes for Food Applications*. Wiley Blackwell, 2010.

[9] Silvestre, C, Duraccio, D, and Cimmino, S. Food packaging based on polymer nanomaterials. *Progress in Polymer Science*, 36(12): 1766-1782, 2011.

[10] Kuswandi, B, Restyana, J A, Abdullah, A, Heng, L Y, and Ahmad, M. A novel colorimetric food package label for fish spoilage based on polyaniline film. *Food Control,* 25(1): 184-189, 2012.

[11] Mills, A. Oxygen indicators and intelligent inks for packaging food. *Chem. Soc. Rev.*, 34(12): 1003-1011, 2005.

[12] Baldini, F, Bacci, M, Cosi, F, and Bianco, A D B. Absorption-based optical-fibre oxygen sensor. *Sensors and Actuators B*, 7(1-3): 752-757, 1992.

[13] Del Bianco, A, Baldini, F, Bacci, M, Klimant, I, and Wolfbeis, O S. A new kind of oxygen-sensitive transducer based on an immobilized metallo-organic compound. *Sensors and Actuators B,* 11 *Sensors and Actuators B* 11: 347-350, 1993.

[14] Erskine, R W, and Field, B O. Reversible oxygenation. *Struc Bond*, 28: 1-50, 1976.

[15] Lawrie, K, Mills, A, and Hazafy, D. Simple inkjet-printed UV-activated oxygen indicator. *Sensors and Actuators B*,176: 1154-1159, 2013.

[16] Amao, Y. Probes and Polymers for Optical Sensing of Oxygen. *Microchimica Acta*, 143(1): 1-12, 2003.

[17] Klimant, I, Kühl, M, Glud, R, and Holst, G. Optical measurement of oxygen and temperature in microscale: strategies and biological applications. *Sensors and Actuators B*, 38(1-3): 29-37, 1997.

[18] Quaranta, M, Borisov, S M, and Kliman, I. Indicators for optical oxygen sensor. Bioanal Rev., 4(2-4): 115-157, 2012.

[19]   Rharbi, Y, Yekta, A, and Winnik, M A. A Method for Measuring Oxygen Diffusion and Oxygen Permeation in Polymer Films Based on Fluorescence Quenching. Anal. Chem, 71(22): 5045-5053, 1994.

[20]   Wolfbeis, O S. Fiber optic chemical sensors and biosensors. Anal. Chem., 80(12):4269-4823, 2008.

[21]   Dobrucki, J W. Interaction of oxygen-sensitive luminescent probes Ru(phen)32+ and Ru(bipy)32+ with animal and plant cells in vitro: Mechanism of phototoxicity and conditions for non-invasive oxygen measurements. Journal of Photochemistry and Photobiology B, 65(2-3): 136-144, 2001.

[22]   Draxler, S, Lippitsch, M E, Klimant, I, Kraus, H, and Wolfbeis, S O. Effects of polymer matrices on the time-resolved luminescence of a ruthenium complex quenched by oxygen. J. Phys. Chem., 99(10): 31623167, 1995.

[23]   Kane, J, Martin, R, and Perkovich, A. Ratiometric fluorescence method of making for measuring oxygen. US Patent 5,728,422, 1998.

[24]   Park, E J, Reid, K R, Tang, W, Kennedy, R T,and Kopelman, R. Ratiometric fiber optic sensors for the detection of inter- and intra- cellular dissolved oxygen. J. Mater. Chem., 15: 2913-2919, 2005.

[25]   Xu, H, Aylott, J W, Kopelman, R, Miller, T J, and Philbert, M A. A realtime Ratiometric method for the determination of molecular oxygen inside living cells using sol–gel based spherical optical nanosensors with applications to rat C6 glioma. Anal. Chem., 73(17): 4124-4133, 2001.

[26]   Santoro, S, Moro, A J, Portugal, C M, Crespo, J G, Coelhoso, I M, Lima, J C, 2016, Development of Oxygen and Temperature Sensitive Membranes Using Molecular Probes as Ratiometric Sensor, Journal of Membrane Science (submitted).

[27]   Cywinski, P J, Moro, A J, Stanca, S E, Biskup, C, and Mohr, G J. Ratiometric porphyrin-based layers and nanoparticles for measuring oxygen in biosamples. Sensors and Actuators B, 13:472-477, 2009.

[28]   George, S C, and Thomas, S. Transport Phenomena through polymeric system. Prog. Polym. Sci., 26(6): 985-1017, 2001.

[29]   Zolandz, R R, and Fleming, G K. Gas Permeation theory, In: Membrane Handbook. Springer Link, 2001.

[30]   Guo, J, and Barbari, T A. A Dual Mode, Local Equilibrium Relaxation Model for Small Molecule Diffusion in a Glassy Polymer. Macromolecules, 41(1): 238-245, 2008.

Chapter 4

Development of Fluorescent Nano-thermometers for temperature monitoring on membrane surfaces

4.1 Introduction

Temperature is a key parameter affecting mostly all the chemical processes, included membrane processes. Nowadays, thermocouples are commonly used as accurate and inexpensive technologies with a rapid response time for temperature detection. However, the miniaturization of the sensors is the most critical issue of these technologies. In fact, monitoring the temperature with a high spatial resolution at micron and submicron scale is typically demanded in innovative research fields such as nanomedicine, biotechnology and microfluidics [1-5].

In membrane technology, temperature is a fundamental parameter, affecting the performance of every membrane process. In fact temperature plays a key role in membrane processes, in particular in those where the driving force is guaranteed by gradient of temperature across the membrane, such as direct contact membrane distillation. In these cases, the heat transfer between the boundary layer of streams and membrane surface produces a temperature profile along the membrane surface (thermal polarization) witch dramatically affects the global performance of the process [6-7]. Efforts towards a better understanding of this phenomenon have been performed through the development of modelling studies. However, these studies have been limited by the lack of experimental data, since the non-invasive monitoring of temperature at the membrane surface with high enough spatial resolution conditions is a challenging task. *Ali et al.* studied the effect of various hydrodynamic and thermal conditions on heat and mass transport in direct contact membrane distillation using a cell containing different thermocouples [8]. Optical techniques present the advantage of a non invasive monitoring and were employed for evaluation of temperature polarization in spacer-filled by means of Thermochromic Liquid Crystals [9].

In the recent years, luminescent molecular probes have been considered a powerful tool for the monitoring of the temperature at nanoscale, since the properties of their emissions (fluorescence or phosphoresce) are generally affected by the temperature [10-12]. Luminescent nanoparticles have been studied as a promising alternative to molecular probes since their immobilization in nanoparticles increases their optical properties (i.e. photostability, emission quantum yield, isolation from possible quenchers) [13,14]. Luminescent molecular probes silica-doped nanoparticles have been considered ideal for monitoring biochemical processes, since they are chemically inert, biocompatible, not subjected to microbial attack and with easy tailoring [15,16]. Several molecular probes were successful immobilized in growing silica nanoparticles for the development of nano-thermometers, such as rhodamine 6G, acridine orange, $Ru(bpy)_3$ and $Ru(phen)_3$ [17-21]. In fact, Ruthenium(II) polypyridyl complexes, in particular $Ru(phen)_3$ and $Ru(byp)_3$, are widely explored as luminescent probes for temperature detection because of the strong temperature dependence of their photochemical properties [22]. The thermal quenching of the emission is attributed to the thermal-driven non-radiative decay of the excited state, which leads to a decrease of the intensity of the emission and life time of the excited state, described by an Arrhenius-type model, approximated to a linear relationship at low temperature [23].

Temperature sensitive paints (TSP) based on the dispersion of emissive doped nanobeads or nanoparticles are successful employed for two dimension temperature mapping in aerodynamics, providing information on aerodynamic performance and on heat transfer in structures [24,25]. This

technology could be of interest for the development of smart coatings for monitoring the temperature on membrane surfaces.

The aim of this work is the development of a nano-thermometer for the measurement of the temperature on the surface of a membrane based on the attachment of fluorescent silica nanoparticles on its surface. Two different approaches will be evaluated for the immobilization of Ru(phen)$_3$ in silica nanoparticles: i) immobilization of the probe in the silica matrix (Ru(phen)$_3$-Core SiO$_2$NPs), ii) immobilization of the probe in an external shell (Ru(phen)$_3$-Shell SiO$_2$NPs) grown in a second step on bare silica nanoparticles (Bare SiO$_2$NPs). Efforts have been devoted on finding a compromise between the photophysical properties and the nanoparticle morphology, in particular, size and polydispersity. Subsequently, Ru(phen)$_3$-Shell SiO$_2$NPs will be functionalized to confer to the nanoparticles an hydrophobic behaviour and then immobilized on membrane surface via dip-coating procedure. The stability of the attached nanoparticles will be studied, as well as, the sensitivity to the temperature of the modified membrane.

In this work, silica nanoparticles doped with a luminescent molecule sensitive towards the temperature are proposed as an innovative technology for non–invasive, on-line, in-situ monitoring of the temperature in different processes. In particular, the membrane community will be benefit from this tool and will be able to validate theoretical models and answer important questions related to heat transfer and temperature polarization in membrane processes.

4.2. Experimental section

4.2.1. Materials

SiO$_2$NPs were prepared employing Tetraethoxysilane (TEOS, Sigma–Aldrich, Spain), ammonium hydroxide (Ammonia, ACS reagent 28%, Spain), absolute ethanol (EtOH, Sigma Aldrich, Spain) and distilled water. Dodecyltriethoxysilane employed for the functionalization of the nanoparticles and the molecular probe tris(phenantroline)ruthenium(II) chloride (Ru(phen)$_3$) was purchased from Sigma–Aldrich (Spain).

Hydrophobic porous membranes made of poly (vinylidenefluoride) ((PVDF) Solef® 6012, Solvay Specialty Polymers, Italy) were prepared using the non-solvent induced phase separation (NIPS) technique. The solvent was N-methylpyrrolidone (NMP, 99%, Carlo Erba Reagents, Spain), whereas distilled water and lithium chloride (LiCl, 98%, Carlo Erba Reagents, Spain) were employed as additives. The phase inversion step was induced by a coagulation bath containing distilled water and propan-2-ol (99.9%, Carlo Erba Reagents, Spain) 50/50 wt./wt. PDMS elastomer (Sylgard 184, Dow Corning, USA) was used to attach silica nanoparticles on membrane surface.

4.2.2. Synthesis of SiO$_2$NPs

For the preparation of the tris(phenantroline)ruthenium(II)-doped silica nanoparticles two different immobilization approaches were employed: a) inside of a silica core, b) in a silica shell grown on a bare silica core. The two different methods are summarized in Figure 4.1.
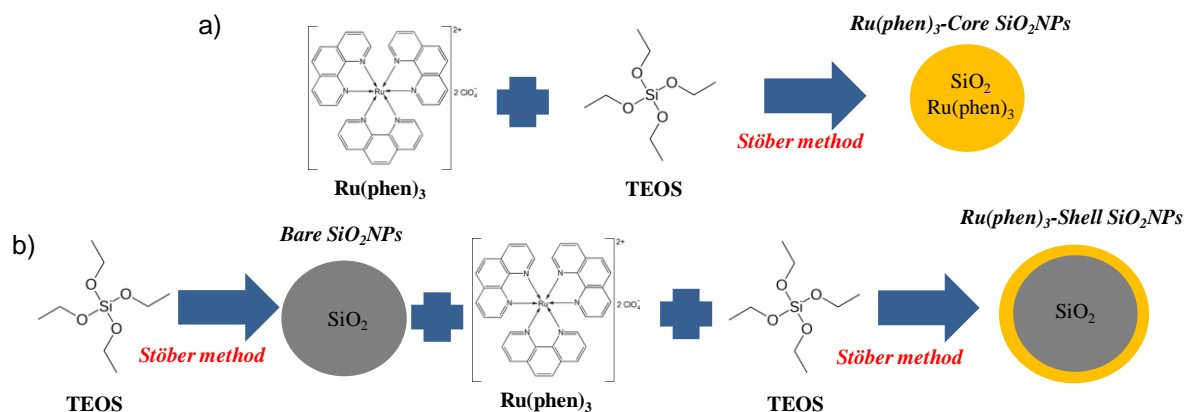
Figure 4.1: Scheme of preparation of Core and Shell doped silica nanoparticles.

Bare SiO$_2$NPs were synthesized following the procedure proposed by Stöber [16], which is based on the hydrolysis and condensation reaction of TEOS in presence of NH$_3$ and H$_2$O in EtOH (molar ratio TEOS: EtOH: NH$_4$OH$_{aq}$=1: 187: 22). Briefly, 6 ml of ammonia were added to 43.1 ml of ethanol and stirred for 5 min. Subsequently, 0.91 ml of TEOS was added to the basic solution. The solution was magnetically stirred at 400 rpm for 3 hours at 50°C. The SiO$_2$NPs were collected by centrifugation, washed 3 times with ethanol and re-dispersed in 20 ml of water.

Ru(phen)$_3$-Core SiO$_2$NPs were prepared by immobilizing Ru(phen)$_3$ in SiO$_2$ during the Stöber reaction. In fact, the method of the preparation is similar to that one employed for the preparation of Bare SiO$_2$NPs. However, in this case the Ru(phen)$_3$ was solubilized in the alcoholic solution (0.04 mg/ml). The concentration of Ru(phen)$_3$ with respect to SiO$_2$ is 0.066mol% (0.8wt%).

Ru(phen)$_3$-Shell SiO$_2$NPs were prepared by immobilizing the molecular probe in a shell of silica grown on the surface of bare core SiO$_2$NPs based on the procedure previously reported by *Mirenda et al* [26] for tris(bipyridine)ruthenium(II)-doped silica nanoparticles. Two parameters have been optimized for the synthesis of Ru(phen)$_3$-Shell SiO$_2$NPs: i) the amount of Ru(phen)$_3$ fluorophore on the silica shell, that was varied from 0 to 27%wt, in respect to the total silica weight on the shell and ii) the shell size, i.e. amount of TEOS and chemicals for growing the shell (see Table 4.1) which were decreased with respect to previous reported procedure (Ru(phen)$_3$-Shell SiO$_2$NPs 100%) by a factor of 2 (Ru(phen)$_3$-Shell SiO$_2$NPs 50%), 4 (Ru(phen)$_3$-Shell SiO$_2$NPs 25%), 10 (Ru(phen)$_3$-Shell SiO$_2$NPs 10%) and 20 (Ru(phen)$_3$-Shell SiO$_2$NPs 5%). In all the cases the weight fraction of fluorophore in the silica shell was kept constant at 1.35%wt.

The procedure for the synthesis is as follows in the case of Ru(phen)$_3$-Shell SiO$_2$NPs 100%, (see Table 4.1), 2.8 micromole of Ru(phen)$_3$ solubilized in 2 ml of EtOH and 0.55 ml of TEOS were added to a solution of 15 ml of bare core SiO$_2$NPs in EtOH (c=5.5 mg ml^{-1}). Then, 1.5 ml of NH$_3$

(30%) diluted with 12 ml of H_2O were added in order to initiate the condensation of TEOS. The solution was stirred for 2 hours at 40°C and then kept overnight at room temperature. Finally the $Ru(phen)_3$-Shell SiO_2NPs were collected by centrifugation, washed with ethanol and dispersed in 15 ml of EtOH. In this case, the $Ru(phen)_3$-Shell SiO_2NPs contain equimolar amounts of the molecular probe with respect to the $Ru(phen)_3$ -Core SiO_2NPs.

After washing (3 times with EtOH), the nanoparticles were re-dispersed in water.

Table 4.1: Preparation of solutions used for the growth of the shell on bare SiO_2NPs.

$Ru(phen)_3$-Shell SiO_2NPs	100%	50%	25%	10%	5%
EtOH+ Bare SiO_2NPs [ml]	15	15	15	15	15
$Ru(phen)_3$ [µmol]	2.80	1.40	0.70	0.28	0.14
TEOS [ml]	0.55	0.275	0.138	0.055	0.027
H_2O [ml]	12	6	3	1.2	0.6
Ammonia [ml]	1.5	0.75	0.375	0.15	0.075
$mSiO_2$ shell/m BareSiO_2NPs	1.788	0.894	0.447	0.179	0.089

4.2.3 Immobilization of SiO_2NPs on PVDF membranes

PVDF membranes were prepared according to the protocol reported in literature by *Drobek et al.* [27]. Briefly, PVDF (18wt%) was slowly added under magnetically vigorous stirring to NMP solution containing LiCl (2wt%) and H_2O (5wt%) as pore former additives. The polymeric solution was stirred overnight at 80°C to guarantee the complete dissolution of the polymer and then kept at 80°C for 30 min without stirring to remove air bubbles. Finally the dope solution was cast by means of a knife of 0.25 mm and immersed in the coagulation bath (50wt% H_2O-50wt% propan-2-ol) for 3 hours ensuring the NIPS process. Finally, the coagulated membranes were washed for 3 hours in a pure water bath to remove all the residual solvents and then were dried for 24 hours at 50°C.

In order to turn the hydrophilic character of silica into hydrophobic, $Ru(phen)_3$-Shell SiO_2NPs were functionalized with Dodecyltriethoxysilane, a TEOS derivative with long aliphatic chains. 40 ml of $Ru(phen)_3$-Shell SiO_2NPs dispersed in EtOH were centrifuged to remove the solvent and re-dispersed in toluene (40 ml). The functionalization was carried out at 60°C under reflux (N_2 inert atmosphere): the solution was heated-up to 60°C and magnetically stirred, then 1 ml of dodecyltriethoxysilane was injected. After 3 hours, the solution was cooled-down at room temperature and the nanoparticles washed with EtOH 3 times in order to remove traces of toluene.

Hydrophobic Ru(phen)$_3$-Shell SiO$_2$NPs were immobilized on surfaces of PVDF membranes via dip-coating procedure. PDMS was employed to favor the adhesion of the NPs on PVDF surfaces and solubilized in toluene at a concentration of 0.4mg ml^{-1}. After the solubilization of PDMS (3 hours), functionalized 100% Ru(phen)$_3$-Shell SiO$_2$NPs (0.4mg ml^{-1}) were added to the polymeric solution and stirred for 2 hours. Then, the silicon curing agent (wt% 40.0-60.0 Dimethyl, methylhydrogen siloxane) was added (10wt% with respect to PDMS). Finally, the polymeric solution was sonicated for 30 min. Subsequently, the dip-coating was performed by immersing PVDF membranes for 5 min in the PDMS solution containing Ru(phen)$_3$-Shell SiO$_2$NPs. The membranes were then dried for 2 hours at room temperature, immersed for 5 hours in distilled water to remove non-immobilized NPs and dried once again.

4.2.4 Characterization

SEM imaging analyses were acquired in a scanning electron microscope, FEI Quanta FEG-250. TEM images were obtained with a transmission electron microscope FEI TECNAI T20, working at 200 kV. These microscopes belong to the Laboratory of Advanced Microscopies, LMA, in the installations at the Institute of Nanoscience of Aragon (INA), University of Zaragoza. Particle-size distribution and shell thickness of the resulting nanoparticles during the different synthesis steps were obtained using statistical analysis (N>100 particles) of SEM images. Results were compared with the NPs size and polydispersion evaluated by Dynamic Light Scattering (DLS) using a Brookhaven 90 (Brookhaven Instruments Corp.) photo correlation spectroscope. The same equipment was employed for Z-Potential measurements.

Experiments of fluorescence were performed using a LS 55 Fluorescence Spectrometer (Perkin-Elmer) setting the excitation wavelength at 450 nm, excitation and emission slits at 7.5 nm and a velocity of scanning of 400 nm/min. For evaluating the sensitivity towards the temperature, 0.5 ml of the prepared SiO$_2$NPs were diluted to 10 ml, heated-up with a thermostatic bath at different temperatures and, then, 3 ml were transferred into a quartz cuvette, evaluated the real temperature by means of a thermocouple and the intensity of the emission was measured.

In the case of the evaluation of the fluorescence of PVDF membranes, the sample was placed in the cuvette on a porous support of glass fixing the angle between the exciting source and the membrane surface at 45°C.

The hydrophobicity of the membranes was evaluated by contact angle measurements employing a Dataphysics OCA Series (Neurtex instruments) equipped with 500 μL Hamilton syringe. Membrane porosity was determined by gravimetric method following the procedure reported in literature [28]. Briefly, membranes were weighted dry (w$_d$) and wet after the immersion in kerosene for 24 hours (w$_h$). Porosity (P) was calculated according to the following equation:

$$P = \frac{\frac{w_h - w_d}{\rho_w}}{\frac{w_d}{\rho_{PVDF}} + \frac{w_h - w_d}{\rho_w}} ; \quad (4.1)$$

where ρ_w is the kerosene density (0.82g cm^{-3}) ρ_{PVDF} is the PVDF density (1.78 g cm^{-3} [29]).

Liquid Entry Pressure (LEP) was determined by placing the membrane in a membrane module filled up with distilled water. The pressure of the compartment was increased 0.2 bar every 5 minutes until water passed through the membrane (LEP).

4.3 Results and Discussion

4.3.1 Optimization of fluorescent silica nanoparticles as nanothermomethers

Bare SiO_2NPs were prepared using the well-known Stöber method based on the hydrolysis followed by the condensation of TEOS catalyzed by ammonia. According to SEM analysed micrographs (Figure 4.2), monodispersed Bare SiO_2NPs with an average diameter of 296±19 nm were prepared, as confirmed by DLS measurements (275±16 nm) reported in Table 4.2. Bare SiO_2NPs showed a narrow size distribution with a polydispersity index of 0.05. On the other hand; Ru(phen)$_3$-Core SiO_2NPs presented a wide size distribution showing a polydispersity index of 0.26. Moreover, the average diameter was 555±90 nm according to SEM analyses and 544±88 nm according to DLS measurements. On the contrary, Ru(phen)$_3$-Shell $SiO_2$100%NPs prepared by coating Bare SiO_2NPs with an extra layer of SiO_2 load with Ru(phen)$_3$ presented a narrow size distribution (polydispersity index of 0.05) with an average diameter of 419±20 nm according to SEM picture, coherent with the value of 394±6 nm obtained by DLS measurements.

Table 4.2: Size and polydispersity index of Bare, Ru(phen)$_3$-Core and Ru(phen)$_3$-Shell SiO_2NPs.

SiO_2NPs	*Diameter [1] (nm)*	*Diameter[2] (nm)*	*Polydispersity index[2]*
Bare	296±19	275±16	0.05
Ru(phen)$_3$-Core	555±90	544±88	0.26
Ru(phen)$_3$-Shell 100%	419±20	394±6	0.05

[1]SEM analysis   **[2] DLS analysis**
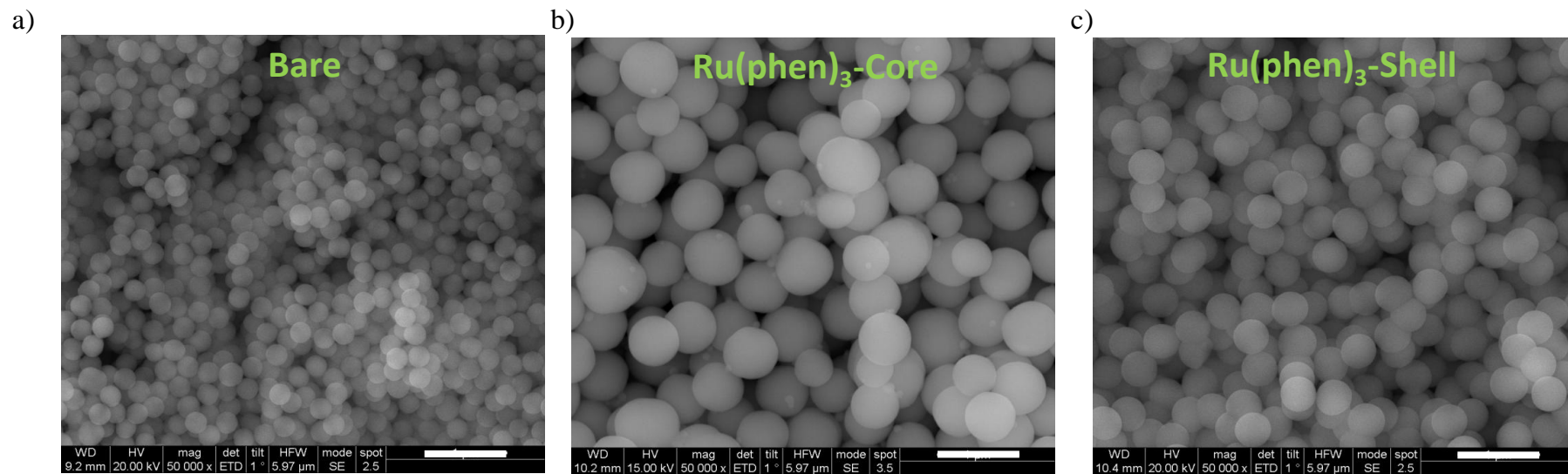
Figure 4.2: SEM pictures of a) Bare, b) Ru(phen)₃-Core and c) Ru(phen)₃-Shell SiO₂100% NPs. The size of the scale bar corresponds to 1 micron in all the images.
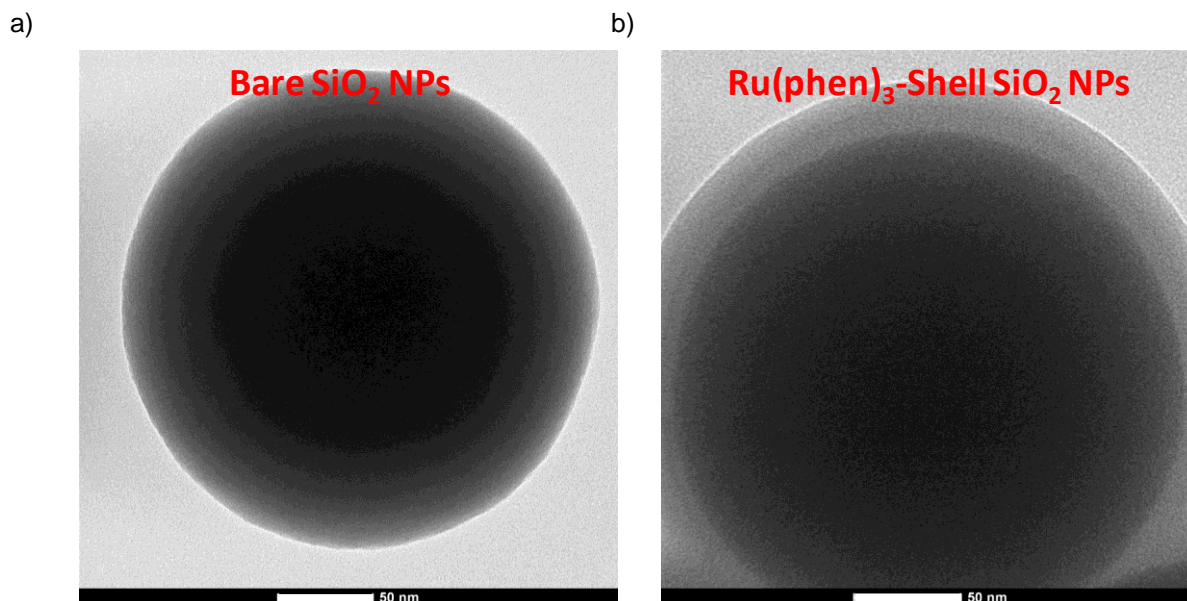
Figure 4.3: TEM picture of Bare SiO₂NP (a) and Ru(phen)₃-Shell SiO₂ 5%NP. The size of the scale bar corresponds to 50nm in all the images.

In general, the Stöber protocol generates electrostatically stabilised, spherical and monodisperse particles. This is consequence of the hydrolysis and condensation of silica precursors, such as TEOS, in ethanol solution in the presence of aqueous ammonium hydroxide mixture as a condensation reaction catalyst. Indeed, in the case of Bare SiO_2NPs homogeneous nucleation forms silica particles of 296 nm in size.

This method is rather simple and it can enable the incorporation of both organic and inorganic markers [30]. However, the immobilization of the probes may lead to a non-uniform particle size [31]. The high polydispersion of Ru(phen)₃-Core SiO_2NPs suggested that the injection of the complex of ruthenium disturbed the Stöber reaction due to the steric effect of phenantroline ligands affecting the hydrolysis and the condensation reactions. On the contrary, the Ru(phen)₃-Shell grew on a well-organized structure as the Bare SiO_2NPs leading to a narrow size distribution and a low polydispersity index (Figure 4.2 and Table 4.2). The presence of the external Ru(phen)₃-Shell is also confirmed by TEM analyses of the single NPs (Figure 4.3). In fact, the diameter of the Ru(phen)₃-Shell SiO_2 NP is higher compared to that one observed for Bare SiO_2NPs due to the condensation of extra amount of silica. Moreover, at high voltage the Ru(phen)₃-Shell appeared lighter due to the burning of the organic ligands of the complex of Ruthenium.

In Figure 4.4 are reported the excitation and emission spectra of Bare, Ru(phen)₃-Core and Ru(phen)₃-Shell 100% SiO_2NPs. Measurements evidenced that Bare SiO_2NPs are not emissive, as expected, whereas the immobilization of the molecular probe in silica conferred to NPs luminescent properties. In fact, an evident peak of emission with a maximum at 590 nm by exciting the NPs dispersed in water at 450 nm (maximum of excitation). Moreover, Ru(phen)₃-Shell SiO_2NPs prepared by the immobilization of the molecular probe in an external shell made of silica, growth in a second

step, presented higher emission with respect to those prepared by the injection of the luminophore at the beginning of the Stöber reaction (Ru(phen)$_3$-Core SiO$_2$NPs). In fact, the hydrolysis and condensation of TEOS is fast under the catalysis of the ammonia and the complex of Ruthenium molecules tend to aggregate in the silica core leading to non emissive aggregates of the molecular probe by introducing Ru(phen)$_3$ at the beginning of the reaction [33]. On the other hand, if the luminophores were added in a second step (Ru(phen)$_3$-Shell SiO$_2$NPS), they will be gradually absorbed by polar interaction on the layers of the growing silica shell upon the deposition of the remaining monomers of silica.
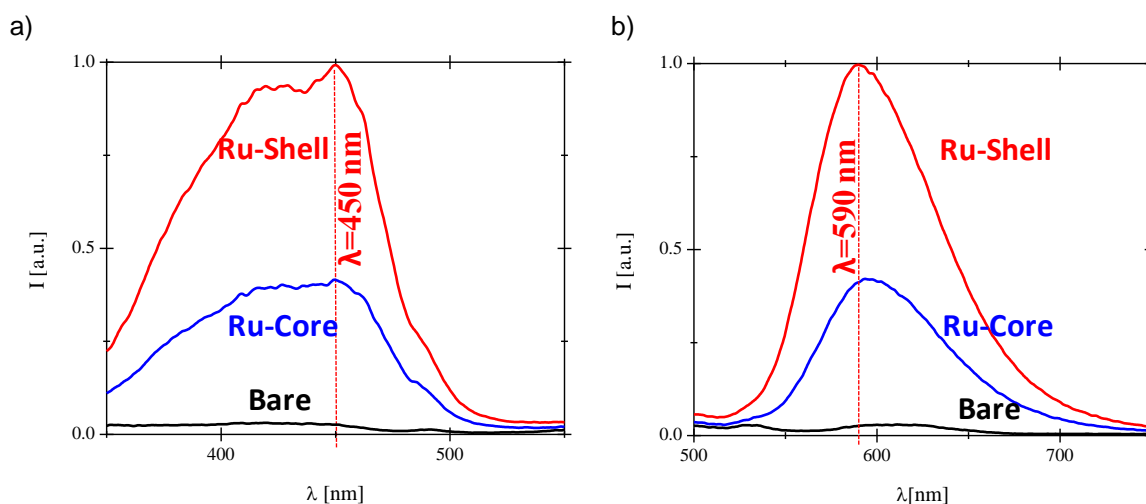
Figure 4.4: Normalized a) excitation and b) emission spectra of Bare, Ru(phen)$_3$-Core and Ru(phen)$_3$-Shell 100% SiO$_2$NPs.

As shown in Figure 4.5, by increasing the amount of the luminescent probe till 1.35 wt% the emission from the nanoparticles increased as expected. On the contrary, for values above 1.35% the intensity of the emission decreased. This is due to the fact that increasing the amount of the probes the formation of non-emissive aggregates is favored. Moreover, luminescent activity was noticed in the supernatant solution evidencing that Ru(phen)$_3$ was partially immobilized in the silica matrices due to the limited number of sides of interaction and the relatively fast growth of the Shell.

For these reasons, Ru(phen)$_3$-Shell SiO$_2$NPs were doped with different amounts of Ru(phen)$_3$ by fixing their concentration with respect to the SiO$_2$ used to make the Shell at a value of 1.35wt% in order to maximize the intensity of the emission.
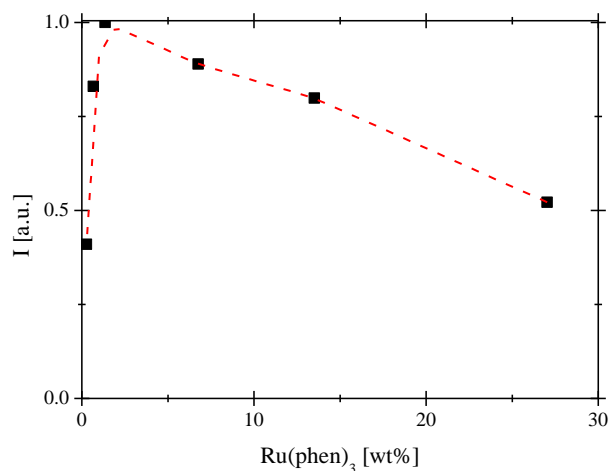
Figure 4.5: Normalized Intensity of emission with respect to SiO₂ 5% NPs doped with 1.35 wt% of Ru(phen)₃ at 590 nm of Ru(phen)₃-Shell SiO₂ 5% NPs prepared with different concentrations of Ru(phen)₃.

The sensitivity of the emission of SiO_2NPs doped with Ru(phen)$_3$ is shown in Figure 4.6 by plotting the maximum of the emission (590 nm) as a function of the temperature. In both cases, Ru(phen)$_3$-Shell 100% and Ru(phen)$_3$-Core SiO_2NPs the intensity of the emission linearly decreased by increasing the temperature of the aqueous solution. This is due to the fact that the increase of the temperature favours the non-radiative deactivation pathways of the molecular probe, in particular internal conversion. During the internal conversion, the electronic energy is converted to the vibrational energy of the molecular probe itself accounting for the commonly observed decrease in fluorescence/phosphorescence intensity with temperature rising [34].
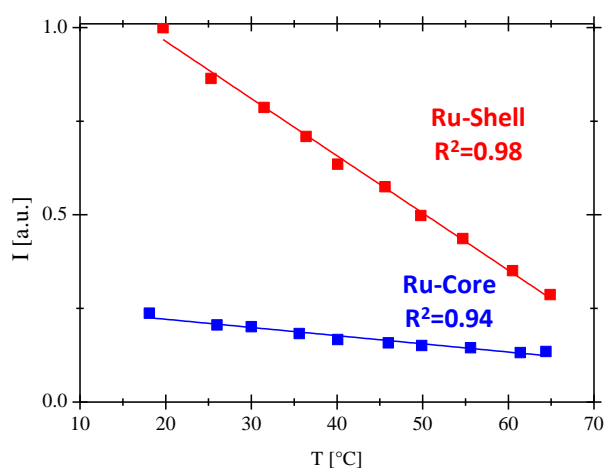
Figure 4.6: Temperature sensitivity of the maximum emission (590 nm) of Ru(phen)₃-Core and Ru(phen)₃-Shell SiO₂ 100%NPs.

Furthermore Ru(phen)$_3$-Shell 100% SiO$_2$NPs showed higher sensitivity to the temperature with respect to Ru(phen)$_3$-Core SiO$_2$ NPs. In fact a decrease of 1.45% °C^{-1} was observed in the emission of Ru(phen)$_3$-Shell SiO$_2$NPs, comparable with the data reported in literature for Ru(byp)$_3$-Shell SiO$_2$NPs [26], whereas a lowering of 0.37 % °C^{-1} was recorded in the case of Ru(phen)$_3$-Core SiO$_2$NPs. The dye-SiO$_2$ architectures dramatically affect the optical properties of the luminophore due to different bonding and spatial hindrance. Studies have shown that doped core NPs present a considerable excimeric emission, whereas a monomeric emission is usually observed in the Shell leading different responses of the emission to external factors [35]. Finally, it is obvious that luminophore immobilized on the external Shell are more prone to variations of temperature since they are more exposed to the water. On the other hand, the Ru(phen)$_3$ immobilized in the Core of NPS is less prone to change of the temperature of aqueous solution and others environmental parameters. Ru(phen)$_3$-Shell SiO$_2$NPs showed more promising results as nano-thermometer on the basis of their uniform shape combined with high emission and sensitivity towards the temperature. As reported in Table 4.1, different amount of TEOS were employed for the preparation of the shell made of silica in order to tune the properties of the developed nano-thermometer. Results in terms of Ru(phen)$_3$-Shell SiO$_2$NPs diameter and shell thickness are reported in Figure 4.7.
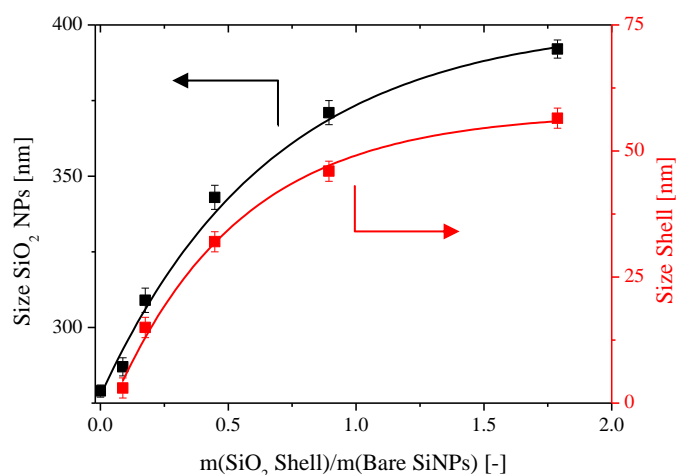
Figure 4.7: Particle size (black) and shell thickness (red) as a function of the mass ratio of silica precursor employed to grow the shell and the mass of Bare SiO$_2$NPs coated. The values correspond to DLS measurements.

Measurements of the size of the NPs confirmed the presence of the external shell. In fact the diameter of the of the SiO$_2$NPs exponentially increased from 275 nm observed for Bare SiO$_2$NPs to 394 nm for 100% Ru(phen)$_3$-Shell SiO$_2$NPs as a function of the amount of SiO$_2$ employed to make the shell. This is due to the fact that the thickness of the shell exponentially increased by increasing the silica precursor employed during the preparation, as expected, from 3 nm (5% Ru(phen)$_3$-Shell SiO$_2$) to 57 nm (100% Ru(phen)$_3$-Shell SiO$_2$). On the other hand, the growth of the shell did not affect the polydispersity of the nanoparticles which is in all the cases of ca. 0.05.

From the emission spectra reported in Figure 4.8, it is possible to notice that the intensity of the emission increase by increasing the total amount of molecular probe immobilized in the shell. In particular, the intensity of the maximum of emission (590 nm) linearly increased by increasing the molar concentration of Ru(phen)$_3$ immobilized in the Ru(phen)$_3$-Shell SiO$_2$NPs (Figure 4.9.b). This is due to the fact that the total amount of the luminophore in the aqueous solution containing the NPs increases as the shell size increases and the intensity of the emission, I, linearly increases with the concentration of the luminescent molecule (c) as predicted by the following equation:

$$I = kI_{exc}\Phi[\varepsilon bc]; \quad (4.2)$$

where I$_{exc}$ is the intensity of the exciting light, ε the molar extinction coefficient, and b is the optical path of the cuvette (1 cm). This confirms the absence of additional interfering phenomena due to the aggregation of the probe since no deviation from linear trend of the intensity of the emission as a function of the mole of Ru(phen)$_3$.

Figure 4.8: a) Normalized emission spectra of Ru(phen)$_3$-Shell SiO$_2$NPs doped with different
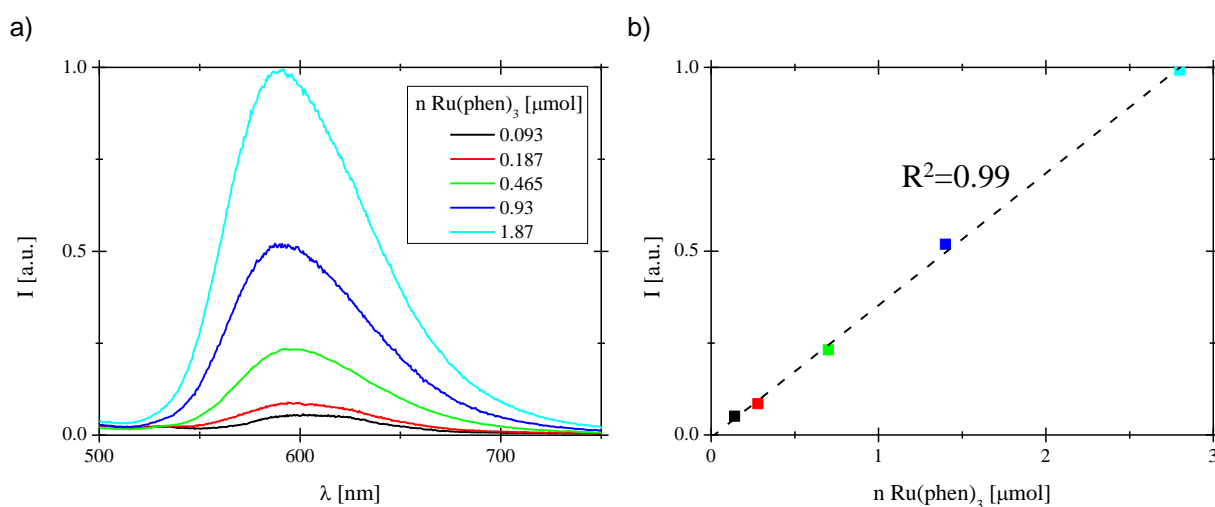
amounts of Ru(phen)$_3$, b) Intensity of the emission at 590 nm as a function of the moles of Ru(phen)$_3$.

As shown in Figure 4.9.a, in all the cases, the intensity of the emission of the Ru(phen)$_3$-Shell SiO$_2$NPs linearly decreased (R^2>0.99) by increasing the temperature, as expected, from 20°C to 65°C which is the range of interest for membrane distillation processes. The increase of mole of Ru(phen)$_3$ in the nano-thermometer could promote higher degree of energy transfer between Ru(phen)$_3$ molecules, which results in a stronger emission quenching, producing a higher sensitivity towards temperature changes by increasing the number of molecular probes immobilized in the shell.
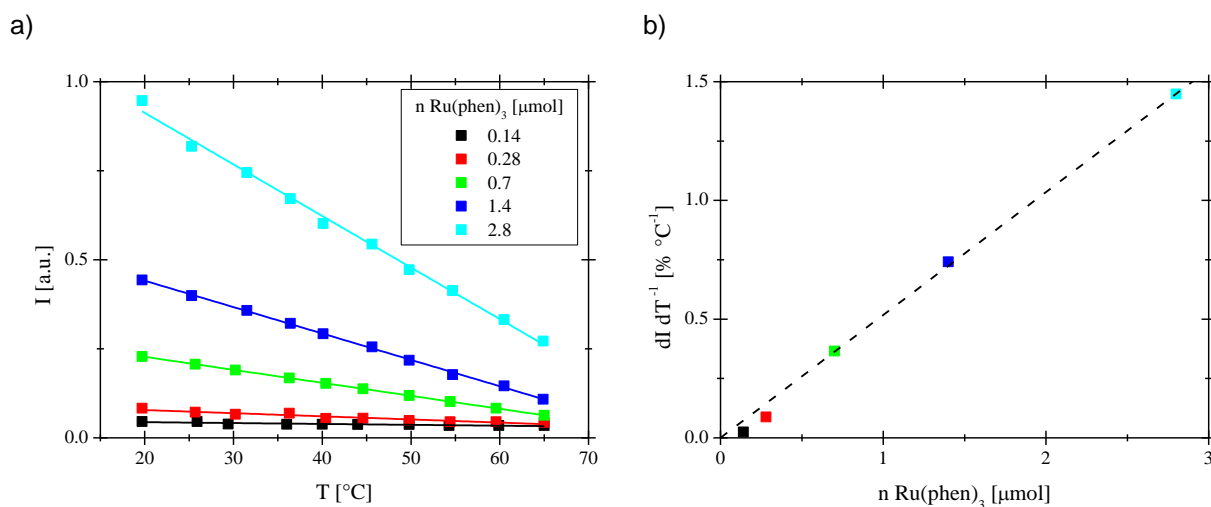
Figure 4.9: a) Effect of the temperature on the intensity of the emission at 590 nm of Ru(phen)$_3$-Shell SiO$_2$NPs doped with different amounts of Ru(phen)$_3$; b). Temperature sensitivity of Shell SiO$_2$NPs as a function of Ru(phen)$_3$ immobilized.

4.3.2 Fluorescent Ru(phen)$_3$-Shell SiO$_2$NPs immobilized in the surface of membranes as nanothermometers

On the basis of the higher intensity of the emission and higher temperature sensitivity 100% Ru(phen)$_3$-Shell SiO$_2$NPs were considered as the most promising candidate as nano-thermometer for monitoring the temperature on membrane surface.

Ru(phen)$_3$-Shell SiO$_2$NPs were functionalized with dodecyltriethoxysilane obtaining hydrophobic NPs made of silica. Measurements of Z-potential of Ru(phen)$_3$-Shell SiO$_2$NPs in water confirmed the success of the reaction. In fact, the Z-potential increased from -43±1 mV to +36±2 mV as a consequence of the functionalization of the silica with the dodecyl aliphatic chain which made the silica hydrophobic. This step is important in order to not affect the hydrophobicity of membrane surface required in such membrane processes (i.e. membrane distillation).

In Figure 4.10 is depicted the cross-section micrographs of PVDF membrane load with 100% Ru(phen)$_3$-Shell SiO$_2$NPs via dip-coating (a) compared with bare PVDF membrane (b). In both the cases, PVDF membranes of ca 106 µm of thickness presented a finger-like structure of ca 50 µm supported on a spherulitical-like layer.

SEM micrograph evidenced that the nano-thermometer NPs were immobilized on membrane surface (Figure 4.11).
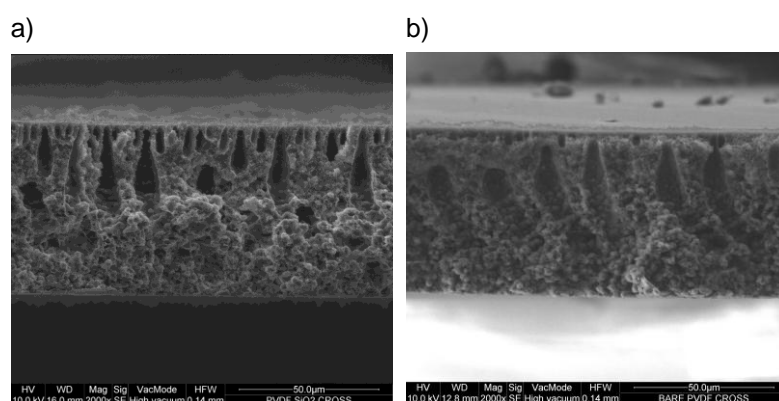
Figure 4.10: SEM picture of PVDF membrane load with hydrophobic 100% Ru- Ru(phen)$_3$-Shell SiO$_2$NPs (a) compared with bare PVDF membrane (b).
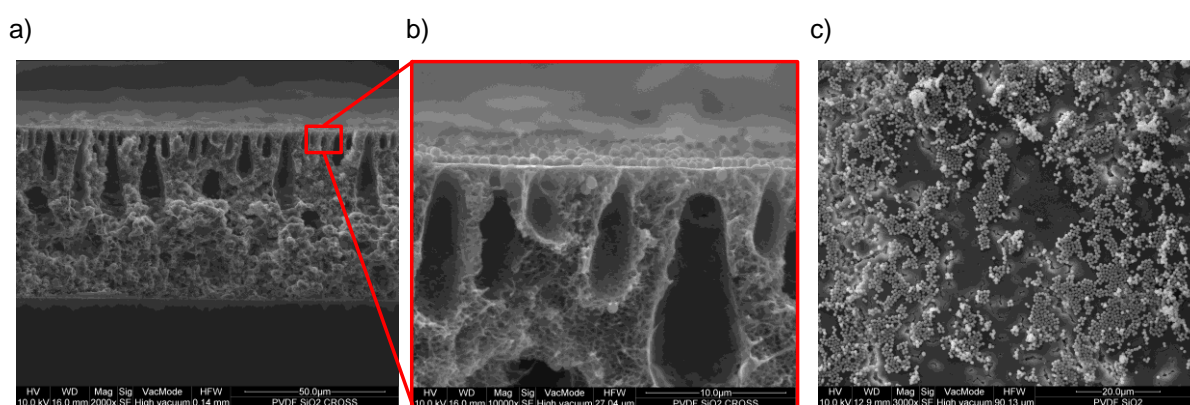
Figure 4.11: SEM picture of PVDF membrane load with hydrophobic 100% Ru- Ru(phen)$_3$-Shell SiO$_2$NPs: a) cross-section, b) zoom of the cross-section in proximity of the surface, c) top view of the surface.

By comparing the characterization and the morphology of bare PVDF with PVDF load with Ru(phen)$_3$-Shell SiO$_2$NPs membranes it is possible to conclude that the immobilization of the nano-thermometer did not affect the morphology of the membrane. In fact the contact angle is 109±2° in the case of bare PVDF and 114±3° in the case of PVDF loaded with functionalized SiO$_2$ NPs. The increase of contact angle is due to the hydrophobicity of the functionalized SiO$_2$NPs doped with Ru(phen)$_3$ and the increase of the roughness of membrane surface as a consequence of the immobilization of the probes. In both cases the membrane porosity is in the range of 88±3% and LEP of 2.0±0.2 bar, confirming that PVDF membranes preserved their morphology and integrity after immobilization of the nano-thermometer.

Furthermore upon membrane excitation it was observed an emission peak unmistakable attributed to the nano-thermometer doped with Ru(phen)$_3$. The maximum of emission was observed at 614 nm, red–shifted of 24 nm with respect to the emission observed for Ru(phen)$_3$-SiO$_2$NPs. The red shift in the peak can be attributed to the higher refractive index of PVDF surface and coupling effect due to the higher packing density of nanoparticles on the surface. This configuration leads higher sensitivity

towards the temperature with respect to membrane prepare by immobilizing the molecular probe in dense film made of PS (dI/dT=0.33% °C^{-1}) [36]. In fact, the by the immobilization of Shell SiO$_2$NPs on membrane surface, the nano-thermometer are keep in touch with the environment and as a consequence more prone to temperature variation. On the other hand, the immobilization in silica allows the protection of the probe from interfering agent (i.e. oxygen) and limits the photo-bleanching.
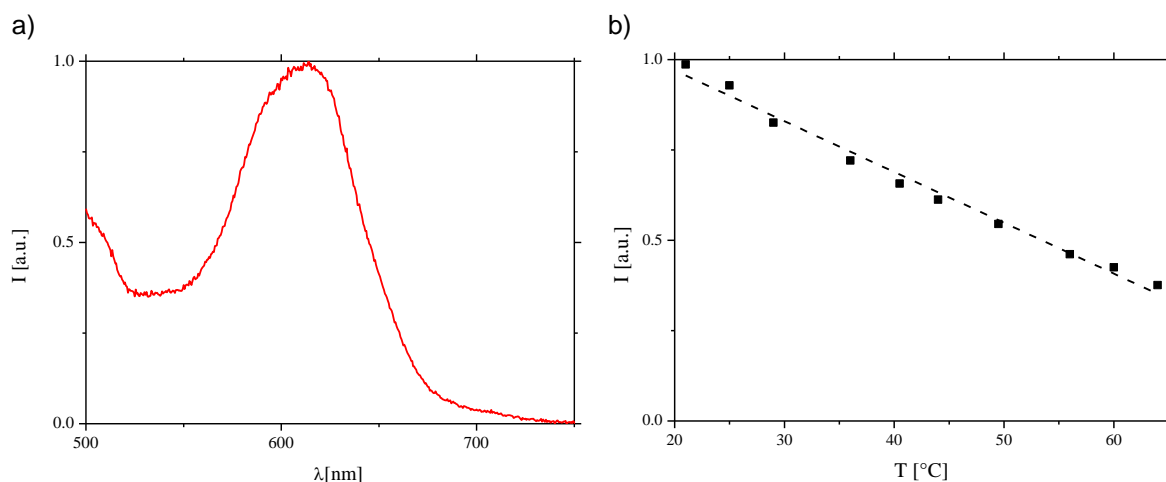
Figure 4.12: (a) Normalized emission of Ru(phen)$_3$-Shell SiO$_2$NPs immobilized on PVDF membranes and (b) their temperature sensitivity.

To test the mechanical stability of the NPs attached to the surface, two membrane samples of area 2x2 cm immersed in 50 ml were subjected to sonication for 10 min, after that the membranes were dried and the fluorescence was measured. The immobilization of the nanoparticles is reasonable stable. In fact, after 10 min of sonication a decrease of 8% due to a minimal leak of the 100% Ru(phen)$_3$-Shell SiO$_2$NPs is observed. It must be considered that sonication is a severe method to evaluate the stability of the coating. In fact, the immersion of the samples for 24 hours in water did not compromise the photochemical properties of the membrane since no variation of the intensity of the emission was observed. These experiments confirm the stability of the NPs immobilized on the surface of PVDF membranes.

SiO$_2$NPs are one of the most widely used inorganic materials for the fabrication of PVDF/SiO$_2$ composite membranes via blending method to enhanced hydrophilic properties of the membrane reducing membrane fouling. In general, SiO$_2$NPs nanoparticles can be modified to form hybrid nanomaterials by chemically bonding or physically adsorbing polymers on silica surface to chemically anchor polymer chains on surface via "grafting to" or "grafting from". This technique could be of interest in facilitating the immobilization of SiO$_2$ NPs on polymeric surface improving the stability the nano-thermometer on membrane surface.

4.4 Conclusions

A nano-thermometer based on silica nanoparticles doped with Tris(1,10-phenanthroline)ruthenium(II) (Ru(phen)$_3$) was prepared. The immobilization of the luminophore in an external shell made of silica consented to prepare monodisperse nanoparticles. On the other hand the immobilization of the luminescent molecule in the core, made of silica, dramatically affect the polydispersion of the NPs. As expected, the thickness of the shell was affected by the concentration of the silica precursor, whereas the mono-dispersity was maintained. The produced nanoparticles showed high photochemical activity and a strong phosphorescence ascribable to Ru(phen)$_3$. The intensity of the emission is modulated by the probe concentration. A systematic study showed that, on the basis of the concentration of the chemicals employed for the preparation of the Shell SiO$_2$ NPs it is possible to prepare monodisperse nano-thermometer with controlled and tuneable properties in terms of particle size, luminescent activity and temperature sensitivity.

Furthermore, the intensity of the emission of the nanoparticles decreased linearly by increasing the temperature and is affected by the probe concentration. These results suggest the employment of the developed system as nano-thermometer offering the possibility of the imaging and mapping of the temperature in a wide range of applications (i.e. bio-medical).

The luminescent nanoparticles were immobilized on PVDF membrane maintaining their temperature sensitivity and providing information about the temperature on membrane surface. The coating was stable since the emission of the membrane remains constant after immersion of the membrane for 24h in water and decrease by a 8% after sonication for 10 minutes. The deposition of the produced nanoparticles on the surface of the hyrophobic polymeric membrane is an innovative technology which could enable the monitoring and the mapping of temperature on membrane surfaces in real membrane process (i.e. membrane distillation).

4.5 References

[1] Vetrone, F, Naccache, R, Zamarrón, A, De La Fuente, A J, Sanz-Rodríguez, F, Maestro, L M,Rodriguez, E M, Jaque, D,Sole, J G, and Capobianco, J A. Temperature sensing using fluorescent nanothermometer. *ACS Nano*, 4(6): 3254-3258, 2010.

[2] Yang, J M, Yang, H, and Lin, L. Quantum dot nano thermometers reveal heterogeneous local thermogenesis in living cells. *ACS Nano*, 5(6): 5067-5071, 2001.

[3] Ross, D, Gaitan, M, and Locascio, L E. Temperature Measurement in Microfluidic Systems Using a Temperature-Dependent Fluorescent Dye. *Anal. Chem.*, 73(17): 4117-4123, 2001.

[4] Filevich, O, and Etchenique, R. 1D and 2D Temperature Imaging with a Fluorescent Ruthenium Complex. *Anal. Chem.,*78(21): 7499-7503, 2006.

[5] Thamdrup, L H, Larsen, N B, and Kristensen, A. Light-induced local heating for thermophoretic manipulation of DNA in polymer micro- and nanochannels. *Nano Lett.,*10(3): 826-832, 2010.

[6] Alsaadi, A S, Francis, L, Amy, G L, and Ghaffour, N. Experimental and theoretical analyses of temperature polarization effect in vacuum membrane distillation. *Journal of Membrane Science*, 471: 138-148, 2014.

[7] Martínez-Díez, L, and Vázquez-González, M I. A method to evaluate coefficients affecting flux in membrane distillation. *Journal of Membrane Science*, 173(2): 225-234, 2000.

[8] Ali, A, Macedonio, F, Drioli, E, Aljlil, S, Alharbi, O A. Experimental and theoretical evaluation of temperature polarization phenomenon in direct contact membrane distillation. *Chemical Engineering Research and Design*, 91(10): 1966-1977, 2013.

[9] Tamburini, A, Pitò, P, Cipollina, A, Micale, G, and Ciofalo, M. A. Thermochromic Liquid Crystals Image Analysis technique to investigate temperature polarization in spacer-filled channels for Membrane Distillation. *Journal of Membrane Science*, 447: 260-273, 2013.

[10] Wang, S, Westcott, S, and Chen, W. Nanoparticle Luminescence Thermometry. *J. Phys. Chem. B*, 106(43): 11203-11209, 2002.

[11] Wang, X D, Song, X H,He, C Y, Yang, C J, Chen, G, Chen, X. Preparation of Reversible Colorimetric Temperature Nanosensors and Their Application in Quantitative Two-Dimensional Thermo-Imaging. Anal. Chem., 83 (7): 2434-2437, 2011.

[12] Brites, C D S, Lima, P P, Silva, N J O, Milla, A, Amaral, V S, Palacio, F, and Carlos, L D. Thermometry at the nanoscale. *Nanoscale*, 4(16): 4799-4829, 2012.

[13] Santra, S, Zhang, P, Wang, K. M, Tapec, R, and Tan, W H. Conjugation of Biomolecules with Luminophore-Doped Silica Nanoparticles for Photostable Biomarkers. *Anal. Chem.*, 73(20): 4988-4993, 2001.

[14] Canfarotta, F, Whitcombe, M J, and Piletsky, S A. Polymeric nanoparticles for optical sensing. *Biotechnology Advances*, 31(8): 1585-1599, 2013.

[15] Arduini, M, Marcuz, S, Montolli, M, Rampazzo, E, Mancin, F, Gross, S, Armelao, L, Tecilla, P, and Tonellato, U. Turning Fluorescent Dyes into Cu(II) Nanosensors. *Langmuir*, 21(20): 9314-9321, 2005.

[16] Stober, W, Fink A, and Bohn, E. Controlled Growth of Monodisperse Silica Spheres in the Micron Size Range. J. Colloid Interface Sci., 26(1): 62-69, 1968.

[17] Bele, M, Siiman, O, and Matijevic´, E. Preparation and Flow Cytometry of Uniform Silica-Fluorescent Dye Microspheres. *J. Colloid Interface Sci.*, 254(2): 274-282, 2002.

[18] Zhang, D, Wu, Z, Xu, J, Liang, J, Li, J, and Yang, W. Tuning the Emission Properties of Ru(phen)32+ Doped Silica Nanoparticles by Changing the Addition Time of the Dye during the Stöber Process. *Langmuir*, 26(9): 6657-6662, 2010.

[19] Rossi, L M, Shi, L, Quina, F H, and Rosenzweig, Z. Stöber Synthesis of Monodispersed Luminescent Silica Nanoparticles for Bioanalytical Assays. *Langmuir*, 21(10): 4277-4280, 2005.

[20] Bagwe, R P, Yang, C, Hilliard, L R, and Tan, W. Optimization of Dye-Doped Silica Nanoparticles Prepared Using a Reverse Microemulsion Method. *Langmuir*, 20(19): 8336-8342, 2004.

[21] Qian, L, and Yang, X. One-Step Synthesis of Ru(2,2′-Bipyridine)3Cl2-Immobilized Silica Nanoparticles for Use in Electrogenerated Chemiluminescence Detection. *Adv. Funct. Mater.*, 17(8): 1353-1358, 2007.

[22] Demas, J N, and DeGraff, B A. Applications of Luminescent Transition Platinum Group Metal Complexes to Sensor Technology and Molecular Probes. Coor. Chem Rev., 211: 317- 351, 2001.

[23] Liebsch, G, Klimant, I, and Wolfbeis, O S. Luminescence Lifetime Temperature Sensing Based on Sol-Gels and Poly(acrylonitrile)s Dyed with Ruthenium Metal–Ligand Complexes. Adv. Mater., 11(15): 1296-1299, 1999.

[24] Barja, B C, Chesta, C A, Atvars, T D Z, and Aramendía, P F. Fluorescent polymer coatings with tuneable sensitive range for remote temperature sensing. S*pectrochimica Acta Part A: Molecular and Biomolecular Spectroscopy,*116: 13-16, 2013.

[25] Liu, T, and Sullivan, J P. Physical Properties of Paints, in: Pressure and Temperature Sensitive Paints. Wiley, 2005.

[26] Mirenda, M, Levi, V, Bossi, M L, Bruno, L, Bordoni, A, Regazzoni, A E, and Wolosiuk, A. Temperature response of luminescent tris(bipyridine)ruthenium(II)-doped silica nanoparticles. J. *Colloid Interface Sci.*, 392: 96–101, 2013.

[27] Drobek, M, Figoli, A, Santoro, S, Navascués, N, Motuzas, J, Simone, S, Algieri, C, Gaeta, N, Querze, L, Trotta, A, Barbieri, G, Mallada, R, Julbe, A, and Drioli, E. PVDF-mixed matrix membranes as VOCs adsorbers. *Microporous and Mesoporous Materials*, 207: 126-133, 2015.

[28] Feng, C S, Shi, B, and Li, G. Preparation and properties of microporous membrane from poly (vinylidene fluoride-co-tetrafluoroethylene)(F2. 4) for membrane distillation. *J. Membr. Sci.*, 237(1-2): 15-24, 2004.

[29] Drioli, E, Santoro, S, Simone, S, Barbieri, G, Brunetti, A, Macedonio, F, and Figoli, A. ECTFE membrane preparation for recovery of humidified gas streams using membrane condenser. *Reactive & Functional Polymers*, 79: 1-7, 2015.

[30] Shibata, S, Taniguchi, T, Yano, T, and Yamane, M. Formation of Water-Soluble Dye-Doped Silica Particles. *J. Sol-Gel Sci. Technol.*, 10(3): 263-268, 1997.

[31] Auger, A, Samuel, J, Poncelet, O, and Raccurt, O. A comparative study of non-covalent encapsulation methods for organic dyes into silica nanoparticles. *Nanoscale Res Lett.*, 6: 328, 2011.

[32] Van Blaaderen, A, and Vrij, A. Synthesis and characterization of colloidal dispersions of fluorescent, monodisperse silica spheres. *Langmuir*, 8(12): 2921-2931, 1992.

[33] Zhang, D, Wu, Z, Xu, J, Liang, J, Li, J, and Yang, W. Tuning the emission properties of Ru(phen)3(2+) doped silica nanoparticles by changing the addition time of the dye during the Stöber process. *Langmuir,* 26(9): 6657-6662, 2010.

[34] Sauer, M, Hofkens, J,and Enderlein, J. Basic Principles of Fluorescence Spectroscopy, in: *Handbook of Fluorescence Spectroscopy and Imaging: From Single Molecules to Ensembles.* Wiley, 2011.

[35] Rampazzo, E, Bonacchi, S, Montalti, M, Prodi, L, and Zaccheroni, N. Self-Organizing Core−Shell Nanostructures: Spontaneous Accumulation of Dye in the Core of Doped Silica Nanoparticles*. J. Am. Chem. Soc*, 129(46): 14251-14256, 2007.

[36] Santoro, S, Moro, A J, Portugal, C M, Crespo, J G, Coelhoso, I M, Lima, J C, 2016, Development of Oxygen and Temperature Sensitive Membranes Using Molecular Probes as Ratiometric Sensor. *Journal of Membrane Science* (submitted).

Chapter 5

On-line and non-invasive mapping of temperature on electrospun nanofibrous PVDF membrane in direct contact membrane distillation by means of molecular probes

5.1 Introduction

Membrane distillation (MD) is a relative new coming and emerging non-isothermal separation process allowing vapour molecules to permeate through a micro-porous hydrophobic membrane, whereas theoretical 100% rejection of ions, macromolecules, colloids, cells and other non-volatiles is obtained [1-3]. MD is considered a promising technology in a wide range of applications in water treatment such as desalination, purification of contaminates and organic matter, concentration of aqueous solutions [4]. In fact, MD is an non-intensive energetic cost-saving separation process operating at lower pressure than conventional pressure-driven membrane separation processes and requiring minimal heat with respect to conventional distillation that could be provided by thermal renewable energy sources (i.e. solar) making the process economical viable [5].

Nevertheless, several drawbacks have limited the implementation of MD at industrial scale and hindered commercial visibility, such as the development of membranes with adequate and devoted properties and improvement on the module design and operating conditions in order to limit polarization phenomena occurring in the boundary layers adjacent to the membrane [6-7].

Ideal membrane for MD should present superhydrophobic surface to avoid pore wetting and a well-designed pore structure to favour water vapour transport [8-9].

Poly(vinylidene fluoride) (PVDF) has gained great attention as a membrane material with regard to its outstanding properties such as high mechanical strength, thermal stability, chemical resistance, combined with solubility in a wide number of common solvents which favoured the preparation of membranes with designed morphology using different techniques [10]. Among them, electrospinning is a promising technique which enables to produce self-sustained electrospun nanofibrous membranes (ENMs) with both interconnected open pore morphology made of a 3D network of nano-fibers and super-hydrophobicity, due to higher surface roughness, leading to high performance in terms of mass transport in MD process [11-16]. The most studied configuration in MD is the direct contact membrane distillation (DCMD), where the membrane is an interface between two aqueous streams at different temperature producing a gradient of vapour pressure across the membrane that represents the driving force for the process. As shown in Figure 5.1, mass and heat transfers are correlated: energy is transferred from the feed to the permeate by the evaporation and the condensation of the permeating species and by the thermal conductivity of the membrane matrix [17]. As a consequence of the thermal polarization in the boundary layer (Figure 5.1), the membrane temperature at the feed side ($T_{F,M}$) is lower than the value of bulk feed (T_F) and the driving force dramatically decreases along the module negatively affecting the performance of MD processes [18]. Opposite effect takes place in the distillate compartment where the temperature of the membrane (T_{DM}) is higher than the value of bulk (T_D).

Efforts have been devoted to the development of membrane modules in order to minimize this phenomenon by improving the fluid dynamics [19-20]. On the other hand, several mathematical models based on the heat and mass transfer equations have been developed to evaluate the thermal polarization [21-22]. Basically, studies have been focused on the evaluation of effects of the thermal

polarization by referring only to the overall performance in terms of heat or mass flux of the process. On the other hand minor attention was dedicated to the local characterization of the thermal polarization which affects the global performance. It is desirable to have a method able to monitor on–line and in-situ the temperature in the membrane module and on membrane surface. Recently, invasive techniques such as thermocouples located on the membrane surface [23] and spacer filled by thermochromic liquid crystals [24] have been proposed for the evaluation of the thermal polarization.
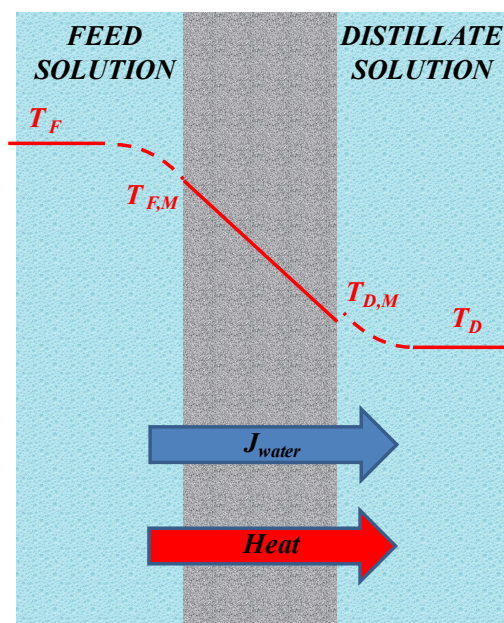
Figure 5.1: Thermal polarization.

The aim of this work is to propose a luminescent molecular probe as an innovative technology for non-invasive and spatial monitoring temperature in membrane processes. In fact, the employment of optical sensor based on the dispersion luminescent molecules in polymeric matrix is an actual technology for the temperature sensing in several innovative fields of nano-science [25-26]. In our previous work, we have demonstrated that the immobilization of molecular probe in dense membrane made of PS enables the non-invasive, on-line and in-situ monitoring of the temperature and oxygen concentration [27]. Nevertheless, this is the first time that the concept is applied to membrane distillation.

Tris(phenantroline)ruthenium(II) chloride ($Ru(phen)_3$) was selected as temperature sensitive luminescent probe and immobilized in a PVDF ENM prepared via electrospinning. The PVDF ENM was then tested in DCMD. The immobilization of the molecular probe and the design of a devoted membrane module connected to a spectrofluorometer, by means of an optical fiber, allowed monitoring on-line the temperature of the membrane at feed side ($T_{F,M}$) during the DCMD process. On the other hand, the employment of an IR-camera allowed monitoring the temperature of the bulk feed (T_F). The combination of these two optical techniques is really promising since it enables the on-line

and non-contact characterization of difference of temperature between the feed bulk and the membrane at the feed side unrevealing the thermal polarization along the membrane module during DCMD experiments.

5.2 Materials and methods

5.2.1 Materials

The luminescent molecular probe tris(phenantroline)ruthenium(II) chloride (Ru(phen)$_3$) was purchased by Sigma–Aldrich, Spain. Poly(vinylidenefluoride) ((PVDF) Solef® 6012, Solvay Specialty Polymers, Bollate, Italy) was solubilised in a blend of solvents such as N,N-Dimethylformamide (DMF, 99.8%, Sigma Aldrich, Spain) and acetone (Panreac, Spain). Lithium chloride (LiCl, Fisher Chemicals, Spain) was employed as additive.

5.2.2 Membrane preparation

PVDF solutions were prepared by adding the polymeric powder to 12 mL mixture of DMF/Acetone (6:4 wt:wt). The polymer concentration was varied from 6wt% to 10wt%. Homogeneous solutions were obtained by stirring at a temperature of 70°C the mixture of solvents and, then, adding PVDF. In the case of membranes doped with the molecular probe, 10 mg of Ru(phen)$_3$ (0.83wt% with respect to the PVDF) and 5mg of LiCl (0.43wt% with respect to PVDF) were first solubilized in the mixture of DMF/Acetone (6:4 wt:wt) and then PVDF was added and stirred at 70°C until an homogeneous solution was reached. After cooling at room temperature, the solution was transferred in a syringe and connected to the electrospinning set-up.
The solution properties were characterized using a Fungilab Visco Basic Plus Viscometer and a ABB X400 conductivimeter.

5.2.3 Electrospinning

Yflow 2.2 D500 electrospinner with a 20-gauge needle was used to obtain the fibers. The flow rate of the solution was adjusted to 1mL h^{-1}. The needle was placed 15 cm away from a flat collector. The optimum voltage was adjusted to +16KV in the needle and -2KV in the collector. In order to obtain homogeneous films, the needle was moved in 2 dimensions (80 mm left-right, 150 mm front-rear) to cover all the electrospinning area and obtain a homogeneous thickness of the membrane.
After electrospinning the PVDF ENM was dried in oven at 70 °C overnight to remove traces of solvents and to improve the cohesion between the nano-fibers (post-treatment).

5.2.4 Membrane characterization

The novel PVDF membranes prepared via electrospinning were characterized by several conventional techniques:

Thickness- The thickness of membranes was evaluated by means of a digital micrometer Carl Mahr D 7300 (Esslingen AN, Gottingen, Germany) with an accuracy of ± 0.1 μm. For each membrane, ten measurements were taken.

Scanning Electron Microscopy (SEM) analysis- The morphology of membranes was observed by scanning electron microscope (SEM; Steroscan 360, Cambridge Instruments, Cambridge, UK). Cross-section samples were freeze fractured in liquid nitrogen to produce a clean brittle fracture. All samples were sputter-coated with gold immediately before observation.

Contact angle (CA)- The contact angles with distilled water on both the surfaces were measured using a CAM 200 contact angle meter (KSV Instruments, Finland) by the sessile drop method at ambient temperature. After taken 10 measurements, the average value and the corresponding standard deviation were calculated.

Porosity (P)- Membrane porosity was evaluated by the gravimetric method consisting in weighing the membrane in dry and wet conditions (24 hr in kerosene). The overall porosity was calculated according to the following equation [28]:

$$P = \frac{\frac{w_h - w_d}{\rho_w}}{\frac{w_d}{\rho_{PVDF}} + \frac{w_h - w_d}{\rho_w}} ; \quad (5.1)$$

where w_h is the weight of the wet membrane; w_d is the weight of the dry membrane; ρ_w is the kerosene density (0.82 g cm^{-3}) and ρ_{PVDF} is the polymer density (1.72 g cm^{-3}). For each membrane, three measurements were performed; the average value and the corresponding standard deviation were, then, calculated.

Bubble point (BP) and pore size (d_p)- Membrane bubble point and pore size were measured using a PMI Capillary Flow porometer (Porous Materials Inc., US). According to the procedure reported in literature [29], membranes were immersed for 24 hours in Porewick (16 dyne cm^{-1}) and then tested in the membrane module of the porometer using wet-up/dry-up method programmed by the software Capwin. The method is based on the increasing of the pressure in a compartment of the membrane cell to remove the Porewick from the pores and, then, repeating the test using the dry sample. The data were processed using the software Caprep which correlates the applied pressure P to the pore size d_P according to the Laplace equation:

$$d_p = \frac{4 \, \tau \cos \theta}{P} ; \quad (5.2)$$

where τ is the surface tension of the liquid, θ is the contact angle of the liquid (assumed to be 0 in case of full wetting, which means cosθ=1).

Liquid Entry Pressure (LEP)- The liquid entry pressures (LEPs) of the membranes were measured by means of a static liquid chamber filled-up with 200 mL of DI water at ambient temperature accommodating the membrane sample (area 4 cm^2). The pressure in the chamber was increased at a constant rate of 0.1 bar per 10 min until the water permeated trough the membrane. Experiment was repeated twice with different membrane samples at the same conditions and the average value evaluated was the LEP.

Monitoring of temperature on membrane surface during direct contact membrane distillation (DCMD) experiments

DCMD experiments were performed using the set-up presented in Figure 5.2. The membrane is employed as an interface between two streams of water kept at different temperature. The permeate stream was kept at an inlet temperature of 15°C, whereas the feed was heated-up to 40, 50 and 60°C by a heater (Thermo Haake® heating circulator C10). Thermocouples (HD9214, Delta OHM, accuracy ±0.1 °C) placed in proximity of the inlets and outlets of the membrane module were employed to monitor the temperature of the two streams that were fed at a flow rate of 12 L h^{-1} by means of two peristaltic pumps (Masterflex ® 7518-10). An analytical balance (Europe 6000, Gibertini) was used for weighing the distillate.

The membrane module made of Nylon (Figure 5.3) in which the membrane sample is placed (size: 16 cm x 5.5 cm) has a polymeric window transparent in the near-UV/visible region which allowed to excite the molecular probes immobilized into/onto the membrane and to collect their emission by means of a bifurcated fiber-optical bundle UV/Visible (Ocean Optics) connected to a spectrofluorimeter (Avantes). The excitation wavelength was fixed at 450 nm. The acquisition time of spectra was set at 0.2 s and 10 spectra were averaged for each measurement in order to obtain the maximum signal to noise ratio.

A membrane module cover with 42 holes displaced in 3 rows (x_1=1.7 cm (1), x_2=2.7 cm (2), x_3=3.7 cm (3)) allowed to fix the optical fiber at 90° with respect to the sample surface, and allowed to excite the membrane and detect the emitted fluorescence from each holes.

Before each session of measurement, the spectrophotometer setup was calibrated by acquiring dark signal. The dark signal was obtained by turning off the LED. Then the fluorescence spectrum acquired for each hole was therefore normalized with respect to dark signal. We performed a calibration procedure to extrapolate the temperature from the acquired fluorescence signal for each holes. Calibration curves of the amplitude of the fluorescence at 572 nm as a function of the temperature were obtained by keeping the two water streams (feed and distillate) at the same temperature (40, 50 and 60°C), in order to avoid simultaneous heat and mass transfer across the membrane. The thermocouples placed in the proximity of the membrane module were used to check the temperature change along the membrane module. For each experimental measurement we extracted the slope of

the linear regression of the fluorescence amplitude vs temperature ($R^2 > 0.96$). Then, a cold stream at 15°C was fed to one compartment of the membrane module and, after 60 min, necessary to achieve the steady state; the flux was registered for 4 hours of DCMD test. The fluorescence was also measured during the DCMD process and the temperature of the membrane surface evaluated.
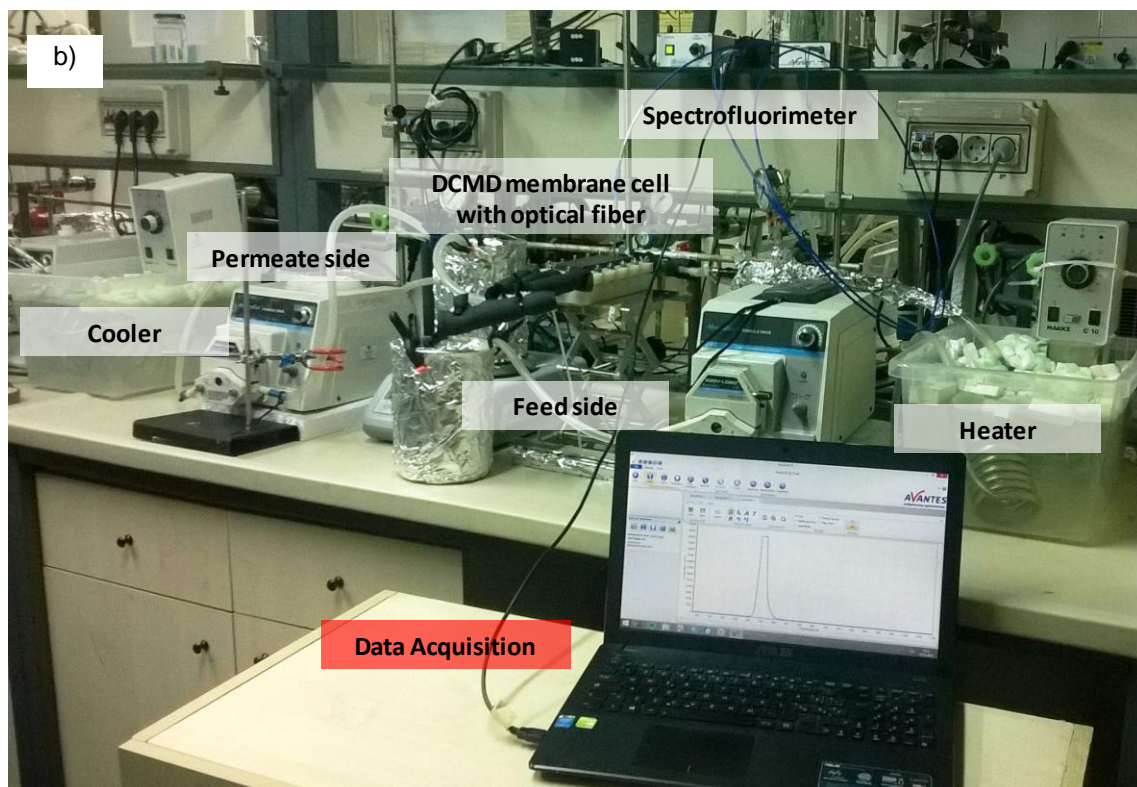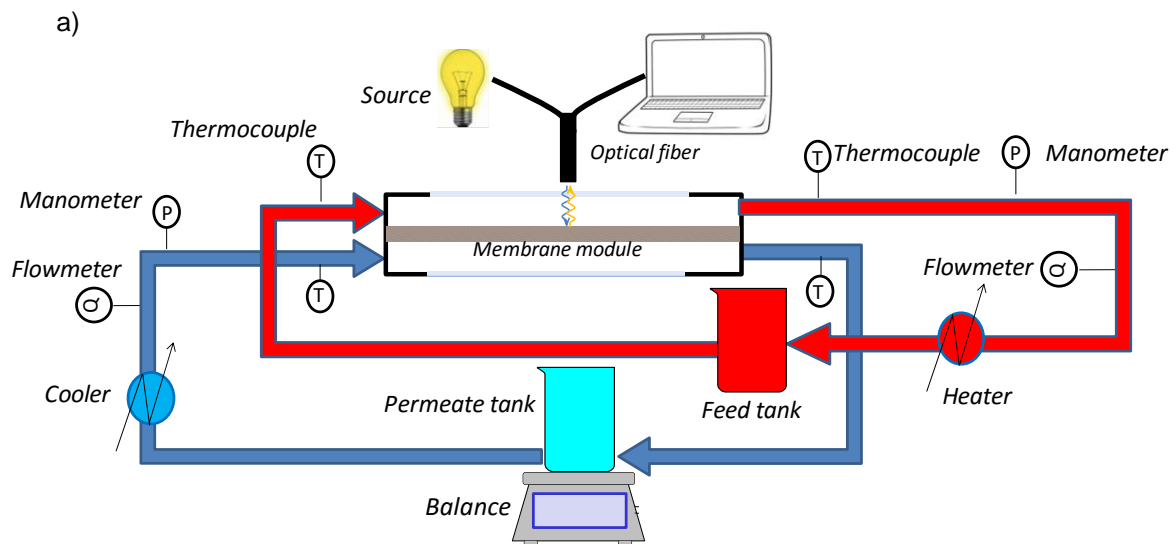
Figure 5.2: a) Scheme of the set-up used for monitoring the temperature in DCMD process, b) Picture of the set-up.

A two-dimensional mapping of the temperature on the membrane surface was derived by linear interpolation of the temperature values in each hole. For this purpose a numerical processing was

performed by writing a custom Matlab routine (Matlab, The MathWorks Inc., Natick, MA, USA) using the *griddedinterpolant* function.

The temperature of membrane bulk was evaluated by means of an IR CAMERA (model FLIR E40) with a thermal sensitivity of 0.07°C at 30°C. Infra-red pictures of a resolution of 160x120 pixels were acquired in the spectral range from 7.5 µm to 13 µm.
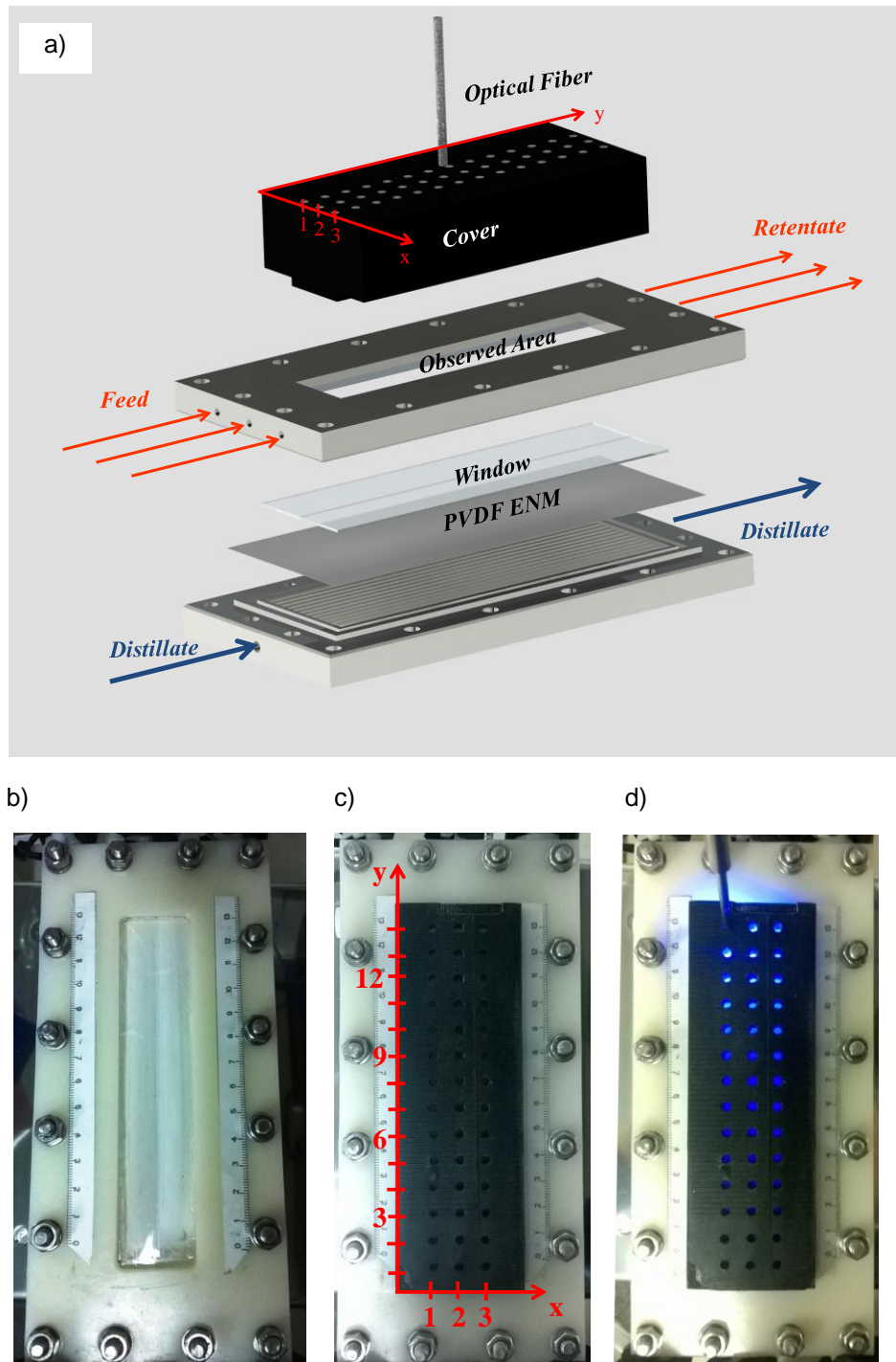
Figure 5.3: Scheme of the developed membrane module for optical observations (a). Pictures evidencing the window (b), the cover (c) and the optical-fiber (d).

5.3 Results and Discussion

5.3.1 Membrane composition and morphology

PVDF ENMs were electrospun starting from a polymeric solution prepared using a mixture of DMF/Acetone. Basically, DMF is used as good solvent for PVDF whereas acetone has the key role to accelerate solvent evaporation due to its superior vapour pressure facilitating the formation of the 3D network [30].
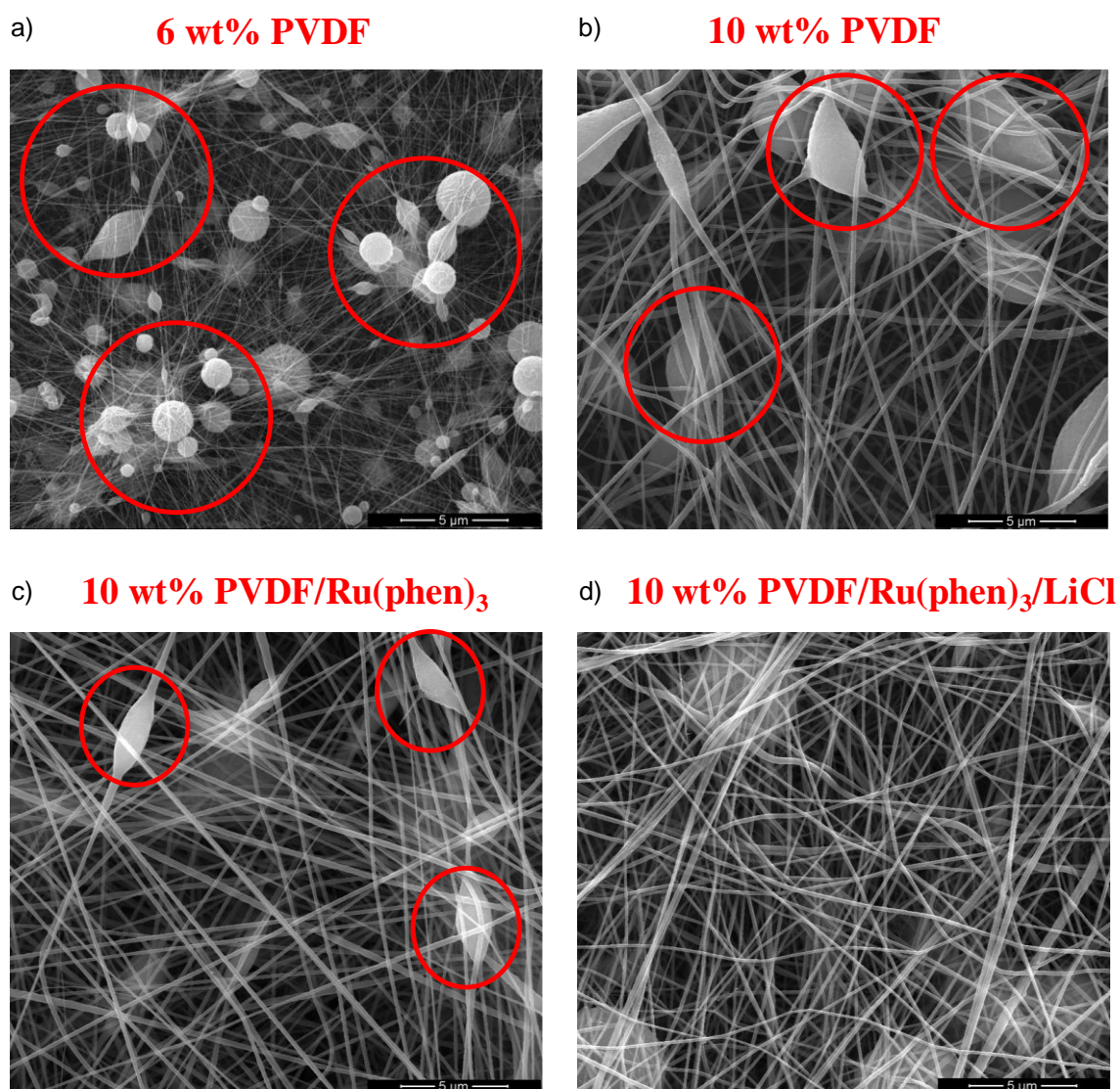
Figure 5.4: SEM picture of PVDF ENMs (Magnification: 10,000 X): a) PVDF 6wt%, b) PVDF 10wt%, c) PVDF 10wt%+0.85wt% Ru(phen)₃, d) PVDF 10wt%+0.85wt% Ru(phen)₃+0.43wt% LiCl.

The optimal concentration to electrospin the nano-fibers was found to be 10wt% (Figure 5.4b). In fact, for higher concentration the viscosity of the polymeric solution was too high to be electrospun, whereas at lower concentration (i.e. 6wt %) the nano-fibers presented defects. This is due to the fact that at low viscosities (24.3 cP) the surface tension becomes the dominant factor during the electrospinning process and drops are formed instead of nano-fibers as is visible in the Figure 5.4.a [31]. By looking at Figure 5.5, it is possible to notice that the increase of the concentration of PVDF to 10wt% dramatically improves the quality of the fibers as a consequence of the increasing of the viscosity of the polymeric solution to a value of 94.6 cP. However, ENM prepared with 10wt% of PVDF presented defects too (Figure 5.4.b.).
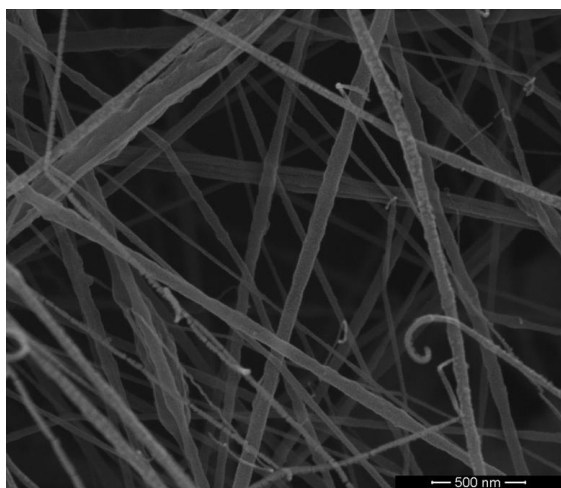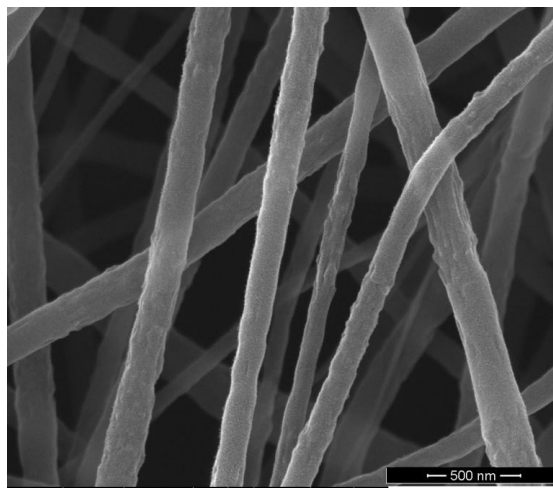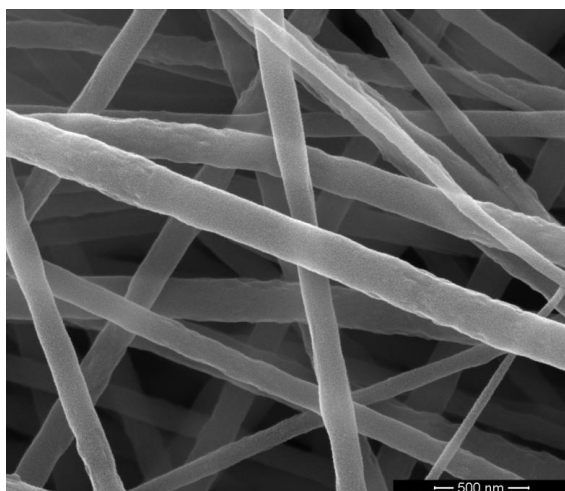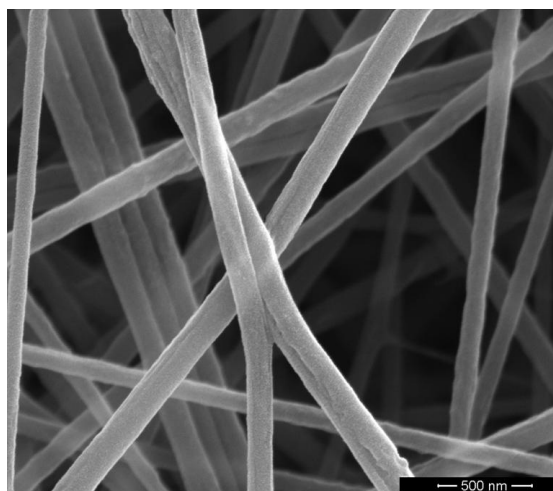
Figure 5.5: SEM picture of PVDF ENMs (Magnification: 100,000 X): a) PVDF 6wt%, b) PVDF 10wt%, c) PVDF 10wt%+0.85wt% Ru(phen)$_3$, d) PVDF 10wt%+0.85wt% Ru(phen)$_3$+0.43wt% LiCl.

The addition of Ru(phen)$_3$ decreased the number and the size of drops (Figure 5.4.c), that disappeared by the addition of LiCl. This is explained by the nature of the molecular probe and the additive that are salts and that affect the electrical conductivity of the polymeric solution. In fact the electrical conductivity of the polymeric solution containing 10wt% of PVDF in DMF/Acetone (6:4 wt:wt) was really low (0.8 µS cm^{-1}), whilst raised to 76.3 µS cm^{-1} by the addition of the molecular probes and up to 375 µS cm^{-1} by the employment of LiCl as additive. PVDF polymeric solution prepared with both Ru(phen)$_3$ and LiCl presented an electrical conductivity of 394 µS cm^{-1}.

The use of salts, in particular LiCl, is quite common in electrospinning membrane preparation in order to improve the conductivity of polymeric solution generating a higher charge density on the surface of the charged jet, thus favouring the formation of nano-fibers [30-32].

Table 5.1: Electrical conductivity (s) and viscosity (v) of PVDF polymeric solutions.

| Polymeric Solution	PVDF [wt%]	Ru(phen)$_3$ [wt%]*	LiCl [wt%]*	s [µS cm^{-1}]	v [cP]
6% PVDF	6			1.4 ± 0.1	24.3 ± 0.1
10% PVDF	10			0.8 ± 0.1	94.6 ± 0.5
10% PVDF/LiCl	10		0.83	375.0 ± 2.6	107.2 ± 0.4
10% PVDF/Ru(phen)$_3$	10	0.43		76.3 ± 0.2	98.3 ± 0.6
10% PVDF/LiCl/Ru(phen)$_3$	10	0.43	0.83	394.0 ± 6.1	108.1 ± 0.7

***wt% with respect to PVDF**

In fact, 10wt%PVDF/ Ru(phen)$_3$/LiCl ENM (Figures 5.4.d, 5.5.d) showed a 3D network defect-free of nanofibers with a diameter of 145±12 nm.

Accordingly, PVDF ENMs prepared by solubilising 10wt% of polymer in the blend of the solvents doped with Ru(phen)$_3$ and LiCl were selected for DCMD experiments.

5.3.2 Membrane Characterization

The properties of the developed 10wt%PVDF/ Ru(phen)$_3$/LiCl ENM are reported in Table 5.1.

Table 5.2 : Characterization results of 10wt%PVDF/ Ru(phen)$_3$/LiCl ENM.

	10wt%PVDF/ Ru(phen)$_3$/LiCl
Thickness [µm]	48±1
Contact Angle [°]	115±4
Porosity [%]	89±1
LEP [bar]	1.0±0.1
Average Pore diameter [µm]	0.75±0.01

PVDF ENMs is really thin, providing low resistance to the mass transport. Moreover the membrane showed a hydrophobic character with a contact angle of 115°. Hydrophobicity, that is a function of the chemical texture of the surface as well as its roughness [33], is crucial for MD processes for avoiding the permeation of liquid water through the membrane and for ensuring good rejection values. Electrospinning is a competitive fabrication technique for developing hydrophobic membranes due to the greater surface roughness that can be achieved. In fact, the PVDF ENMs prepared by electrospinning showed a higher hydrophobic character than the PVDF membranes obtained by phase inversion, that typically have a contact angle of 80° [34]. Furthermore, the electrospinning allows to easy production of membranes with uniform pore size distribution and significantly high porosity. Specially, the produced PVDF membrane presented a porosity of 89% and narrow pore size distribution with an average pore diameter of 0.75 µm.

5.3.3 DCMD results

Figure 5.6.b shows the DCMD permeate fluxes as a function of different feed temperatures. The permeate flux increased exponentially with the feed temperature following an Arrhenius type of dependence as expected. In fact, the flux raises from 9 kg m^{-2} h^{-1} to 15.7 kg m^{-2} h^{-1} increasing the temperature from 40°C to 60°C.
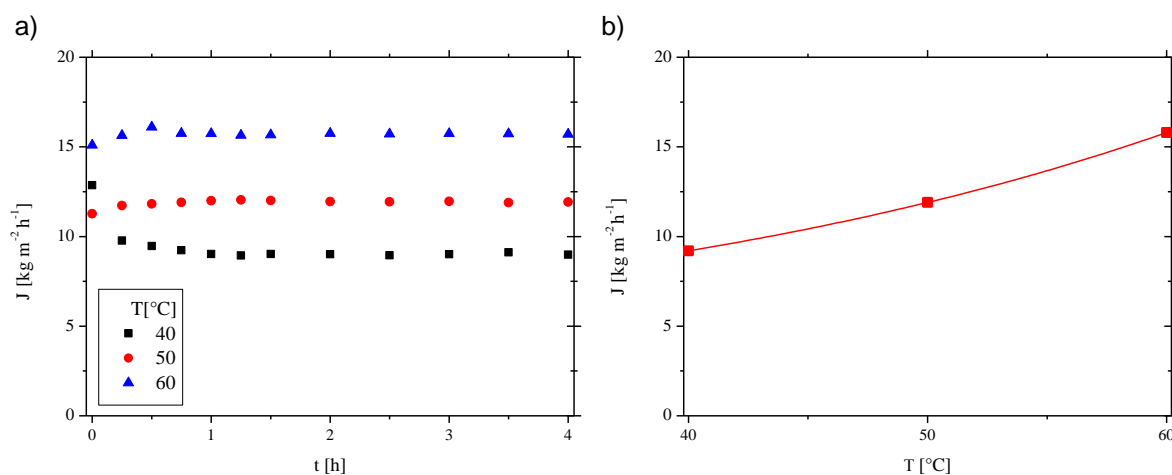
Figure 5.6: Flux of 10wt%PVDF/ Ru(phen)$_3$/LiCl prepared via electrospinning for 4 hours at different temperatures (a) and mean value at the steady state (b).

The high fluxes of the novel PVDF membrane are related to the low thickness and high porosity [35]. The thickness of the PVDF ENM lies between 30 and 60 µm, considered the optimal range for DCMD providing enough heat transfer resistance to establish a water vapour pressure difference across the membrane, together with a reduced membrane resistance [36-37]. Moreover, the high porosity of the PVDF ENM minimizes the heat loss by conduction since the thermal conductivity of air is an order of

magnitude lower than that of the polymeric membrane material and also offers a lower resistance to the mass transport [6].

Finally, the 10wt%PVDF/Ru(phen)$_3$/LiCl showed stable performance for 3 hours for each temperature, with a quite low experimental error (<2%) and no wetting was observed during the 20 hours DCMD operating period.

Experiments show the outstanding performance of the PVDF ENM in DCMD. In fact ENMs generally present superior flux with respect to conventional flat-sheet membrane due to their excellent properties in terms of porosity, thickness and hydrophobicity.

From Table 5.2, it is possible to notice that the PVDF ENM developed in this work presents competitive performance with literature data. In fact, PVDF ENM doped with Ru(phen)$_3$ and prepared using LiCl as additive shows similar flux with respect to PVDF ENMs reported in the literature [38-40]. However, several studies showed that the performance of PVDF ENMs is improved by inorganic fillers, such as silica nanoparticles of nanoparticles as carbon nanotubes that can enhance the mechanical strength and thermal stability of the membrane, and enhance its hydrophobicity [41-43].

Table 5.3: DCMD performance of the present study in comparison with ENMs reported in literature (Feed inlet temperature: 60°C).

Material	d_p [μm]	P[%]	CA [°]	J [kg m^{-2} h^{-1}]	Reference
PVDF Kynar 761	*0.05-0.63*	*-*	*87-151*	*3-10**	*[38]*
PVDF Kynar 761	*0.58-0.64*	*81-82*	*128-154*	*<5***	*[39]*
PVDF	*2.9-5.2*	*85-93*	*137-141*	*7.2-28.8***	*[40]*
PVDF+SiO$_2$	*0.69*	*82*	*156*	*18.9*	*[41]*
Silica-PVDF/PVDF	*0.32-0.36*	*80*	*150-154*	*21**	*[42]*
CNT/PVDF-co-HFP	*0.29*	*>84*	*158*	*29.5**	*[43]*
10wt%PVDF/ Ru(phen)$_3$/LiCl	*0.75*	*89*	*115*	*15.7*	*This Study*

*35 g L^{-1} NaCl feed

**30 g L^{-1} NaCl feed

5.3.4 Evaluation of temperature on the membrane surface

The temperature on the membrane surface was evaluated on the basis of the pronounced thermal quenching of the emission of Ru(phen)$_3$ immobilized in the PVDF membrane. In Figure 5.7 it is reported the emission collected from 10wt%PVDF/Ru(phen)$_3$/LiCl and the calibration curve of the fluorescence vs temperature of the hole x=2, y=3.

Doped PVDF ENM presents an unmatched emission attributed to the complex of Ru with a maximum emission at 572 nm. The amplitude of the phosphoresce peak linearly decreased as the temperature

increases. This effect is well known in photochemistry: the increasing of the temperature favour the non-radiative deactivation pathways of the molecular probe converting the absorbed light to the vibrational energy leading to the commonly observed decrease in phosphorescence intensity with rising temperature [33].

After the calibration of fluorescence of the probe as a function of the temperature, the temperature of membrane surface in real DCMD process at three different feed temperatures (40, 50 and 60°C) was monitored on-line by measuring the intensity of phosphorescence.

The data are presented in Figures 5.8 and 5.9 and it is possible to notice that in all cases the temperature on the membrane surface is lower than the temperature of feed at the inlet of the membrane module, because of the temperature polarization inside the liquid and the heat loss both by evaporation and by conduction through the membrane matrix.
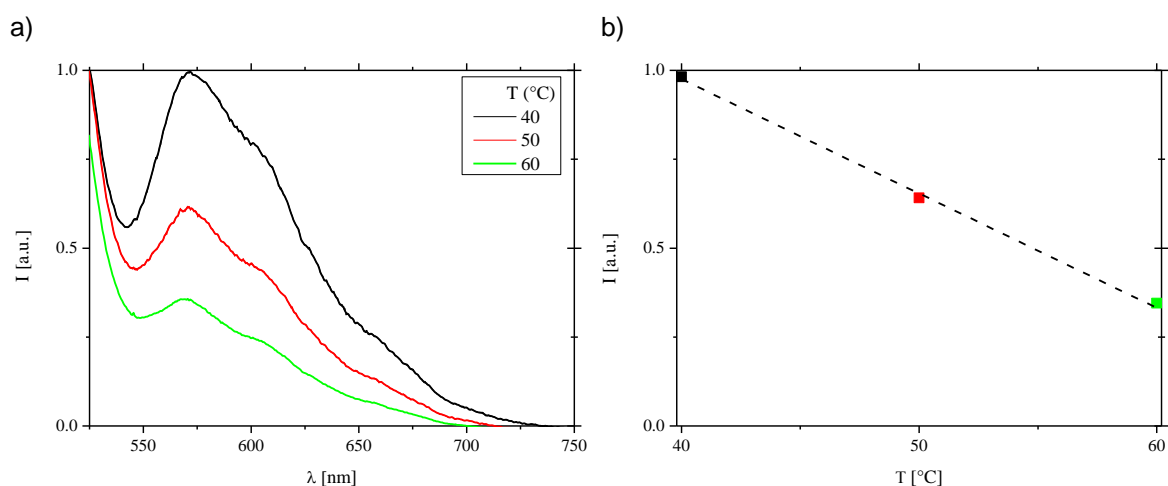
Figure 5.7: Emission spectra of Ru(phen)₃ immobilized in PVDF ENM normalized with respect the value of the maximum of the emission (572 nm) collected at 40°C (a) and temperature sensitivity of the maximum of the emission (572 nm) (b).

Furthermore, because of the heat transfer, the temperature of the membrane surface decreases along the membrane module. In fact, in all the cases the temperature of the membrane surface in proximity of the outlet of the membrane module is of ca. 20°C lower with respect to the temperature of the feed. However different behaviours were observed by varying the temperature of the feed. In particular, the effect is more pronounced at 60°C due to the fact that an increase in the temperature of the feed leads to a higher driving force across the membrane and then to a higher heat loss by both evaporation and conduction. As a result, the temperature polarization effect is significant and the temperature seems to linearly decrease along the membrane module (Figure 5.8.a).
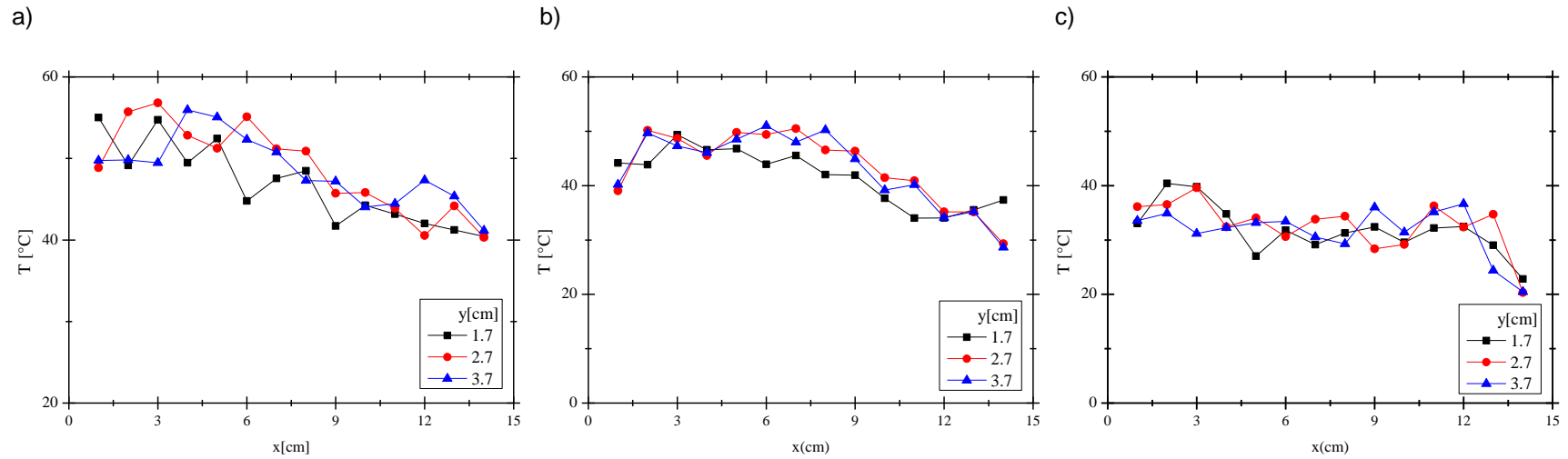
Figure 5.8: Profile of temperature on the membrane surface along membrane module at different temperature of the feed: a) 60°C, b) 50°C, c) 40°C.

On the other hand, at an inlet temperature of 40°C the lower difference of temperature across the membrane decreases the heat transfer from feed side to permeate side and as a consequence the profile of temperature on membrane surface appeared smoother for the larger part of the surface, whereas a considerable drop of the temperature (13±2°C) was observed in the last 2 cm of the membrane surface in proximity of the outlet (Figure 5.8.c).

Furthermore in Figures 5.9, it is possible to notice that the rate of cooling is more marked in the lateral region of the module. This effect is probably induced by the decreasing of the feed velocity close to the membrane module edges. As a consequence of the lower velocity, water persists for longer time in the marginal regions of the membrane module transferring higher amount of heat and leading, then, to a higher rate of cooling of membrane surface.
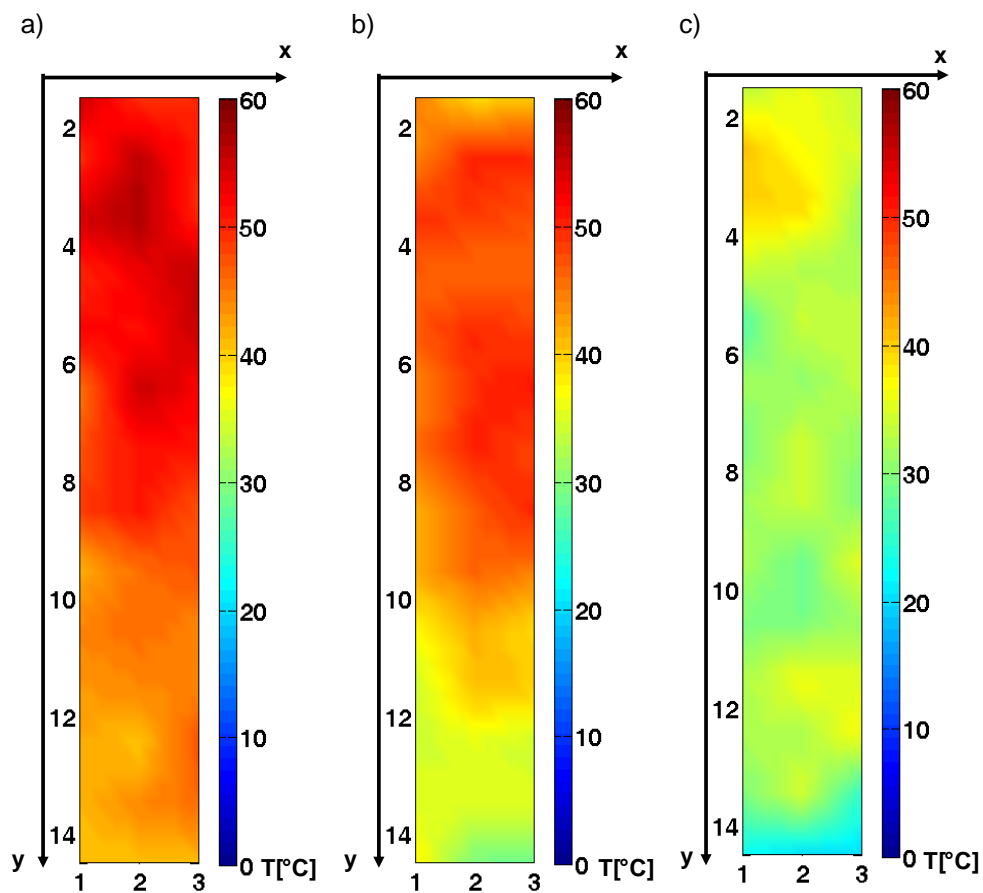
Figure 5.9: *Topographic Maps of the temperature on membrane PVDF ENM using discrete optical fiber measurements together with griddedinterpolant function, Matlab, at different temperature of the feed: a) 60°C, b) 50°C, c) 40°C.*
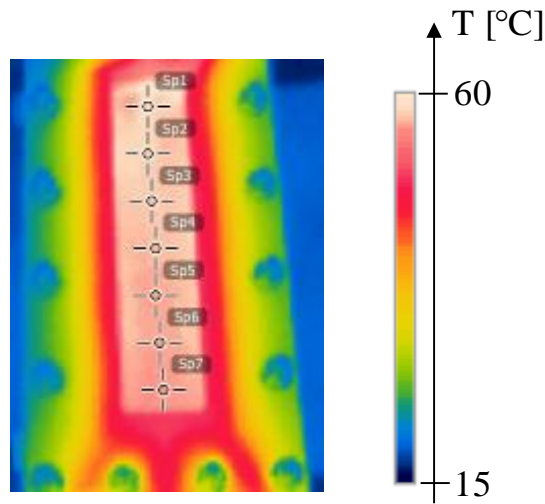
Figure 5.10: Infrared picture of the membrane module at a feed inlet temperature of 60°C.
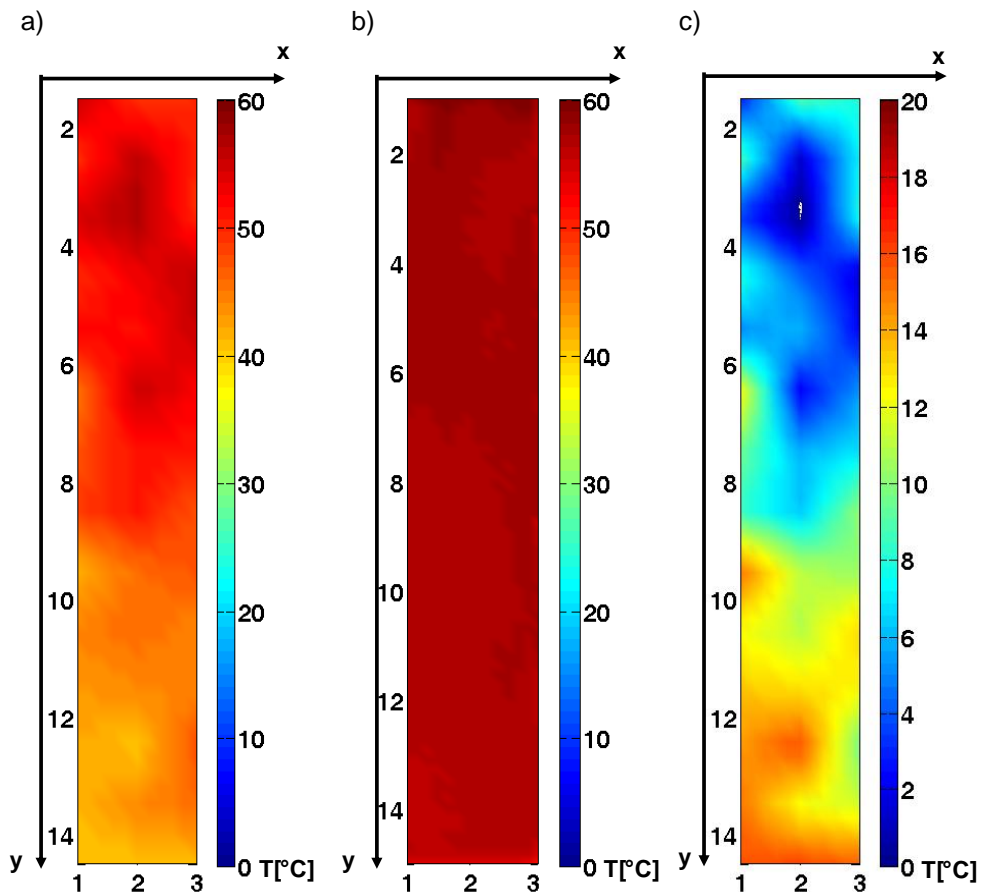
Figure 5.11: Topographic Maps of the temperature in DCMD experiment (feed temperature=60°C). a) on the surface PVDF ENM, measured by optical fiber, b) Measurement using IR camera, c) temperature polarization along membrane surface obtained by subtracting temperatures reported in a) from temperatures reported in b).

Besides the temperature profile on the membrane surface, a decay of temperature was also observed in the feed bulk, by means of an IR-camera (Figure 5.10 shows the thermograph picture obtained during a DCMD experiment carried out at 60°C). The picture evidenced the external part of the module at room temperature, whereas the central region in contact with the feed is at a temperature close to 60°C. The membrane module exposed to this difference of temperature is subjected to heat transfer and as a consequence lateral regions of the feed present a lower temperature.

In Figure 5.11, it is possible to compare the topographic maps of the temperature on the surface PVDF ENM measured using the optical fiber (a) with those of the feed bulk obtained by IR picture (b) for the DCMD experiment carried out at 60°C. First observation is that the map corresponding to the IR camera shows a constant temperature along the area occupied by the membrane, this temperature corresponding to the temperature of the bulk fluid. However a clear temperature gradient is observed in the map produced by the optical fiber measurements. As previous discussed, due to the thermal polarization the temperature on membrane surface dramatically decreases with respect to the bulk. In fact, the membrane surface temperature decreases to a value of 40.6±0.3°C in proximity of the outlet of the membrane module. On the other hand, the temperature of the bulk is affected by a minimal heat loss and the temperature decrease along the membrane module is of only 1.5±0.2°C. On the basis of these results, the thermal polarization becomes more pronounced along the membrane module. In fact, the difference of the temperature between the bulk and the membrane increases along the direction of the feed flow (Figure 5.11.c).

5.4 Conclusions

A PVDF membrane prepared via electrospinning and loaded with a molecular probe was successfully developed. The homogeneity of the membrane made by a 3D network of nano-fibers was optimized indicating the key role of the concentration of the polymer on the dope solution and its electrical conductivity. In fact, the addition of salts, in particular LiCl and Ru(phen)$_3$ in the polymeric solution lead to the preparation of homogeneous membrane defect-free.

The membrane showed promising results in terms of water flux and stability in DCMD experiments. Furthermore, the doping with Ru(phen)$_3$ conferees to the PVDF membrane photochemical activity and, as expected, its emission intensity linearly decreases by increasing the temperature. These properties combined with the development of a devoted membrane module with a transparent window allowed the monitoring of the temperature of the membrane surface in-real time, non-invasive and in-situ.

Using an IR-Camera, it was possible to monitor the temperature of the bulk and the heat lost by the membrane module. The combination of the two optical techniques (IR camera and fluorescence) led to the mapping of the difference of temperature between the bulk and membrane surface, which increases along the membrane module.

According to these results, molecular probes could be considered an innovative and interesting technology for monitoring temperature on membrane surfaces providing an important feedback in the development of high performance membranes and membrane modules and optimization of the operating conditions.

5.5 References

[1] Drioli, E, Criscuoli, A, and Curcio, E. Membrane contactors: fundamentals, applications and potentialities, in: *Membrane Science and Technology Series.* Elsevier, 2006.

[2] Criscuoli, A, Zhong, J, Figoli, A, Carnevale, M C, Huang, R R, and Drioli, E. Treatment of dye solutions by vacuum membrane distillation. *Water Research*, 42(2): 5031-5037, 2008.

[3] Alkhudhiri, A, Darwish, N, and Hilal, N. Membrane distillation: A comprehensive review. *Desalination*, 287: 2-18, 2012.

[4] García-Payo, M C, Essalhi, M, and Khayet, M. Effects of PVDF-HFP concentration on membrane distillation performance and structural morphology of hollow fiber membranes. *Journal of Membrane Science,* 347:209-219, 2010.

[5] Cipollina, A, Di Sparti, M G, Tamburini, A, and Micale, G. Development of a Membrane Distillation module for solar energy seawater desalination. *Chemical Engineering Research and Design*, 90:(12) 2101-2121, 2012.

[6] Alklaibi, A M, and Lior, L. Membrane-distillation desalination: Status and potential. *Desalination*,17(2), 111-131,2005 .

[7] Essalhi, M, and Khayet, M. Fundamentals of membrane distillation, in: *Pervaporation,Vapour Permeation and Membrane Distillation*. Elsevier, 2015.

[8] Phattaranawik, J, Jiraratananon, R, and Fane, A G. Effect of pore size distribution and air flux on mass transport in direct contact membrane distillation. *J Journal of Membrane Science*, 215, (1-2):75-85, 2003.

[9] Gryta, M. Influence of polypropylene membrane surface porosity on the performance of membrane distillation process. *Journal of Membrane Science*, 287(1): 67-78, 2007.

[10] Liu, F, Hashim, N A, Liu, Y, Abed, M R M, and Li, K. Progress in the production and modification of PVDF membranes. *Journal of Membrane Science*, 375(1-2):1-27, 2011.

[11] Tijing, L D, Choi, J, Lee, S, Kim, S, and Shon, H K. Recent progress of membrane distillation using electrospun nanofibrous membrane. *Journal of Membrane Science,* 453:435-462, 2014.

[12] Prince, J A, Rana, D, Singh, G, Matsuura, T, Jun Kai, T, and Shanmugasundaram, T S. Nanofiber based triple layer hydro-philic/-phobic membrane-a solution for pore wetting in membrane distillation. *Sci. Rep.*, 4: 6949-6955, 2014.

[13] Khayet, M, and García-Payo, M C. Nanostructured Flat Membranes for Direct Contact Membrane Distillation. *PCT/ES2011/000091, WO/2011/117443*, 2011.

[14] Feng, C, Khulbe, K C, Matsuura, T, Gopal, R, Kaur, S, Ramakrishna, S, and Khayet, M. Production of drinking water from saline water by air-gap membrane distillation using polyvinylidene fluoride nanofiber membrane. *Journal of Membrane Science*, 311(1-2):1-6, 2008.

[15] Feng, C, Khulbe, K C, and Tabe, S. Volatile organic compound removal by membrane gas stripping using electro-spun nanofiber membrane. *Desalination*, 287:98-102, 2012.

[16] Liao, Y, Wang, R, , M, Qiu, C, and Fane, A G. Fabrication of polyvinylidene fluoride (PVDF) nanofiber membranes by electro-spinning for direct contact membrane distillation. *Journal of Membrane Science*, 425-426:30-39, 2013.

[17] Hitsov, I, Maere, T, De Sitter, K, Dotremont, C, and Nopens, I. Modelling approaches in membrane distillation: A critical review. *Separation and Purification Technology* ,142:48-64, 2015.

[18] Martinez-Diez, L, and Vázquez-González, M I. A method to evaluate coefficients affecting flux in membrane distillation. *Journal of Membrane Science*, 173(2):225-234, 2000.

[19] Martínez-Díez, L, and Rodríguez-Maroto, J M. Characterization of membrane distillation modules and analysis of mass flux enhancement by channel spacers. *Journal of Membrane Science*, 274(1-2): 123-137, 2006

[20] Cheng, L, Wu, P, and Chen, J. Modeling and optimization of hollow fiber DCMD module for desalination. *Journal of Membrane Science*, 318(1-2):154-166, 2008.

[21] Chen, T CHo, C D, and Yeh, H M. Theoretical modeling and experimental analysis of direct membrane distillation. *Journal of Membrane Science*, 330(2): 279-287, 2009.

[22] Ding, Z, Ma, R, and Fane, A G. A new model for mass transfer in direct contact membrane distillation. *Desalination*, 151(3): 217-227, 2002.

[23] Ali, A, Macedonio, F, Drioli, E, Aljlil, S, and Alharbi, A O. Experimental and theoretical evaluation of temperature polarization phenomenon in direct contact membrane distillation. *Chemical Engineering Research and Design*, 91(10):1966-1977, 2013.

[24] Tamburini, A, Pitò, P, Cipollina, A, Micale, G, and Ciofalo, M. A Thermochromic Liquid Crystals Image Analysis technique to investigate temperature polarization in spacer-filled channels for Membrane Distillation. *Journal of Membrane Science*, 447:260-273, 2013.

[25] Yang, J M, Yang, H, and Lin, L. Quantum dot nano thermometers reveal heterogeneous local thermogenesis in living cells. *ACS Nano*, 5(6): 5067-5071, 2011.

[26] Filevich, O, and Etchenique, R. ID and 2D temperature imaging with a fluorescent ruthenium complex. *Analytical Chemistry*, 78(21): 7499-7503, 2006.

[27] Santoro, S, Moro, A J, Portugal, C M, Crespo, J G, Coelhoso, I M, Lima, J C, 2016, Development of Oxygen and Temperature Sensitive Membranes Using Molecular Probes as Ratiometric Sensor. *Journal of Membrane Science* (submitted).

[28] Figoli, A, Simone, S, Criscuoli, A, AL-Jlil, S A, Al Shabouna, F S, Al-Romaih, H S, Di Nicolò, E, Al-Harbi, O A, and Drioli, E. Hollow fibers for seawater desalination from blends of PVDF with different molecular weights: Morphology, properties and VMD performance. *Polymer*, 55: 1296-1306, 2014.

[29] Chan, L S, Cheung, W H, and McKay, G. Adsorption of acid dyes by bamboo derived activated carbon. *Desalination*, 218(1-3): 304-312, 2008.

[30] Liao, Y, Wang, R, Tian, M, Qiu, C, and Fane, A G. Fabrication of polyvinylidene fluoride (PVDF) nanofiber membranes by electro-spinning for direct contact membrane distillation. *Journal of Membrane Science*, 425-426:30-39, 2013.

[31] Deitzel, J M, Kleinmeyer, J, Harris, D, and Beck Tan, N C. The effect of processing variables on the morphology of electrospun nanofibers and textiles. *Polymer*, 42(1):261-272, 2001.

[32] Zong, X, Kim, K, Fang, D, Ran, S, Hsiao, B S, and Chu, S. Structure and process, relationship of electrospun bioabsorbable nanofiber membranes. *Polymer*, 43(16):4403-4412, 2002.

[33] Wenzel, R N. *Ind. Eng. Chem.,* 28(8): 988-994, 1936.

[34] Solef® & Hylar® PVDF Polyvinylidene fluoride Design and Processing Guide.

[35] Lei, Z, Chen, B, and Ding, Z. Membrane distillation, in: *Special Distillation Processes*. Elsevier Science, 2005.

[36] Wu, H Y, Wang, H G, and Field, R T W. Direct contact membrane distillation: An experimental and analytical investigation of the effect of membrane thickness upon transmembrane flux. *Journal of Membrane Science*, 470: 257-265, 2014.

[37] Laganà, F, Barbieri, G, and Drioli, E. Direct contact membrane distillation: modelling and concentration experiments. *Journal of Membrane Science*, 16(1):1-11, 2001.

[38] Prince, J A, Rana, D, Singh, G, Matsuura, T, Jun Kai, T, and Shanmugasundaram, T S. Effect of hydrophobic surface modifying macromolecules on differently produced PVDF membranes for direct contact membrane distillation. *Chem. Eng. J.*, 242:387-396, 2014.

[39] Prince, J A, Singh, G, Rana, D, Matsuura, T, Anbharasi, V, and Shanmugasundaram, T S. Preparation and characterization of highly hydrophobic poly(vinylidene fluoride) – clay nanocomposite nanofiber membranes PVDF–clay NNMs) for desalination using direct contact membrane distillation. *Journal of Membrane Science*, 397–398: 80-86, 2012.

[40] Essalhi, M, and Khayet, M.Self-sustained webs of polyvinylidene fluoride electrospun nanofibers at different electrospinning times: 1. Desalination by direct contact membrane distillation. *Journal of Membrane Science*, 433:167-179, 2013.

[41] Liao, Y, Wang, R, and Fane, A G. Fabrication of bioinspired composite nanofiber membranes with robust superhydrophobicity for direct contact membrane distillation. Environ. Sci. Technol. 48(11) (2014) 6335-6341.

[42] Liao, Y, Loh, C-H, Wang, R, and Fane, A G. Electrospun superhydrophobic membranes with unique structures for membrane distillation. *ACS Appl. Mater.Interfaces*, 6(18):16035-16048, 2014.

[43] Tijing, L D, Woo, Y C, Shim, W-G, He, T, Choi, J-S, Kim, S-H, and Shon, H K. Superhydrophobic nanofiber membrane containing carbon nanotubes for high-performance direct contact membrane distillation. *Journal of Membrane Science*, 502:158-170, 2016.

[44] Sauer, M, Hofkens, J, and Enderlein, J. Basic Principles of Fluorescence Spectroscopy, in: *Handbook of Fluorescence Spectroscopy and Imaging: From Single Molecules to Ensembles*. Wiley, 2011.

Chapter 6

Conclusions

Efforts in membrane science have been devoted on the development of innovative materials and optimization of the operating conditions in order to maximize the chemical-physical interactions at molecular level between membrane surface and target permeant scale that govern the mass transport.

Conventional techniques enable the evaluation of the effects of these interactions on the global performance of the membrane and of the membrane processes, but fail in providing information at a molecular level and in-situ (i.e. membrane surface).

The main objective of the work presented in this thesis was to address the potential employment of molecular probes as an innovative technique for monitoring membrane processes overcoming specific drawbacks of the conventional techniques. The main achievements are highlighted in this chapter with a particular emphasis on future developments and perspectives towards the implementation of the proposed technologies in different membrane processes.

6.1 Oxygen monitoring

The aim of this part of the work was to develop smart membranes to detect oxygen concentration by the dispersion of molecular probes in a membrane matrix.

The immobilization of Ru(phen)$_3$, a luminophore known for its sensitivity to the oxygen, in PS and PHVB conferred to the membrane photochemical activity. Experiments showed that the intensity of the emission of the membrane decreases by increasing the oxygen concentration due to the collision quenching that occurs between the complex of Ruthenium and the oxygen which permeates through the membrane.

Studies demonstrated that the rate of quenching depends on the oxygen permeability of the membrane. In fact, PS guaranteed higher degree of interaction between oxygen and Ru(phen)$_3$ with respect to PHVB due to its higher oxygen permeability leading to a lower intensity of the emission at parity of oxygen concentration. This aspect is of extreme interest in membrane science since the molecular probe could be useful for the evaluation of oxygen permeability. Furthermore, the amount of probe required for these studies is minimal (from nanomole to micromole of Ru(phen)$_3$ per gram of polymer) avoiding alteration of chemical-physical and transport properties of the membranes.

A serious limitation of optical technique is that the measurements are prone to errors due to unknown fluctuation of the operating conditions (i.e. optical path, source intensity). This critical issue was successfully dealt by dispersion of a second molecular probe non-sensitive to the oxygen employed as reference in developing a ratiometric sensor. Coumarin was selected with respect to Dansyl Chloride, Quinine Sulphate for development of the ratiometric response because of its non-sensitivity to oxygen and well discernible emission band from the Ruthenium complex.

The ratiometric response allows the correction of artefacts induced by the operative conditions leading to the precise monitoring of oxygen concentration.

On the other hand, the matched sensitivity to the temperature of both the probes was restricted by the implementation of a simple algorithm allowing to obtain a signal that depends solely on the oxygen concentration.

The developed ratiometric sensor was successful employed for monitoring of the permeation of oxygen trough polymeric films with different oxygen permeability. The oxygen sensitive membranes were placed in a degassed atmosphere enclosed by the polymeric film mimicking a typical configuration in food packaging. Indeed, in this situation the packaging film is an interface between the enclosed degassed chamber (without oxygen) and the external atmosphere (oxygen concentration: 21%). The oxygen sensitive membrane placed in the enclosed atmosphere was stimulated by the exciting light passing through the polymeric packaging material and the emitted light supplied information about the rate of oxygen content in the package, consequently, about the rate of oxygen permeation due to the gradient of concentration across the package. The sensitive membrane allowed the monitoring of oxygen transport through polymeric films with different oxygen permeability, such as PDMS and BOPP. The evolvement of oxygen concentration inside the package made of PDMS was predicted by the solution diffusion model assuming constant permeability (Fist Fick Law), whereas a dual-mode sorption model (non-fickian) was observed for BOPP packaging in the initial phase.

6.2 Temperature monitoring

In the first part of the studies, it was noticed that the increase of the temperature favors the non-radiative deactivation of the probes decreasing the insensitive of the emission as expected. This usual behavior of luminophores suggests one more appealing opportunity of molecular probes in membrane technology: the monitoring of the temperature. The second part of the thesis was devoted on the development of systems providing information on-line and in-situ of the temperature of the membrane. The immobilization of $Ru(phen)_3$ in silica nano-particles allowed the development of nano-thermometer. The nano-sensor was prepared starting from a colloidal solution of bare silica coated, in a second step, by a shell of silica doped with the luminophore. The polar interactions between the silica and the Ruthenium complex favored the immobilization of the probe and protect it from environmental conditions (i.e. oxygen concentration). Studies showed that employing this procedure it was possible to obtained mono-dispersed nano-particles. On the contrary, the homogeneity in terms of shape and monodispersivity was compromised by the immobilization of the molecular probe in the core made of silica due to steric effects of the complex of Ruthenium which disturbed the condensation of the silica precursor. A systematic study showed it is possible to control the properties of the nano-thermometer in terms of size by varying the concentration of the amount of silica precursor (TEOS) used to growth the shell, whereas the concentration of the probe affected the intensity of the emission and the temperature sensitivity. Furthermore it was possible to turn the character of the silica nano-particles, from hydrophilic to hydrophobic by the functionalization of their surface with a silane-derivated with a long aliphatic chain.

The temperature sensitive nano-particles were immobilized via dip-coating on the surface of PVDF porous membranes prepared via NIPS. The immobilization of the SiO_2NPs did not affect the basic properties of PVDF membrane that presented an unmatched temperature sensitive photochemical activity attributed to the nano-particles doped with $Ru(phen)_3$. This system is a really promising since could allow the monitoring of the temperature on membrane surface and also in biomedical applications, such as the monitoring of the temperature of nano-particles employed in hyperthermia. In this therapy, silica nano-particles covered with gold shell release heat as a consequence of the absorption of IR light, destroying cancer tissues. The immobilization of the molecular probes could be of interest not only for marking the nano-particles, but also in detecting the temperature achieved by the nano-particles offering information about the efficiency of the system.

One different approach was the direct immobilization of the molecular probe in the polymeric membrane. Once again $Ru(phen)_3$ was immobilized in PVDF self-sustained electrospun nano-fibrous membranes (ENMs). SEM analyses showed the key-role of the molecular probe on the preparation of defect-free nanofibers due to its salty nature. In fact, the employment of the luminophore and LiCl increased the conductivity of the polymeric solution increasing its spinnability allowing for the preparation of homogeneous nano-fibers. This method allowed the preparation of membranes with super-hydrophobicity surface and interconnected open pore morphology made of a 3D network of nano-fibers. PVDF ENM showed an evident emission related to the presence of $Ru(phen)_3$ immobilized in the PVDF chains. The developed PVDF ENM presented excellent performance on DCMD experiments due to its low thickness and high porosity combined with high hydrophobicity.

By employing a devoted membrane module with a transparent window and a fluorometer equipped with a biforcuted optical fiber, it was possible to monitor the fluorescence raising from the PVDF ENM doped with $Ru(phen)_3$. As expected, the intensity of the emission linearly decreased by increasing the temperature, providing information in-situ about the temperature on the membrane surface. After calibration, it was possible the on-line and non-invasive monitoring of the temperature of the membrane surface during the DCMD processes in different spots of the active area. Subsequently the map of the temperature on membrane surface was obtained by using the temperatures of the different spots as inputs in a model that from discrete points extrapolates a continuous trend. Moreover, the map of temperature of the feed bulk was obtained by means of an IR-camera. Results evidenced that the temperature on membrane surface is lower with respect to the bulk as expected due to the thermal polarization. Furthermore, due to the energy required for producing water vapour and the thermal conductivity of the membrane, the difference of temperature between the bulk and the membrane surface increases along the membrane module. These experiments evidenced the employment of molecular probe as an innovative technology for studying the phenomena of thermal polarization providing crucial information for DCMD process producing advances in term of scientific knowledge that could be used to improve the efficiency of the process.

6.3 Future works

As further developments of this thesis, several are the possibilities concerning both oxygen and temperature monitoring. Results claim molecular probes as a really interesting technology for the on-line, non invasive and in-situ technology for the on line monitoring of oxygen and temperature in real process.

However there is one more advantage (not deeply explored) in the employment of luminophore for monitoring oxygen: the molecular size of the probe. This benefit is of extreme interest in evaluation the oxygen concentration at molecular scale on membrane surface in processes where oxygen production or consumption takes place, such as membrane bioreactor. Furthermore, the immobilization of oxygen sensitive molecular probes on membrane surface could provide crucial information about the oxygen concentration consumed on boundary layer related to the growth of aerobic biofouling. With respect to this, the nano-thermometers based on the immobilization of $Ru(phen)_3$ in silica nano-particles could be of interest, since silica nano-particles are widely employed as antifouling agent, whereas $Ru(phen)_3$ could detect the local dissolved oxygen concentration.

Preliminary experiments showed that using and adequate technology, such as fluorescent microscopy, it is possible not only the detection of the oxygen concentration on membrane surface, but also to follow the profile of oxygen in membrane bulk.

The employment of optical techniques based on the use of molecular probe for monitoring the temperature at membrane surface and IR-camera for the detection of the temperature of the bulk streams could describe the thermal polarization in every respect. In this work, efforts have been devoted in proving the concept and developing an adequate devoted technology, in particular the membrane module, exploring the map of the temperature on membrane surface and bulk on the feed side. Nevertheless, the same configuration could be used to monitor the permeate side, obtaining all the data required to evaluate the heat transfer during the process and studying the thermal polarization. In this sense, further studies about the effects of the streams flow rate and membrane properties on thermal polarization are crucial.

Several molecular probes are also known for their sensitivity to CO_2, Ca^{2+}, pH and solvent polarity offering several potential applications for the monitoring of membrane processes. Nevertheless, opportunities are also envisaged for the study of the membrane preparation in conventional techniques (i.e. rate solvent exchange in NIPS by using molecular probe sensitive to the solvent polarity).

At the end of this manuscript, it could be affirmed that this thesis concerns about the monitoring of oxygen and temperature in membrane processes on-line in situ, non-invasive and at sub-micron scale using molecular probes. Thus, this study may be considered as a basis for further developments opening up interesting perspectives on the monitoring of membrane processes.

Capítulo 6

Conclusiones

La ingeniería de membranas ha dedicado especial atención y recursos al desarrollo de materiales innovadores y a la optimización de las condiciones de operación con el fin de maximizar las interacciones físico-químicas a nivel molecular entre la superficie de la membrana y las moléculas a procesar.

Las técnicas convencionales de caracterización permiten la evaluación a nivel global del funcionamiento de la membrana y de los procesos físicos que ocurren en ella. Sin embargo, la información disponible carece de datos referidos a los procesos físico-químicos que tienen lugar a nivel local sobre la superficie de la membrana y que generalmente son fundamentales para el óptimo funcionamiento y operatividad de la membrana.

El principal objetivo del trabajo presentado en esta tesis ha sido desarrollar sondas moleculares como una técnica innovadora para el seguimiento, en tiempo real, de los procesos que tienen lugar en la membrana. Estas sondas moleculares han permitido eliminar algunos de los inconvenientes específicos de las técnicas convencionales, donde la información referente al funcionamiento de la membrana es de una naturaleza más global que la obtenida con las sondas moleculares. En este capítulo se destacan los logros mas destacados en el desarrollo y aplicación de las sondas moleculares, haciendo un particular énfasis en los desarrollos futuros y perspectivas para la aplicación de la tecnología aquí propuesta para los diferentes usos en la ingeniería de membranas.

6.1 Medición de oxígeno

El objetivo de esta parte del trabajo fue desarrollar membranas "inteligentes" capaces de detectar y cuantificar la concentración de oxígeno mediante la dispersión de sondas moleculares en la propia matriz de la membrana.

La inmovilización de Ru (phen)$_3$, una molécula luminiscente conocida por su sensibilidad al oxígeno, en PS y PHVB, confirió a la membrana la propiedad de tener integrado un sensor fotoquímico. Los experimentos mostraron que la intensidad de la emisión de la membrana disminuye al aumentar la concentración de oxígeno debido a la extinción que se produce por la interacción entre el complejo de rutenio y el oxígeno que difunde a través de la membrana.

Los estudios demostraron que la señal de extinción depende directamente de la permeabilidad del oxígeno en la membrana. De hecho, el PS garantiza un mayor grado de interacción entre el oxígeno y Ru (phen)$_3$ con respecto a PHVB debido a su mayor permeabilidad al oxígeno, que conlleva una menor intensidad de la emisión en relación a la concentración de oxígeno. Este aspecto es de gran interés en la ingeniería de membranas, puesto que la sonda molecular podría ser útil para la evaluación de la permeabilidad al oxígeno. Además, la concentración de sondas moleculares necesarias para los estudios es mínima, siendo del orden de nanomoles y micromoles de Ru (phen)$_3$ por gramo de polímero. Es necesario indicar que la existencia de las sondas moleculares no altera las propiedades físico-químicas y de transporte de la membrana.

Una seria limitación técnica de la señal óptica procedente de moléculas luminiscentes es que las medidas de emisión son susceptibles a errores debido a la fluctuación existente en las propias

condiciones de medida, como por ejemplo la trayectoria óptica o la intensidad de la fuente Para abordar esta problemática se dispersó una segunda sonda molecular, no sensible al oxígeno, en el seno de la membrana; obteniendo así un sensor ratiométrico. Como sonda de referencia ratiométrica se utilizó cumarina frente a cloruro de dansilo y sulfato de quinina. Esta dualidad de sondas originó una respuesta ratiométrica, en la que la cumarina debido a su no sensibilidad al oxígeno permitía ser la referencia para el complejo de rutenio. La respuesta ratiométrica obtenida permitía la corrección de artefactos inducidos por las condiciones operativas, permitiendo la monitorización precisa de la concentración de oxígeno.

Por otra parte, la sensibilidad conjunta a la temperatura de las sondas fue restringida por la aplicación de un algoritmo simple que permitía obtener una señal que dependia únicamente de la concentración de oxígeno.

El sensor ratiométrico desarrollado fue exitosamente empleado para determinar la permeación de oxígeno en películas poliméricas con diferente permeabilidad al oxígeno. Las membranas sensibles al oxígeno se colocaron en una atmósfera desgasificada, sellada por una película polimérica imitando una configuración típica en el envasado de alimentos. De hecho, en esta situación, la película de envasado es una interfaz entre la cámara cerrada de desgasificación (sin oxígeno) y el ambiente externo (concentración de oxígeno: 21%). La membrana sensible al oxígeno colocado en la atmósfera encerrada fue estimulada por la luz de excitación que pasa a través del material de envasado polimérico y la información sobre la cantidad de oxígeno en el envase se obtuvo a partir de la luz emitida. En consecuencia, se pudo determinar la velocidad de permeación de oxígeno debido al gradiente de concentración existente a través de la membrana del envase. El sistema membrana con respuesta ratiométrica permitió el seguimiento del transporte de oxígeno a través de películas poliméricas con diferente permeabilidad al oxígeno, tales como PDMS y BOPP. La evolución de la concentración de oxígeno en el interior del envase hecho de PDMS fue predicho por el modelo de difusión-solución suponiendo constante la permeabilidad (Ley de Fick), mientras que la película de BOPP se observó un modelo de adsorción dual (no correlacionado con la ley Fick) en la fase inicial.

6.2 Medición de la temperatura

Como se ha hecho mención en el apartado anterior, se observó que el aumento de la temperatura favorece la desactivación no radiativa de las sondas moleculares, disminuyendo, tal y como correspondería, la intensidad de la emisión. Este comportamiento habitual de los compuestos luminiscentes ha permitido desarrollar una aplicación de las sondas moleculares en la tecnología de membranas: el seguimiento y trazabilidad de la temperatura. La segunda parte de la tesis se dedica por tanto al desarrollo de sistemas que proporcionan información en tiempo real e in situ de la temperatura de la membrana.

La inmovilización de Ru (phen)$_3$ en nano-partículas de sílice permitió el desarrollo de nano-termómetros. El nano-sensor se preparó a partir de un coloide de sílice, sobre el cual se hizo crecer, en una segunda etapa, una capa de sílice dopada con el compuesto luminiscente. Las interacciones

polares entre la sílice y el complejo de rutenio favorecieron la inmovilización de la sonda molecular protegiéndola a su vez de las condiciones ambientales (como por ejemplo la interacción con el oxígeno). Los estudios realizados demostraron que fue posible la producción de nano-partículas con una distribución de tamaños monodispersa. Por el contrario, la homogeneidad en términos de forma y distribución de tamaños se vio comprometida si la inmovilización de la sonda molecular se realizaba directamente en el núcleo de sílice. Este comportamiento es debido a la existencia de efectos estéricos del complejo de rutenio y sílice, que perturban la condensación del precursor de sílice. Un estudio sistemático mostró que es posible controlar las propiedades del nano-termómetro, en términos de tamaño, mediante la variación de la concentración de la cantidad de precursor de sílice (TEOS) que se usa para el crecimiento de la capa externa, mientras que la concentración de la sonda afecta únicamente a la intensidad de la emisión y la sensibilidad a la temperatura. Además, fue posible modificar el carácter de los nanotermómetros entre hidrófilo e hidrófobo. Así el carácter hidrófilo de los termómetros sintetizados en medio acuoso se transformó en hidrófobo mediante la funcionalización de su superficie con un silano de cadena alifática larga.

Las nano-partículas sensibles a la temperatura se inmovilizaron en la superficie de membranas porosas de PVDF preparados a través del proceso de inversión de fase (NIPS). La inmovilización de las nanopartículas de SiO_2 no afectó a las propiedades básicas de separación de la membrana de PVDF. Dicha membrana presentaba una actividad fotoquímica sensible a la temperatura y atribuida a la molécula de Ru (phen)$_3$ que dopaba la superficie de la sílice. Este sistema es un muy prometedor en el campo de la tecnología de las membranas de separación, ya que ha permitido la medición de la temperatura en la superficie de la membrana. También sería de gran utilidad en aplicaciones biomédicas, tales como la medición de la temperatura de nano-partículas empleadas en la hipertermia óptica. En este tipo de terapia, las nanopartículas de sílice están cubiertas además por una capa fina de oro que transforma los fotones de la radiación absorbida en electrones superficiales (plasmon), generando calor. El aumento de temperatura generado por la radiación en el rango infrarrojo IR, permite destruir los tejidos cancerígenos donde están acumuladas las nanopartículas, sin interferir con las células sanas. Por consiguiente, la inmovilización de las sondas moleculares en estas estructuras híbridas de SiO_2-Au podría ser de interés no sólo para el marcado de las nano-partículas, sino también para la detección de la temperatura alcanzada por los nano-partículas, ofreciendo información sobre la eficiencia de calentamiento del sistema.

Un enfoque diferente fue la inmovilización directa de la sonda molecular en la membrana polimérica. Una vez más Ru (phen)$_3$ fue inmovilizado en membranas de PVDF autosoportadas y fabricadas por el sistema de electrohilado. Los análisis de microscopía electrónica de barrido, SEM, mostraron la función de la sonda molecular en la preparación de nanofibras, favoreciendo la regularidad en las fibras como consecuencia de su carácter polar. De hecho, el empleo de la molécula luminiscente y LiCl aumenta la conductividad de la solución polimérica, aumentando su capacidad de hilado y permitiendo la preparación de nano-fibras homogéneas. Este método ha permitido la preparación de membranas con la superficie hidrofóbica y morfología de poros abiertos interconectados entre si. La membrana generada tiene una estructura de red 3D de nano-fibras de PVDF, que mostraban una

emisión relacionada con la presencia de Ru(phen)$_3$ inmovilizado en las cadenas de PVDF. El PVDF presentaba un excelente rendimiento debido a su bajo espesor y elevada porosidad combinada con una alta hidrofobicidad.

Mediante el empleo de un módulo diseñado con una ventana transparente y un fluorímetro equipado con una fibra óptica bifurcada, fue posible monitorizar la fluorescencia generada por la membrana PVDF dopada con Ru(phen)$_3$. Como se esperaba, la intensidad de la emisión disminuyó linealmente al aumentar la temperatura, proporcionando información "in situ" sobre la temperatura en la superficie de las membranas. Después de la calibración, fue posible el control no invasivo y en tiempo real de la temperatura de la superficie de la membrana. Posteriormente y tras tratar los datos de emisión generados, se pudo determinar el mapa de la temperatura en la superficie de la membrana. Por otra parte, el mapa de temperaturas del fluido de alimentación (agua) fue obtenido por medio de una cámara IR. Los resultados evidenciaron que la temperatura en la superficie de la membrana era más baja con respecto al agua, como consecuencia del fenómeno de polarización térmica. Además, se pudo determinar la energía requerida para la producción de vapor de agua y la conductividad térmica de la membrana. También se observó que la diferencia de temperatura entre el agua y la superficie de la membrana se incrementaba a lo largo del módulo de membrana. Estos experimentos evidenciaron que el empleo de la sonda molecular es una tecnología innovadora que ha posibilitado el estudio de los fenómenos de polarización térmica proporcionando información crucial para la proceso de destilación con membranas por contacto directo DCMD. Además está tecnología permite desarrollar conocimientos científicos que podrían ser utilizados para mejorar la eficiencia en los procesos de purificación y separación con membranas.

6.3 Perspectivas futuras

Como desarrollos adicionales de esta tesis, se consideran varias posibilidades de aplicación en relación con la monitorización del oxígeno y de la temperatura. Los resultados obtenidos confirman que estas sondas moleculares son una tecnología muy interesante para la línea de determinación no invasiva y en tiempo real de la monitorización de oxígeno y la temperatura local del proceso.

Sin embargo hay una ventaja más (no explotada en detalle) en el empleo de moléculas luminiscentes para la monitorización de oxígeno: el tamaño molecular de la sonda. Este beneficio es de sumo interés en la evaluación de la concentración de oxígeno a escala molecular en la superficie de la membrana en procesos en los que se efectúe la producción o consumo de oxígeno, tales como bioreactores de membrana. Por otra parte, la inmovilización de sondas moleculares sensibles al oxígeno en la superficie de la membrana podría proporcionar información crucial acerca de la concentración de oxígeno consumido en la capa límite relacionada con el crecimiento de la contaminación biológica aeróbica. A este respecto, los nano-termómetros, basados en la inmovilización de Ru(phen)$_3$, en nano-partículas de sílice podrían ser de interés, ya que las nanopartículas de sílice se emplean ampliamente como agente antiincrustante, mientras que Ru(phen)$_3$ podría detectar la concentración local de oxígeno.

Los experimentos preliminares mostraron que el uso de esta tecnología y su combinación con la microscopía de fluorescencia, posibilitaría no sólo la detección de la concentración de oxígeno en la superficie de la membrana, sino también permitiría seguir el perfil de oxígeno dentro de la membrana. El empleo de técnicas ópticas basadas en el uso de sondas moleculares para el control y medida de la temperatura de la superficie de la membrana, permitiría describir el fenómeno de la polarización térmica en todos sus aspectos más fundamentales. En este trabajo, se ha dedicado también un considerable esfuerzo para demostrar el concepto y el desarrollo de una tecnología dedicada y adecuada, en particular, el módulo de membrana, que explora la correspondencia de la temperatura en la superficie de la membrana y del agua en el lado de la corriente de alimentación. Sin embargo, la misma configuración podría ser utilizada para monitorear el lado del fluido permeado, permitiendo conseguir todos los datos necesarios para evaluar la transferencia de calor durante el proceso y el estudio de la polarización térmica. En este sentido, son cruciales realizar otros estudios sobre los efectos del flujo de las corrientes y las propiedades de la membrana sobra el fenómeno de polarización térmica.

También son conocidas varias sondas moleculares por su sensibilidad al CO_2, Ca^{2+}, el pH y la polaridad del solvente . Dichas sondas ofrecerían varias aplicaciones potenciales para el seguimiento de los procesos de membrana. Sin embargo, también se contemplan las oportunidades para el estudio de la preparación de membranas en las técnicas convencionales (es decir, velocidad de cambio de disolvente en NIPS mediante el uso de sonda molecular sensible a la polaridad del disolvente).

Tras el trabajo desarrollado en esta tesis doctoral, se podría afirmar que esta tesis aporta varias soluciones de gran relevancia sobre el control de la concentración de oxígeno y temperatura en los procesos de membrana. Dicho proceso de control es en tiempo real y no invasivo, con un nivel de resolución sub-micrométrico. Por lo tanto, este estudio puede ser considerado como una base para futuros desarrollos en el campo de la ingeniería de membranas y de los procesos que en ella ocurren.

Capitolo 6

Conclusioni

Nella scienza delle membrane i recenti sforzi sono stati concentrati sullo sviluppo di materiali innovativi e l'ottimizzazione dei parametri operativi dei processi con lo scopo di massimizzare le interazioni chimiche-fisiche a livello molecolare tra la superficie della membrana e le specie permeanti che governano il trasporto di massa.

Le tecniche convenzionali garantiscono la valutazione degli effetti di queste interazioni sulla base della prestazione globale della membrana e del processo a membrana, ma falliscono nel fornire informazioni a livello molecolare ed *in-situ* (es. superficie della membrana).

L'obiettivo principale del lavoro presentato in questa tesi è quello di valutare le potenzialità dell'impiego delle sonde molecolari come una tecnologia innovativa per il monitoraggio dei processi a membrana superando i limiti delle tecniche convenzionali. I principali risultati sono riassunti in questo capitolo dando particolare enfasi agli sviluppi futuri e alla prospettiva di implementare la tecnologia proposta in diversi processi a membrana.

6.1 Monitoraggio dell'ossigeno

Lo scopo di questa parte della tesi è stato lo sviluppo di membrane intelligenti capaci di monitorare la concentrazione di ossigeno attraverso la dispersione di sonde molecolari nella matrice polimerica della membrana.

L'immobilizzazione di $Ru(phen)_3$, un luminoforo noto per la sua sensibilità all'ossigeno, in polistirolo (PS) e poli(3-idrossibutirrato-co-3-idrossivalerato) (PHVB) ha conferito alle membrane attività fotochimica. Esperimenti hanno dimostrato che l'intensità dell'emissione delle membrane decresce incrementando la concentrazione di ossigeno a causa dello smorzamento collisionale (*collisional quenching)* dovuto a interazioni tra il complesso di Rutenio e l'ossigeno che permea attraverso la membrana.

Studi hanno dimostrato che il grado di smorzamento dipende dalla permeabilità all'ossigeno delle membrane. Infatti, PS ha garantito un alto numero di interazioni tra l'ossigeno e il $Ru(phen)_3$ rispetto al PHVB a causa della sua maggiore permeabilità all'ossigeno ottenendo un'intensità di emissione minore a parità di concentrazione di ossigeno. Questo aspetto è estremamente interessante nella scienza delle membrane in quanto le sonde molecolari potrebbero essere impiegate per valutare la permeabilità all'ossigeno delle membrane. Inoltre, la quantità di sonde molecolari richieste è minima (da nano-mole a micro-mole di $Ru(phen)_3$ per grammo di polimero) evitando alterazioni delle proprietà chimico-fisiche e di trasporto di massa delle membrane.

Una seria limitazione delle tecniche ottiche consiste nel fatto che le misure sono affette da errori dovute a fluttuazioni non-controllabili dei parametri operativi (es. cammino ottico, intensità della sorgente luminosa). Questo aspetto critico è stato risolto con successo mediante la dispersione di una seconda sonda molecolare non sensibile all'ossigeno impiegata come riferimento nello sviluppo di un sensore raziometrico. La Cumarina è stata preferita a Cloruro di Dansile e Chinina Solfato per lo sviluppo del sensore raziometrico sulla base della sua non-sensibilità all'ossigeno e banda di emissione ben discernibile da quella del complesso di Rutenio.

La risposta raziometrica del sensore ha consentito la correzione degli artefatti indotti dalle condizioni operative favorendo una precisa valutazione della concentrazione dell'ossigeno.

D'altro canto, la sensibilità alla temperatura di entrambe le molecole è stata limitata dall'implementazione di un semplice algoritmo che ha consentito di ottenere un segnale che dipende esclusivamente dalla concentrazione di ossigeno.

Il sensore raziometrico che abbiamo sviluppato è stato impiegato con successo per monitorare la permeazione dell'ossigeno in film polimerici con diverse permeabilità all'ossigeno. La membrana sensibile all'ossigeno è stata piazzata in un'atmosfera degassata all'interno di un film polimerico imitando la configurazione tipica dell'imballaggio alimentare. In effetti, in questa situazione il materiale da imballaggio è un'interfaccia tra una camera degassata (senza ossigeno) e l'atmosfera esterna (concentrazione di ossigeno: 21%). La membrana sensibile all'ossigeno collocata nell'atmosfera isolata è stata stimolata dalla luce eccitante attraverso il materiale da imballaggio alimentare e la luce che emessa dal sensore conteneva informazioni riguardo la concentrazione di ossigeno nell'imballaggio e, di conseguenza, circa la permeazione di ossigeno attraverso il film di imballaggio.

La membrana sensibile all'ossigeno ha consentito di seguire il trasporto di ossigeno attraverso materiali polimerici con diverse permeabilità, come ad esempio PDMS o BOPP. Lo sviluppo della concentrazione di ossigeno dentro l'imballaggio di PDMS è stato predetto dal modello soluzione diffusione assumendo permeabilità costante (Legge di Fick), mentre un modello di assorbimento a due fasi (*dual-mode*) è stato osservato per l'imballaggio di BOPP nella fase iniziale.

6.2 Monitoraggio della temperatura

Nella prima parte degli studi è stata notato che l'incremento della temperatura favorisce la disattivazione delle sonde molecolari diminuendo l'intensità dell'emissione, come atteso. Questo comportamento usuale dei luminofori suggerisce un'affascinane opportunità delle sonde molecolari nella tecnologia a membrana: il monitoraggio della temperatura. La seconda parte di questa tesi è stata dedicata allo sviluppo di sistemi capaci di fornire informazioni in tempo reale ed *in-situ* circa la temperatura della membrana.

L'immobilizzazione di Ru(phen)$_3$ in nano-particelle di silicio ha consentito lo sviluppo di un nano-termometro. Il nano-sensore è stato preparato partendo da soluzioni colloidali di puro silicio ricoperte in un passaggio successivo da una corona di silice drogata con il luminoforo. Le interazioni polari tra il silicio ed il complesso di Rutenio hanno favorito l'immobilizzazione della sonda molecolare e la sua protezione da fattori ambientali (es. ossigeno). Studi hanno mostrato che l'impiego di questa procedura ha consentito di ottenere nano-particelle monodisperse. Al contrario, l'omogeneità delle nano-particelle in termini di forma e monodispersione è stata compromessa dall'immobilizzazione della sonda molecolare nel nucleo di silicio a causa dell'ingombro sterico del complesso di Rutenio che disturba la condensazione del precursore di silicio. Uno studio sistematico ha dimostrato come sia possibile controllare le proprietà del nano-termometro in termini di dimensione variando la quantità

del precursore di silicio (TEOS) impiegato per crescere la corona, mentre la concentrazione della sonda influenza l'intensità di emissione e la sensibilità alla temperatura. Inoltre, è stato possibile alterare il carattere delle nano-particelle da idrofile a idrofobiche mediante la funzionalizzazione delle loro superficie con un silano-derivato con una lunga catena alifatica.

Le nano-particelle sensibili alla temperatura sono state immobilizzate mediante la tecnica del *dip-coating* su membrane porose di PVDF preparate mediante induzione di fase indotta da non-solvente (NIPS). L'immobilizzazione non ha modificato le proprietà di base delle membrane di PVDF che presentavano un'evidente attività fotochimica sensibile alla temperatura dovuta alla presenza delle nano-particelle caricate con $Ru(phen)_3$. Questo sistema è molto promettente poiché potrebbe permettere la misura della temperatura sulla superficie delle membrane; ma è di interesse anche in ambito biomedico, come ad esempio per studiare l'ipertermia.

In questa terapia, le nano-particelle ricoperte da una corona di oro rilasciano calore come conseguenza dell'assorbimento di luce infrarossa, distruggendo i tessuti cancerogeni. L'immobilizzazione di queste sonde molecolare potrebbe utile non solo per marcare le nano-particelle, ma anche per il monitoraggio della temperatura che le stesse raggiungono durante la terapia fornendo informazioni circa l'efficienza del trattamento.

Un altro approccio diverso è stato l'immobilizzazione della sonda molecolare in membrane polimeriche. Ancora una volta $Ru(phen)_3$ è stato immobilizzato in membrane composte da nano-fibre (ENMs) di PVDF preparate per elettro-filatura (*electrospinning*). Le analisi al microscopio elettronico a scansione hanno evidenziato il ruolo chiave della sonda molecolare nel preparare fibre prive di difetti per effetto della sua natura salina. Infatti, l'impiego della sonda molecolare e del Cloruro di Litio (LiCl) hanno aumentato la conducibilità elettrica della soluzione polimerica aumentando la sua filabilità favorendo la preparazione di fibre omogenee. Questo metodo ha consentito la preparazione di membrane con superficie idrofoba e una struttura con pori interconnessi fatta da una rete di nano-fibre. PVDF ENM hanno mostrato un'evidente emissione correlata alla presenza di $Ru(phen)_3$ immobilizzato nelle catene polimeriche di PVDF. Le membrane PVDF ENM hanno presentato eccellenti prestazioni in distillazione a membrana per contatto diretto (DCMD) grazie al loro limitato spessore e all'alta idrofobicità combinata con un'elevata porosità.

E' stato possibile monitorare l'emissione proveniente dalla membrana PVDF ENM carica di $Ru(phen)_3$ attraverso l'impiego di un apposito modulo a membrana con una finestra trasparente e uno spettrofotometro equipaggiato con una fibra ottica biforcuta. Come atteso, l'intensità dell'emissione decresce con l'aumento della temperatura fornendo informazioni *in-situ* circa la temperatura della superficie della membrana. In seguito a calibrazione, è stata monitorata la temperatura della superficie della membrana in diversi punti durante il processo di DCMD in modo non-invasivo ed in tempo reale. Successivamente, la mappa della temperatura sulla superficie della membrana è stata ottenuta usando la temperatura misurata nei diversi punti come input in un modello capace di estrapolare un andamento continuo da punti discreti. Inoltre, la mappa della temperatura dell'acqua della corrente di alimentazione è stata ottenuta mediante una camera ad infra-rossi. I risultati evidenziano che la temperatura della membrana è minore rispetto a quella della corrente acquosa a

causa della polarizzazione termica. Inoltre, la differenza di temperatura tra la membrana e la corrente acquosa aumenta lungo il modulo a membrana a causa dell'energia spesa per vaporizzare l'acqua e della conducibilità termica della membrana. Questi esperimenti evidenziano le potenzialità delle sonde molecolari come una tecnologia innovativa per studiare i fenomeni di polarizzazione termica fornendo informazioni cruciali per lo studio del processo di distillazione a membrana e producendo progressi in termini di conoscenza scientifica utili a migliorare l'efficienza del processo.

6.3 Prospettive future

Come ulteriori sviluppi di questa tesi esistono sono molte possibilità che riguardano sia il monitoraggio dell'ossigeno che della temperatura. I risultati hanno dimostrato come le sonde molecolari siano estremamente interessanti per il monitoraggio in tempo reale, *in-situ* e non invasivo della temperatura e dell'ossigeno in processi reali.

Comunque esiste un ulteriore vantaggio (non approfonditamente esplorato) nell'uso dei luminofori per monitorare l'ossigeno e la temperatura: la dimensione molecolare della sonda. Questo beneficio è di estremo interesse nella valutazione dell'ossigeno sulla superficie della membrana su scala molecolare in processi in cui avviene il consumo o la produzione di ossigeno, ad esempio reattori a membrana. Inoltre, l'immobilizzazione delle sonde molecolare sulla superficie della membrana potrebbe fornire informazioni sulla concentrazione dell'ossigeno negli strati di soluzioni a contatto con la membrana stessa fornendo informazioni sulla crescita dello sporcamente biologico (*biofouling*). In questo contesto, i nano-termometri basati sull'immobilizzazione del $Ru(phen)_3$ in nano-particelle di silicio potrebbero essere di grande interesse in quanto le nano-particelle di silicio sono largamente impiegate come agenti antibatterici, mentre il $Ru(phen)_3$ potrebbe rilevare la concentrazione di ossigeno disciolto.

Risultati preliminari hanno dimostrato come mediante l'impiego di una tecnologia adeguata, come il microscopio confocale, sia possibile non solo monitorare la concertazione di ossigeno sulla superficie della membrana, ma anche di seguirne il profilo di concentrazione nella matrice della membrana.

L'uso di tecniche ottiche basate sull'impiego delle sonde molecolari per monitorare la temperatura sulla superficie della membrana e di fotocamere ad infra-rossi per misurare la temperatura delle correnti acquose potrebbe descrivere in ogni aspetto la polarizzazione termica. In questo lavoro gli sforzi sono stati concentrati al fine di provare il concetto di base e nello sviluppo di una adeguata tecnologia, in particolare il modulo a membrana, ottenendo le mappe delle temperature dell'acqua e della membrana nel lato di alimentazione. Ad ogni modo, la stessa configurazione potrebbe essere impiegata per misurare le stesse temperature nel lato distillato, ottenendo tutti i dati richiesti per descrivere pienamente il fenomeno di polarizzazione termica. In questa direzione, ulteriori studi circa gli effetti della portata delle correnti e delle proprietà della membrana sulla polarizzazione termica sono cruciali.

Numerose sonde molecolari sono note per la loro sensibilità a CO_2, Ca^{2+}, pH e polarità del solvente offrendo diverse possibilità per monitorare vari parametri di interesse in processi a membrana. Inoltre,

meriterebbero di essere esplorate le potenzialità delle sonde molecolari nello studio dei processi chimici impiegati per preparare le membrane (ad esempio il grado di scambio di solventi in NIPS usando sonde molecolari sensibili alla polarità del solvente).

Al termine di questo manoscritto si può affermare che questa tesi ha riguardato l'impiego delle sonde molecolari al fine di monitorare la temperatura e l'ossigeno in processi a membrana in tempo reale, su scala inferiore al micron, in modo non invasivo ed *in-situ*. Questo studio può essere considerato una base per ulteriori sviluppi poiché apre interessanti prospettive nello studio dei processi a membrana.

Annexes

Annex I: SEM pictures of the cross section of bare PS membrane (a) compared with PS membrane doped with Ru(phen)₃ and Coumarin.
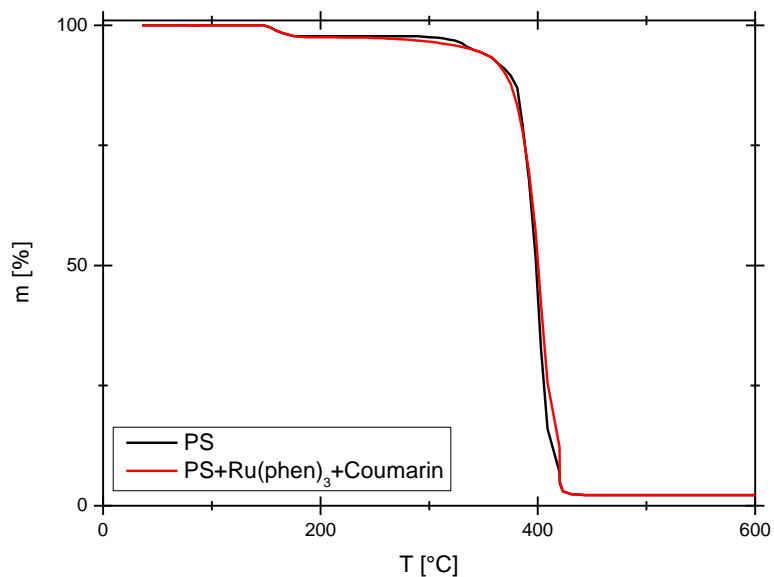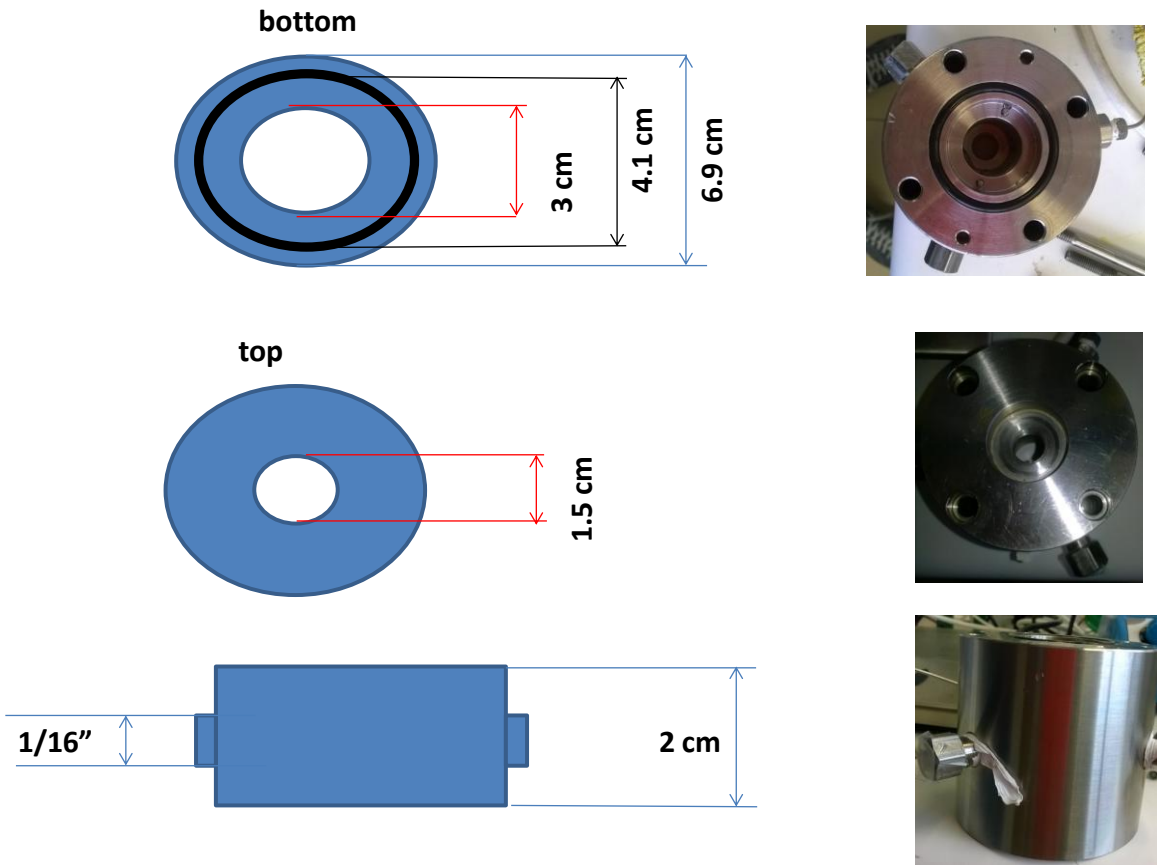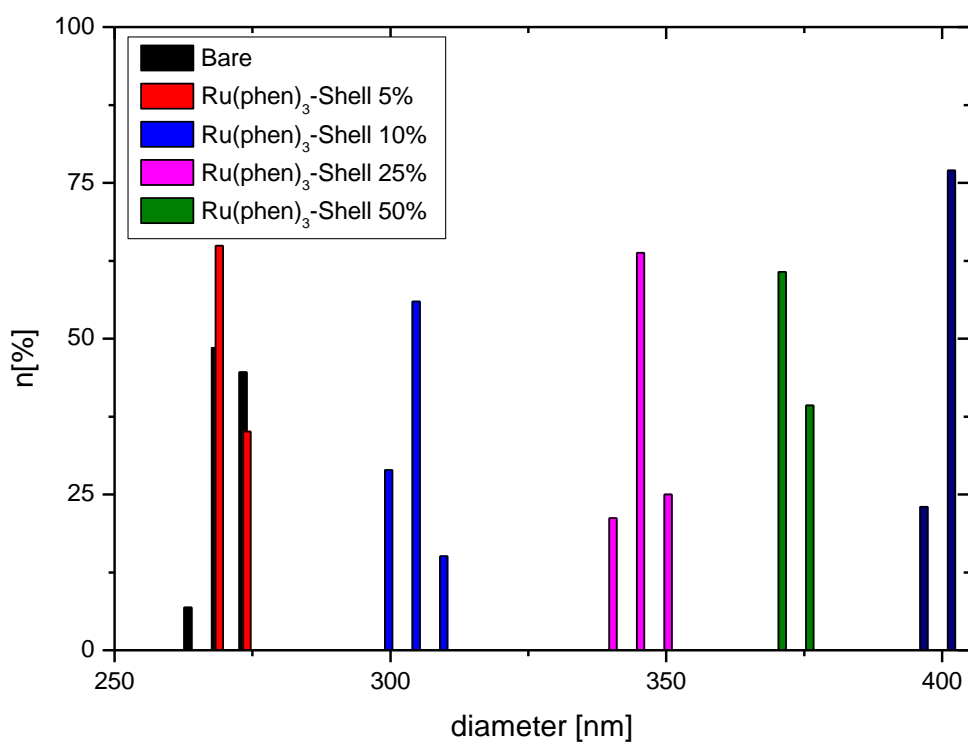
a)
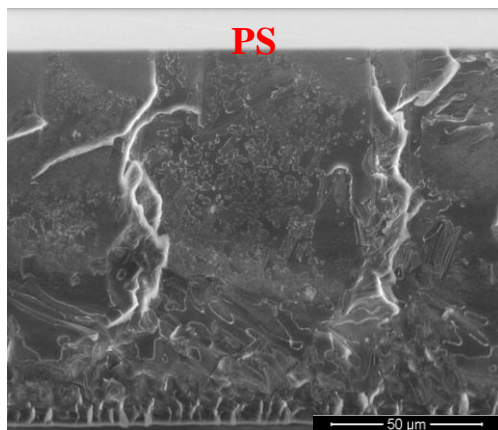
b)

Annex II: Thermogravimetric analyses of bare PS membrane (a) compared with PS membrane doped with Ru(phen)₃ and Coumarin.

Annex III: Scheme and Picture of the membrane module reported in Figure 3.2.

bottom

3 cm
4.1 cm
6.9 cm

top

1.5 cm

1/16"
2 cm

Annex IV: Diameters of Ru(phen)₃-Shell SiO₂NPs compared with Bare SiO₂NPs (DLS analyses).

Annex V: Design of the developed DCMD module employed for online observation of the membrane's fluorescence.

Annex VI: pore size distribution of PVDF ENM.